Western Graduate&PostdoctoralStudies

Western University
Scholarship@Western

Electronic Thesis and Dissertation Repository

11-15-2017 1:45 PM

Design and Evaluation of Neurosurgical Training Simulator

Trinette L. Wright

Supervisor
Roy Eagelson
The University of Western Ontario Co-Supervisor
Sandrine de Ribaupierre
The University of Western Ontario

Graduate Program in Biomedical Engineering
A thesis submitted in partial fulfillment of the requirements for the degree in Master of Engineering Science
© Trinette L. Wright 2017

Follow this and additional works at: https://ir.lib.uwo.ca/etd

Part of the Biomedical Commons, Biomedical Devices and Instrumentation Commons, and the Medical Education Commons

Recommended Citation
Wright, Trinette L., "Design and Evaluation of Neurosurgical Training Simulator" (2017). *Electronic Thesis and Dissertation Repository*. 5115.
https://ir.lib.uwo.ca/etd/5115

This Dissertation/Thesis is brought to you for free and open access by Scholarship@Western. It has been accepted for inclusion in Electronic Thesis and Dissertation Repository by an authorized administrator of Scholarship@Western. For more information, please contact wlswadmin@uwo.ca.

المنارة للاستشارات

www.manaraa.com

Abstract

Surgical simulators are becoming more important in surgical training. Consumer smartphone technology has improved to allow deployment of VR applications and are now being targeted for medical training simulators. A surgical simulator has been designed using a smartphone, Google cardboard 3D glasses, and the Leap Motion (LM) hand controller. Two expert and 16 novice users were tasked with completing the same pointing tasks using both the LM and the medical simulator NeuroTouch. The novice users had an accuracy of 0.2717 bits (SD 0.3899) and the experts had an accuracy of 0.0925 bits (SD 0.1210) while using the NeuroTouch. Novices and experts improved their accuracy to 0.3585 bits (SD 0.4474) and 0.4581 bits (SD 0.3501) while using the LM. There were some tracking problems with the AR display and LM. Users were intrigued by the AR display and most preferred the LM, as they found it to have better usability.

Keywords

Augmented reality, virtual reality, Leap Motion, Unity3d, Google cardboard, NeuroTouch, Vuforia

www.manaraa.com

Co-Authorship Statement (where applicable)

This thesis is presented in the integrated article format, I wish to acknowledge the work of co-authors.

Chapter 2 co-authors:

Ryan Armstrong assisted in the development and testing of the application. He also contributed to the writing of the manuscript. Roy Eagleson and Sandrine de Ribaupierre assisted in the study design, and in the review of the manuscript.

Chapter 3 co-authors:

Roy Eagleson and Sandrine de Ribaupierre assisted in the study design, and in the review of the manuscript.

Chapter 4 co-authors:

Roy Eagleson and Sandrine de Ribaupierre assisted in the study design and testing, and in the review of the manuscript.

المنارة للاستشارات
www.manaraa.com

Acknowledgments (if any)

I would like to acknowledge my supervisors and advisory committee for their guidance and thank the examiners for their time in examining this work.

المنارة للاستشارات

www.manaraa.com

Table of Contents

Abstract i

Co-Authorship Statement (where applicable) ii

Acknowledgments (if any) iii

Table of Contents iv

List of Tables (where applicable) vii

List of Figures (where applicable) viii

Chapter 1 1

1 Introduction 1

- 1.1 Surgical Training 1
  - 1.1.1 Surgical Training Simulators 2
- 1.2 Ventriculosmy Procedures 2
- 1.3 Virtual Reality and Display 3
  - 1.3.1 Virtual Reality Environments 3
  - 1.3.2 Head Mounted Display 3
- 1.4 Virtual Realty Medical Simulators 5
- 1.5 Measures of Performance 5
- 1.6 Research Question 7

Chapter 2 8

2 Medical Simulation System Using Google Cardboard and Vuforia 8

- 2.1 Introduction 8
- 2.2 Methods 10
- 2.3 Results 15
- 2.4 Discussion 16
- 2.5 Conclusion 17

المنارة للاستشارات

www.manaraa.com

Chapter 3 18

3 Targeting Performance of Leap Motion In An Augmented Reality Environment 18

3.1 Introduction 18

3.2 Methods 20

3.2.1 Sphere Targeting Tasks 21

3.2.2 Shape Tracing Tasks 25

3.3 Results 28

3.3.1 Sphere Targeting 28

3.3.2 Shape Tracing 33

3.4 Discussion 48

3.4.1 Sphere Targeting Tasks 48

3.4.2 Shape Tracing Tasks 49

3.5 Conclusion 50

Chapter 4 51

4 Leap Motion Simulator Design and Evaluation 51

4.1 Introduction 51

4.2 Methods 52

4.3 Results 60

4.4 Discussion 73

4.5 Conclusion 74

Chapter 5 75

5 Conclusion 75

5.1 Simulator design 76

5.1.1 HMD 76

5.1.2 Image Tracking 76

المنارة للاستشارات

www.manaraa.com

5.1.3 Leap Motion ... 77
5.1.4 VR and AR Environment ... 77
5.2 Future Directions ... 78
References ... 79
Curriculum Vitae ... 84

www.manaraa.com

List of Tables (where applicable)

Table 1: Average targeting accuracy and task completion times by participant. 15

Table 2: Average time, average combined distance and average distance in each direction for all users based on all target tasks. 32

Table 3: Average time, average combined distance and average distance in each direction for all users based on all target tasks. 38

المنارة للاستشارات

www.manaraa.com

List of Figures (where applicable)

Figure 1: Google cardboard 3D glasses contain two optical lenses and a space for the smartphone at the front. The glasses have an action button to increase the interactive experience the user has with the virtual environment. 4

Figure 2: Image features created by Vuforia. These points are used to calculate the distance and angle between the image and the smartphone camera. 9

Figure 3: The duplicated camera view that when used in combination with the Google cardboard 3D glasses, the user is presented with the stereoscopic view. 11

Figure 4: The base image for the simulator with the associated virtual mannequin head. 11

Figure 5: The tool image and the associated virtual tool. 12

Figure 6: The set up of the physical tool with the tool image. 12

Figure 7: A participant placing the virtual tool through the longest axis of the visible ellipsoid. 13

Figure 8: The selected position of the tooltip with the purple sphere shown as visual feedback for the user. 14

Figure 9: The experimental setup for this simulator. 15

Figure 10: The LM controller with the 3D axis labeled. 19

Figure 11: The setup of the smartphone with the LM controller. The LM uses a USB connector, so a USB to micro USB converter was needed to connect the LM directly to the Nexus 5. 20

Figure 12: Location of all spheres within the AR environment. 21

Figure 13: The base image for all spheres. A) The image that was selected. B) The image in a Unity scene with a sphere. C) The view of the same scene when run on the smartphone. 22

المنارة للاستشارات

www.manaraa.com

Figure 14: The virtual robotic hands used in the application. The virtual hands mimic the movements of the users hands when held above the LM. 23

Figure 15: The setup for the sphere targeting tasks with a participant. 23

Figure 16: The screen view of the application as seen by the participants. The arrows at the top of the screen as for switching between spheres and the green button at the bottom of the screen records the position of the virtual index finger when pressed. 25

Figure 17: The first three shapes the participants were asked to trace. 25

Figure 18: Examples of the change in orientation, position and size for the three different shapes that were presented to the participants. 26

Figure 19: The base image for all shapes. A) The image selected. B) The image and a circle from a Unity scene. C) The same scene when run through the application on the smartphone. 26

Figure 20: The view of the first tracing task to the user. When the participant was ready to start tracing, they pressed it and began tracing. The colour of the button changed to indicate the position information of the index finger was being recorded. The arrows at the top of the screen allowed the user to move between shapes. 27

Figure 21: The information recorded from Unity. The path of the index finger is shown in yellow with the outside edge of the sphere shown in blue. The corners of the base image are shown in red. 28

Figure 22: The distance from the center of the sphere to the fingertip for all participants. Correct fingertip positions are shown in blue. 29

Figure 23: The task completion times by user. 30

Figure 24: The distance from the sphere center to the fingertip position in the x direction (width direction). 31

www.manaraa.com

Figure 25: The distance from the sphere center to the fingertip position in the y direction (height direction). 32

Figure 26: The distance from the sphere center to the fingertip position in the z direction (depth direction). 32

Figure 27: The fingertip path split into before the record button had been pressed, in yellow, and after the record button had been pressed, in purple. The outside edge of the shape was shown in blue with the corners of the base image shown in red. 328

Figure 28: The fingertip path after the record button has been pressed for a “good” trace. 35

Figure 29: The fingertip path after the record button has been pressed for a “poor” trace. 35

Figure 30: The distance from the center over time. A) The “good” trace in blue, the calculated edge of the circle in red. B) The “poor” trace in blue, the calculated edge of the circle in red. 36

Figure 31: The maximum distance for this “good” trace was the top yellow line and the minimum distance was the bottom yellow line. 37

Figure 32: The maximum distance for this “poor” trace was the top yellow line and the minimum distance was the bottom yellow line. The bias was the difference between the minimum and the edge of the circle, as shown in red. 37

Figure 33: The speed and accuracy of circle tracing for all participants 39

Figure 34: The circle tracing times for all participants 40

Figure 35: The fingertip path of a “good” trace after the record button has been pressed. The participants path is shown in yellow, the outside edge of the square is shown in blue and the corners of the base image are shown in red. 40

Figure 36: The distances between the fingertip and the outside edge of the square for the “good” trace. 41

المنارة للاستشارات

www.manaraa.com

Figure 37: The fingertip path of a "poor" trace after the record button had been pressed. The participants path is shown in yellow, the outside edge of the square is shown in blue and the corners of the base image are shown in red. 42

Figure 38: The distances between the fingertip and the outside edge for the square for the "poor" trace. 42

Figure 39: The speed and accuracy of each square traced by side for all participants 43

Figure 40: The square tracing times for all participants. 44

Figure 41: The fingertip path after the record button had been pressed for a "good" trace. The fingertip path is shown in yellow, the outside edge of the triangle is shown in blue and the corners of the base image are shown in red. 44

Figure 42: The distance between the fingertip position and the outside edge of side one of the triangle for the "good" trace. 45

Figure 43: The fingertip path after the record button has been pressed for a "poor" trace. The fingertip path can be seen in yellow, the outside edge of the triangle can be seen in blue and the corners of the base image can be seen in red. 45

Figure 44: The distances between the fingertip position and the outside edge of the triangle for the "poor" trace. 46

Figure 45: The speed and accuracy for the triangle traced by side for all participants.. 47

Figure 46: The triangle tracing times for all participants. 48

Figure 47: The multi-image cube for overlaying the virtual objects on to the physical simulator. 52

Figure 48: The transparent virtual head overlaid with the physical head. 53

Figure 49: The stereoscopic view of the simulator through the Google Cardboard glasses... 54

Figure 50: The LM robotic hand index finger was used as the tool for this simulator. 55

المنارة للاستشارات

www.manaraa.com

Figure 51: The NeuroTouch tool had to be placed on the physical skull and orientation so that the trajectory from the end of the tool would pass through the longest axis of the visible ellipsoid. 56

Figure 52: The LM virtual hands could pass through the virtual head so the index finger could be placed through the ellipsoid. 56

Figure 53: The interface of the program used to copy the position and location of the NeuroTouch tooltip and the task completion time. 57

Figure 54: An example of one of the ventricles with the right anterior horn highlighted in red. 57

Figure 55: An example of how a user would place the NeuroTouch tool so that the trajectory from the tooltip would pass through the highlighted region of the ventricle. 58

Figure 56: An example of how a user would place the LM index finger so that it passes through the highlighted region of the ventricle. 59

Figure 57: The setup of the NeuroTouch. 59

Figure 58: The setup of the LM. 60

Figure 59: An example of a “correct” trajectory through the right anterior horn. 60

Figure 60: An example of a “correct” trajectory and its center through the right anterior horn. 61

Figure 61: An example of a “good” participant trajectory through the right anterior horn using the NeuroTouch. 62

Figure 62: An example of a “poor” participant trajectory through the right anterior horn using the NeuroTouch. 62

Figure 63: An example of a “good” participant NeuroTouch trajectory in red with the “correct” trajectory in gold. 63

المنارة للاستشارات

www.manaraa.com

Figure 64: An example of a “poor” participant NeuroTouch trajectory in red with the “correct” trajectory in gold. 63

Figure 65: The entire path a participant moved their index finger, in red, before selecting the final trajectory. 63

Figure 66: An example of a “good” participant trajectory through the right anterior horn using the LM. 64

Figure 67: An example of a “poor” participant trajectory through the right anterior horn using the LM. 64

Figure 68: An example of a “good” participant LM trajectory in red with the “correct” trajectory in gold. 65

Figure 69: An example of a “poor” participant LM trajectory in red with the “correct” trajectory in gold. 65

Figure 70: Novice distance performance for the NeuroTouch. 66

Figure 71: Expert distance performance for the NeuroTouch. 66

Figure 72: Novice angle performance for the NeuroTouch. 67

Figure 73: Expert angle performance for the NeuroTouch. 68

Figure 74: Novice distance performance for the LM. 69

Figure 75: Expert distance performance for the LM. 69

Figure 76: Novice angle performance for the LM. 70

Figure 77: Expert angle performance for the LM. 71

Figure 78: The average novice task completion times for both NeuroTouch and LM. 72

Figure 79: The average expert task completion times for both NeuroTouch and LM. 72

المنارة للاستشارات

www.manaraa.com

www.manaraa.com

Chapter 1

1 Introduction

The use of surgical simulators as a method of training is a growing field of research. Computer graphics are improving rapidly, which aids in the creation of more realistic simulators. Virtual and augmented reality (VR and AR respectively) are areas being explored for the creation of new simulators. The technology used in the display of VR is also experiencing rapid advancement, leading to more commercially available and user-friendly devices. Some companies are taking advantage of the technology contained within smartphones, a device many consumers now own, to create light weight head mounted displays (HMD) for virtual environments. The purpose of this research is to use the advancements in consumer technology to create a medical simulator and assess both its performance and usability.

1.1 Surgical Training

Surgical training is a very important area of study, as designing a training program that requires fewer hours but does not negatively affect the skills acquisition by students is incredibly difficult. There have been ethical and safety concerns raised about some of the traditional training methods [1][2][3]. These include concerns about patient safety and the ethical use of cadavers in procedure training [2]. Training with cadavers also has a disadvantage in that performing procedures in this environment is not the same as performing these same procedures on a real patient [3]. Surgical training must help students with acquiring the skills they need, ensure high retention of those skills, and must help with transferring those skills to the trainees’ future working environment. Additional resources to help with training are beneficial as they improve patient safety, enhance the training of residents and surgeons, and reduce surgical error [4]. In addition, surgical procedures are becoming more complex, so additional training methods are advantageous. Surgical simulators have been gaining acceptance in this field, as they provide educators with an additional source for this training.

المنارة للاستشارات

www.manaraa.com

1.1.1 Surgical Training simulators

Surgical training simulators have been around for many years, but owing to technological advances, they are becoming more accessible and accurate. Factors such as graphics, haptics, and tissue deformation all affect the realism of the simulator, so there have been many research studies focusing on investigating these areas [5][6][7][8]. Simulators can be used to teach and practice procedures before students and residents preform them on live patients [1]. Simulators can offer students feedback on their performance and can be used to track skill acquisition and improvement [4]. Simulators will be an important facet for training in new and emerging areas of medicine, such as robotic and minimally invasive surgery [1]. Surgical trainers are very expensive which, unfortunately limits the educational institutions that can provide these systems to students [9]. This is often due to proprietary hardware contained within the devices [10]. Much of the cost of these simulators is due to the high-resolution displays that are needed to provide the immersive environment. Immersive environments have been seen to improve skill retention for spatial tasks and have been found to reliably assess and train surgical skills [11][12]. Additionally, interactive 3D models have been found to aid in trainees' skill and knowledge acquisition [13]. Stereoscopic displays aid in the immersive and interactive environments, and afford many benefits in the medical domain.

1.2 Ventriculosmy Procedures

Many types of procedures can be simulated using training simulators. Endoscopic Third Ventriculostomy (ETV) is a neurological procedure that residents frequently perform [14][15]. The procedure is usually performed without medical imaging guidance and is done at a patient's bedside. It is important to place the catheter correctly into the ventricle so that pressure is relieved and prevents any lasting neurological damage [16][15]. There have been many ETV simulators designed, specifically one that has been developed by the National Research Council of Canada (NRC) is the NeuroTouch device [17]. Over 20 Canadian research hospitals worked in partnership with the NRC to develop the NeuroTouch [17]. The NeuroTouch device uses a mechanical arm in combination with graphics for simulation of several types of procedures. Although this system is very beneficial, it is still very expensive which limits its use in an educational setting [18].

المنارة للاستشارات

1.3 Virtual Reality and Display

1.3.1 Virtual Reality Environments

VR and AR are areas that have been greatly impacted by technological advances in recent years [19][20]. While VR is made completely of virtual objects in a virtual environment, AR overlays virtual objects onto the real world as seen through a camera [21][22]. These technological advances have increased accessibility for developers and reduced costs for consumers [19][20]. A number of video game platforms have been created that aid in the development of VR and AR applications. The most popular platforms are Unreal, Valve and Unity [23]. These platforms allow for the development of easily deployable virtual applications. They have also improved the environment around developing these applications, which means more developers are able to create virtual environments. In particular, Unity has some advantages including cross platform development [24][25]. This means applications can be created and deployed on a wide range of devices from iOS, to Android and Windows [24][25]. This is very appealing to developers, as separate applications for the systems do not need to be developed. Unity is also advantageous as it allows for the integration of different devices into the environment. Different types of interaction methods can be used such as image tracking, and applications can be developed that mix virtual and augmented reality environments. Other devices such as different displays and controllers may also be integrated into the Unity environments.

1.3.2 Head Mounted Display

The viewing of virtual reality is moving away from the traditional method of viewing using a large screen, towards a more immersive method of Head-Mounted Displays (HMD) [26]. HMDs improve the user experience over the traditional method by allowing the user to be surrounded by the virtual environment while providing users the freedom to easily move through the virtual world [27][28]. HMDs should have good resolution, a wide field of view, low latency, contain positional and rotational sensors, and be relatively light [28][29], as these parameters affect the immersive experience of the device [28]. Advances in technology such as screen resolution and positional tracking have made these types of devices more affordable [29]. Until recently, stereoscopic

المنارة للاستشارات
www.manaraa.com

displays used for VR were either a dual projection system or a costly headset. Tracking of head movements provided additional difficulties, as an optical or electromagnetically tracked system was needed [30]. There are several popular devices that are now commercially available including the Oculus Rift, HTC Vive, and the Microsoft HoloLens. These are HMDs that developers can specifically develop and deploy new virtual environments on. These are untethered devices; therefore, all hardware, including sensors and camera, is contained within the device [31]. Most of these devices were developed by the video game industry; however, their use as medical training tools and simulators is something that is currently being explored. An issue with these devices is they are still expensive for most consumers. Companies such as Google and Samsung have recently designed different HMDs that use a consumer's smartphone [32]. Virtual reality environments can be designed and deployed using most smartphones [20][32][33][34]. The user would need to purchase an inexpensive set of 3D glasses to be able to view the environments [20][32][33][34]. The smartphone can be placed in the glasses and the user can wear them like the previously mentioned HMDs (Fig. 1).

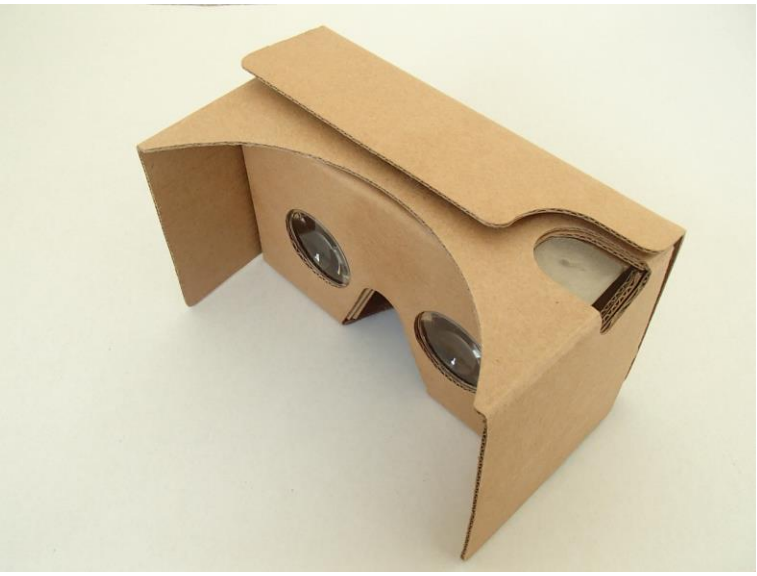

Figure 1: Google cardboard 3D glasses contain two optical lenses and a space for the smartphone at the front. The glasses have an action button to increase the interactive experience the user has with the virtual environment.

المنارة للاستشارات

www.manaraa.com

These types of systems are easier for consumers to purchase and use, as most people have a smartphone that is powerful enough to run the VR applications. There has also been a lot of advancement in the technology, particularly with respect to the graphics, display and positional sensors within the phones, which has led to more powerful gyroscopes that help make applications much more immersive for the users [35]. The google cardboard glasses contain optical lenses with an outer shell that holds the smartphone in place to uses the phone as the display. However, the glasses limit the amount of interaction that can occur between the user and the VR environment. Some interaction can be done using the action button contained on the glasses. Another method of creating this interaction is to combine the glasses with another input method. One of the more popular interaction methods is the hands and body free method [36]. There are a number of devices that can be used to achieve this including the Leap Motion hand controller [37]. Although the use of smartphones as a display for virtual environments has some advantages, there are some limitations. The main limitation is the field of view, which is much smaller for smartphones as compared to systems that contain a display [31]. They also require a different method for providing a stereoscopic view of the virtual environment.

1.4 Virtual Realty Medical Simulators

Mobile phones are beginning to be targeted by developers for medical simulators [37]. There have been previous attempts to lower the cost of these immersive virtual training simulators. HMDs have improved greatly to the point where they are capable of displaying high resolution images such as CT and MRI scans [27]. Immersive virtual environments have been developed for purposes such as anatomical education and surgical planning [27][38][10]. With more affordable and powerful smartphones being developed, the smartphone is becoming a very appealing platform for the development of surgical simulators by developers and educators.

1.5 Measures of Performance

For simulators to be an effective training tool, they must provide feedback to the users about their performance and be designed so that users can easily interact with them [39]. Simulators provide an interesting example of Human Computer Interfaces (HCI). For these

المنارة للاستشارات
www.manaraa.com

HCIs it is important to predict how a user will interact with the device [39]. A common method of measuring performance of an HCI is using Fitts' Law. Fitts' Law is most easily described as being the trade-off between speed and accuracy when performing a targeting task [41] and is used as a quantitative measure for describing the HCI [40]. The Fitts' Law relationship shows that as a user is faster completing a targeting task, they become more inaccurate [40].

$$\mathrm{T} = a + b * log_2(\frac{A}{W} + 1) \qquad (1)$$

T is the time it takes to complete the pointing task, a and b are empirically determined constants, A is distance between the starting point and the target, and W is the width of the target [40]. The index of performance (ID) is the measure of how difficult a task is to complete and is described by:

$$\mathrm{I}D = \ log_2(\frac{A}{W} + 1) \qquad (2)$$

The more difficult a task is, the higher the value of the ID will be [40]. However, Fitts' Law only addresses movement in 2 dimensions. Fitts' Law can be modified so that it is predictive of movement through a tunnel instead of movement between two points:

$$\mathrm{T} = a + b * \frac{A}{W} \qquad (3)$$

With the ID as:

$$\mathrm{I}D = \frac{A}{W} \qquad (4)$$

This is because the difficulty of traveling through this tunnel is related to the relationship between A/W and the logarithm of A/W [40]. When using it to compare movements in 3 dimensions, such as those in a surgical simulator, a modified equation is needed [40]. These types of 3D movements have presented some different challenges then those in 2D [42]. In 3D, objects are more commonly used than points, so Fitts' Law can be modified so that the target is an object [43][40]. The W can also be adjusted so that it is the width of the cursor

www.manaraa.com

instead of the width of the target [43][42]. These concepts will be used when calculating the performance of users while they are using a 3D simulator.

1.6 Research Question

The purpose of this research is to design an affordable, easily accessible and robust virtual reality simulator for neurosurgical procedures, specifically EVT procedures. To make this simulator affordable and highly accessible for students, the simulator should run on commercially available, inexpensive hardware and software. Most students have access to a smartphone, which makes it the ideal choice for a virtual reality display. This will also reduce the cost of the simulator as students will not need to purchase an additional device. They will need a pair of 3D glasses that the smartphone will fit in. Fortunately, due to the popularity of the Google cardboard glasses, the cost of a pair of these glasses is relatively inexpensive. The simulator should also record all movements completed by the users. This will aid in assessing the performance of the students, and the overall usability of the simulator. The simulator should be robust and have high repeatability as students would be using it as a training tool. Performance evaluation will be done using a modified Fitts' Law equation as all tasks the users will complete will be in 3D. Different tasks have been designed that will test the performance of the simulator. Users will be asked to complete simple pointing and tracing tasks to achieve this. The simulator will then be tested against the NeuroTouch medical simulator to assess the performance with that of a commercially available simulator. The next three chapters describe the evolution of the proposed simulator and the metrics used to evaluate the simulator against the listed criteria.

المنارة للاستشارات

www.manaraa.com

Chapter 2

2 Medical Simulation System Using Google Cardboard and Vuforia

An affordable virtual reality simulator has been designed using the video game design engine Unity and the image tracking software Vuforia. This system has been implemented using the Google Cardboard 3D glasses for stereoscopic vision. The simulator was assessed by creating ellipsoid targeting tasks. This comprised of placing a virtual tool through the longest axis of each ellipsoid. The system was tested using eight participants and the overall system performance was measured by user targeting accuracy.

2.1 Introduction

The purpose of this initial study was to design a simulator that is low cost and easily accessible for all users. HMDs are the cost common way for virtual environments to be displayed [26]. Technological advances and prevalence of smartphones have made them a good platform for developing low cost, easily accessible environments [22]. Unity3d is a popular video game design engine that has been used to develop all virtual environments. This program allows for cross platform development, which is advantageous for this application as it can be developed and released for many different mobile devices, such as Android and iOS [24][25]. Unity also allows for integration with other programs, such as image tracking. Image tracking is a popular option that has been added to VR environments. Image tracking requires an image to be loaded into the VR environment during development and a set of virtual objects are associated with this image. To view these objects when running the application, this image must be physically placed within the field of view of the camera embedded within the smartphone. This can be done by printing the image. Vuforia was used, a very popular image tracking library, and can be directly integrated with Unity [22]. Integrating Vuforia with Unity requires the software development kit (SDK) package to be imported and no additional programming is required. When the physical image is detected by the smartphone application, all associated virtual objects are visible to the user. Vuforia calculates the distance of the image from the camera

المنارة للاستشارات

www.manaraa.com

and the angle between the two [44]. Vuforia creates image features and uses these in its calculations (Fig. 2).

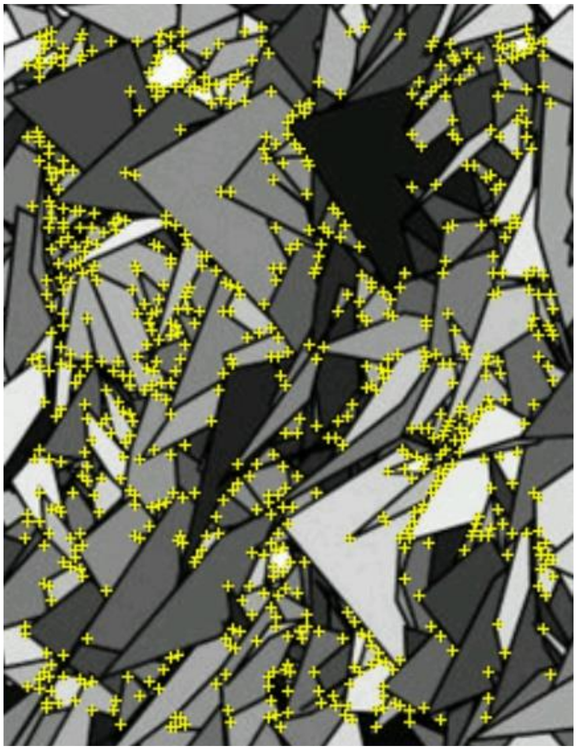

Figure 2: Image features created by Vuforia. These points are used to calculate the distance and angle between the image and the smartphone camera.

These calculations are done so that when the virtual objects are overlaid, they are at the correct scale and angle to the user [44]. If the application loses the image tracking, such as when the image is not within the camera field of view or if the user is too far away for the application to distinguish the needed features, the virtual objects will no longer be displayed. To have the objects reappear, the user would have the bring the image back into the camera field of view and hold the smartphone close enough that the above features can be found by Vuforia’s algorithm.

The overall research goal is to create a neurosurgical training simulator so a virtual mannequin head has been included in the simulator. All the tasks that the users were asked to complete were contained within the head to give it the neurosurgical context. It also assisted the users in orientating themselves within the virtual environment. Many surgical

المنارة للاستشارات

www.manaraa.com

tasks can be divided into several basic tasks with a main task being the selection of a position or of a trajectory within the anatomical setting. Ellipsoids were used as the targeting shape for the tasks as some neurological structures can be abstracted into simpler shapes. Ellipsoids are also advantageous when assessing a trajectory targeting task as the user can be asked to target the shape through the longest axis. The accuracy of the user's ability to target this axis can be more easily calculated using this shape. The simulator was designed to use pointing tasks and was evaluated by assessing the usability and the accuracy of the participants to correctly place a tool through the longest axis of the ellipsoids.

2.2 Methods

The simulator has been developed using Unity3d (version 5) with an android smartphone as the HMD. The LG Nexus 5 and Samsung Galaxy Alpha were specifically chosen for their availability and affordability. Neither of these smartphones contain the most recent hardware and software releases. Most users would not have access to the newest smartphone release so these phones are a more realistic representation of what most users would have. This application was integrated with the Google cardboard glasses so that the virtual environment would be seen by the users in 3D. This integration was done by importing the Google Cardboard SDK in to Unity3d. Google cardboard duplicates the view of the camera so that when viewed with the cardboard glasses, it appears stereoscopic to the user (Fig. 3)[32]. The simulator has been design so that users can interact with the virtual objects. A simple pointer tool has been designed to achieve this. The tool allows users to select the trajectory and position to complete the tasks presented to them. Vuforia is capable of tracking multiple images, so two images for the simulator: one for the base of the simulator (Fig. 4), and one for the tool (Fig. 5).

المنارة للاستشارات

www.manaraa.com

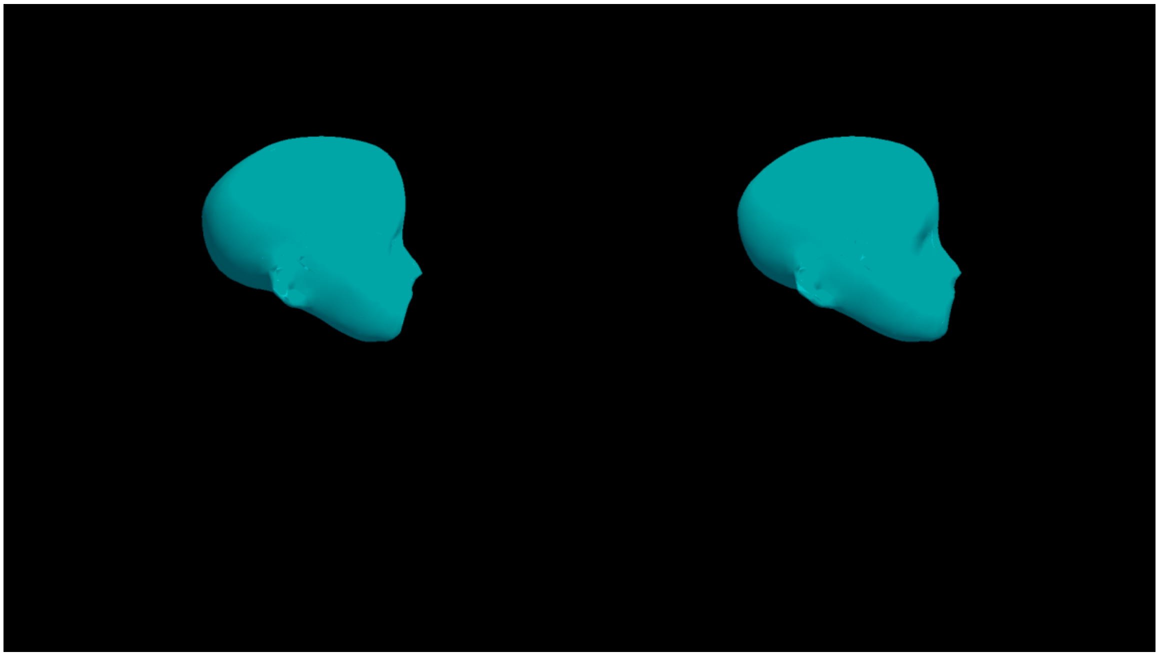

Figure 3: The duplicated camera view that when used in combination with the Google cardboard 3D glasses, the user is presented with the stereoscopic view.

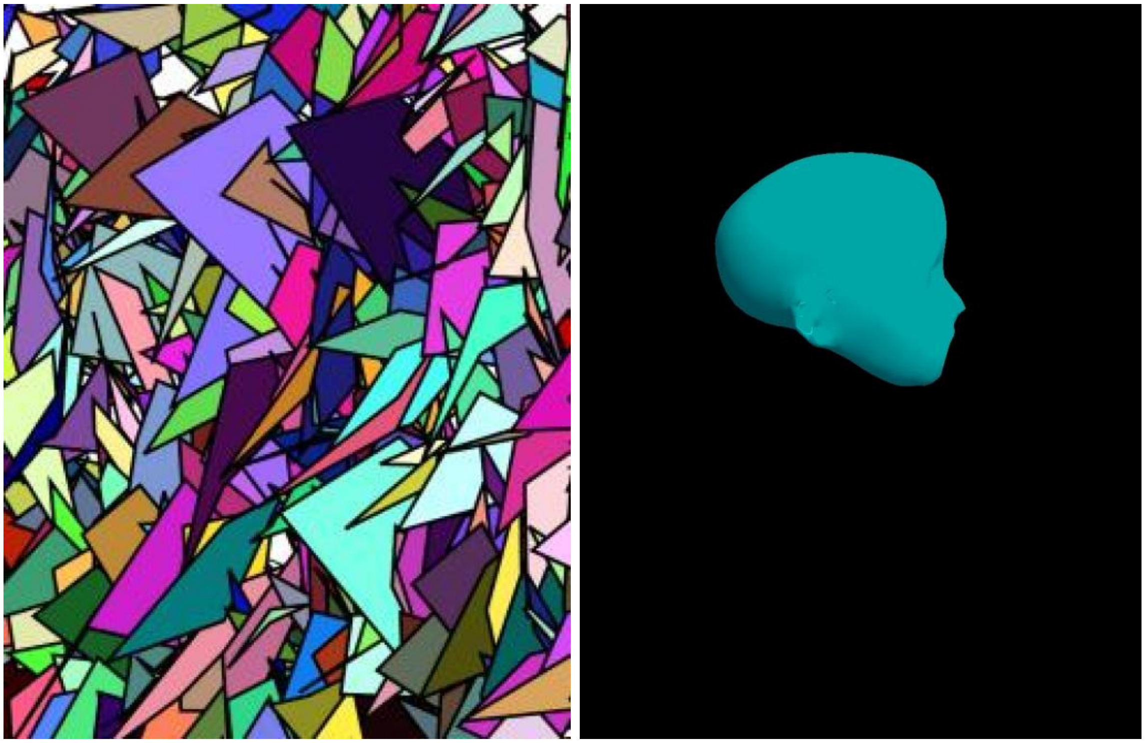

Figure 4: The base image for the simulator with the associated virtual mannequin head.

www.manaraa.com

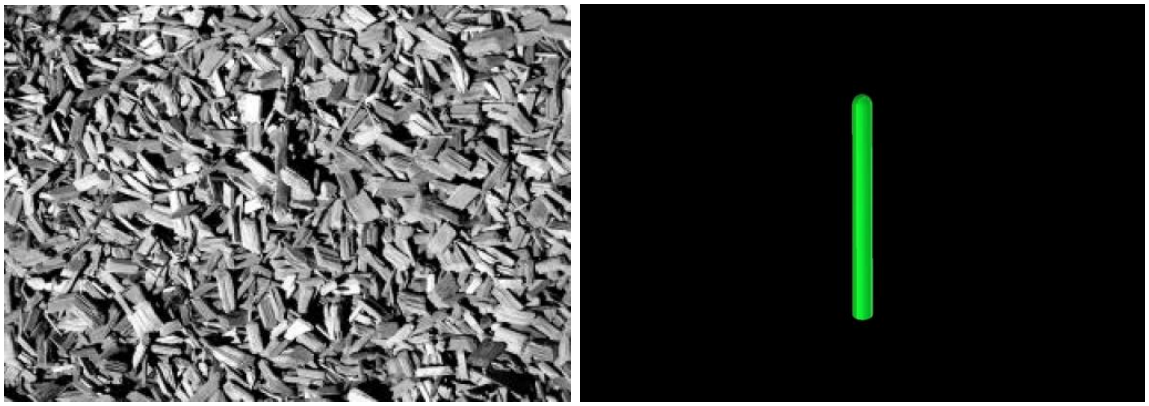

Figure 5: The tool image and the associated virtual tool.

To make the simulator feel as natural as possible, the tool image was attached to a pen. This was done to improve the comfort of the tool in the users' hands and the image was duplicated on both sides (Fig. 6). This was done to maximize the amount of freedom the participants had in moving the tool.

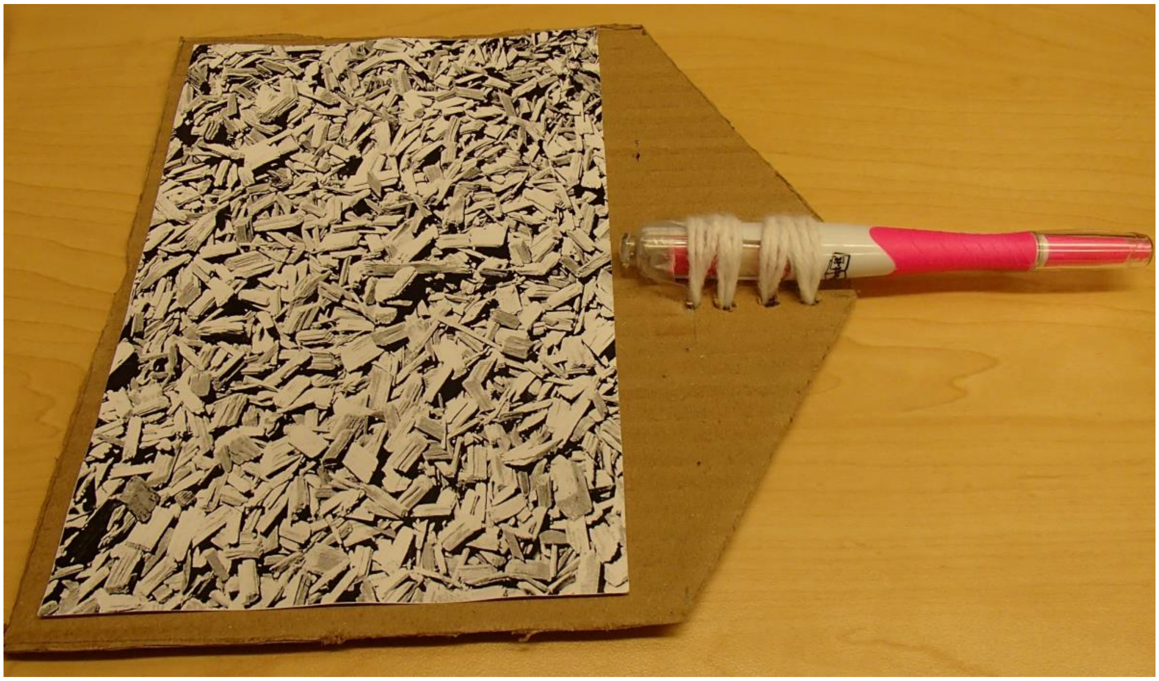

Figure 6: The setup of the physical tool with the tool image.

All the targeting tasks consisted of locating a visible ellipsoid within the virtual head. The users were instructed to place the tool so that it passed through the longest axis of the

www.manaraa.com

ellipsoid and the tip touched the opposite edge of the ellipsoid (Fig. 7). The users were told that they were being timed for each task but that they should complete the tasks as accurately as possible.

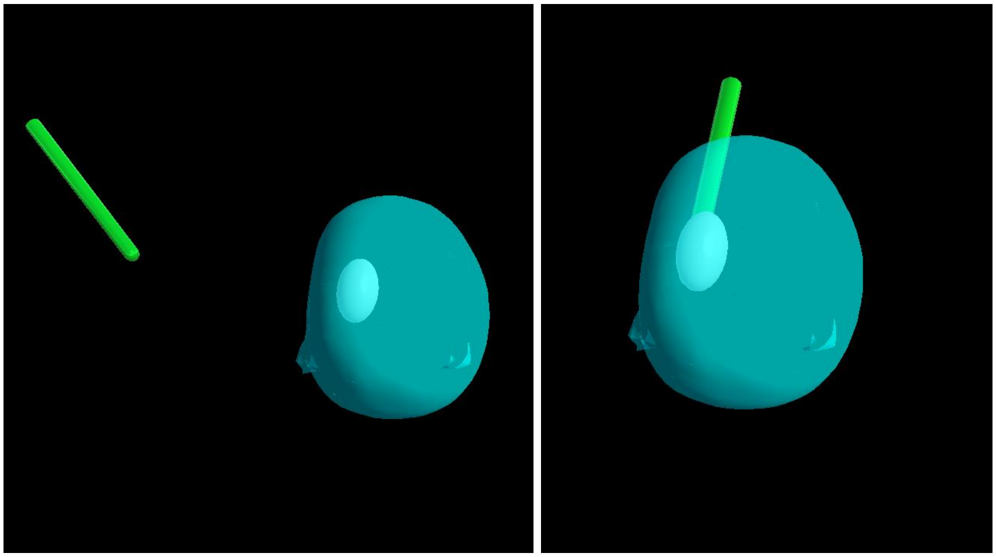

Figure 7: A participant placing the virtual tool through the longest axis of the visible ellipsoid.

When the participant decided the tool was in the correct position, they pressed the action button on the Google Cardboard glasses and a purple sphere appeared (Fig. 8). The action button simulates a tap on the screen which then triggers a script included in the Unity application that makes the sphere visible to the user. The purple sphere appeared in the position of the tooltip to give the participants visual feedback on their selected tooltip position.

المنارة للاستشارات

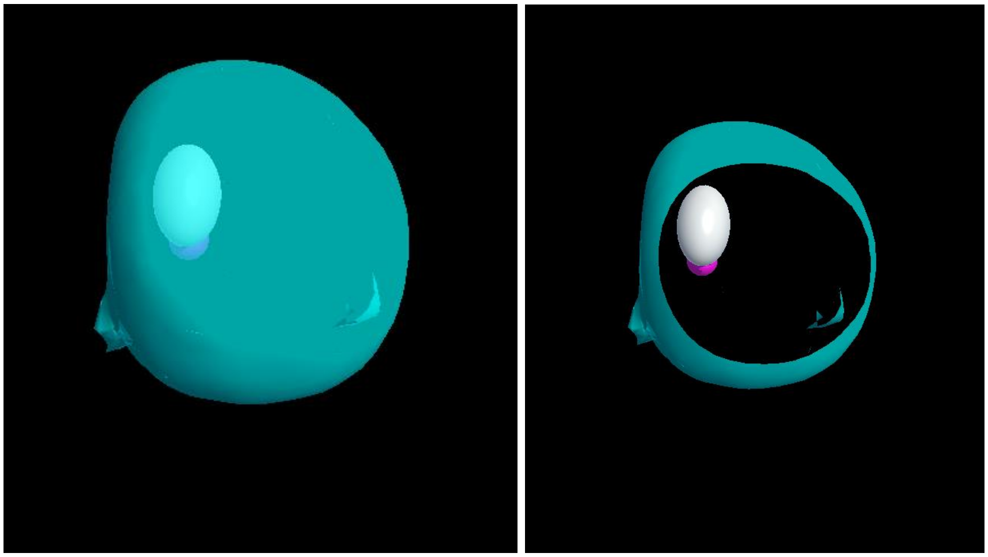

Figure 8: The selected position of the tooltip with the purple sphere shown as visual feedback for the user.

A total of 15 ellipsoids were created using the 3D creation program Blender. The ellipsoids varied in size, location and orientation. They were then imported into Unity and duplicated so participants completed the same 15 ellipsoid targeting tasks twice for a total of 30 tasks. The setup for this experiment consisted of the participants placing the base image in front of them and holding the tool image in the hand they felt most comfortable with (Fig. 9).

المنارة للاستشارات

www.manaraa.com

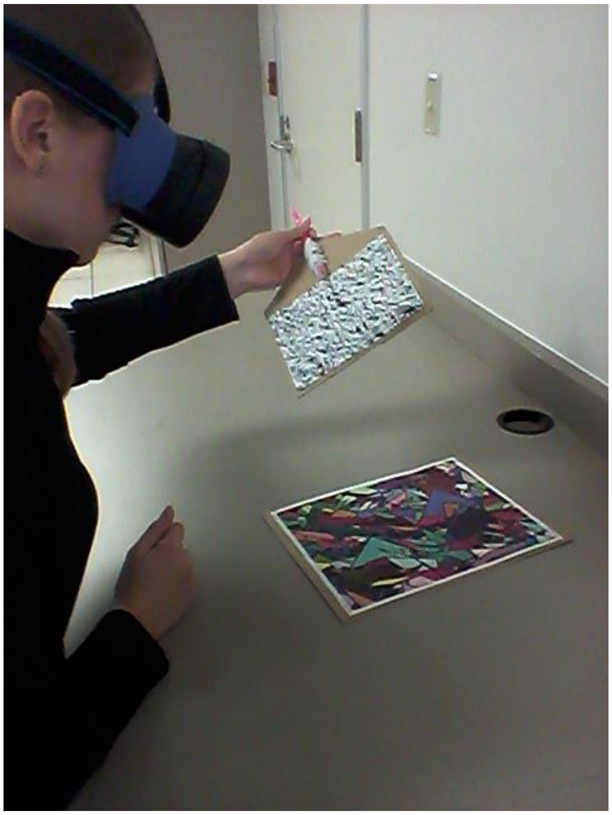

Figure 9: The experimental setup for this simulator.

When the action button is pressed, the amount of time it took the participant to complete the task and if the tooltip was touching the ellipsoid edge were recorded. This was done by a script that was written C# and was integrated with the Unity application. A total of eight participants were recruited for this study. The participants completed a Likert style questionnaire on conclusion of the tasks to provide quantitative feedback.

2.3 Results

The average accuracy for all participants was 62% and the average task completion time was 23.79 s (SD 24.80 s). The individual accuracies and task completion times can be seen in Table 1.

Table 1: Average targeting accuracy and task completion times by participant.

Participant	Targeting Accuracy	Task Time (s)
1	70%	26.32
2	13.33%	22.87

المنارة للاستشارات
www.manaraa.com

3	60%	80.46
4	15.79%	40.18
5	86.67%	2.25
6	83.33%	5.3
7	83.33%	2.9
8	86.67%	10.09

The questionnaires did not report any strong views from the participants. The scale used in the questionnaire ranged from one to seven with seven as the most positive response. The participants felt the environment's visual aspects were immersive, average of 5.12, and that there was a natural feel to the input apparatus, average of 5.13. The participants felt compelled by the objects moving through the environment, average of 5.25, but only slightly felt they were able to explore the environment visually, average of 3.63.

2.4 Discussion

There were no clear trends observed in the accuracy and completion times. There was low variance between individual participant task completion times but high variance between participants. This indicates that the size of the ellipsoid did not affect how the participant targeted the shape. The accuracy and task completion time were more reliant on the method each participant took to completing the tasks. There were cases where the tool image blocked the base image and would cause the image tracking to be lost. When this happened, the mannequin head and ellipsoid would disappear. To resume tracking, the participant would have to either move themselves to a different position so that both the base and tool images were within the field of view of the camera or move the tool image away from the base image. Both cases would cause the task completion time to be longer. Some of the participants felt that this interruption in the task had a negative impact on their performance and on the immersive environment of the simulator. This disruption could be a source of noise within the data which would explain why the results are indistinct. Although the ellipsoids varied in size, location and orientation, there may not have been enough variation between them due to the limited space within the mannequin head. Using an image for the tool made it difficult to avoid occlusion of the base image, and the 2D nature of the image made the tool difficult to continuously track. Participants had to be conscious of the angle that they held the physical tool so that one of the two images was always visible to the

المنارة للاستشارات
www.manaraa.com

camera. This lead to participants holding the tool in orientations that did not feel natural. The participants hand and arm also contributed to the base image occlusion issue.

2.5 Conclusion

This study shows that a low-cost simulator was developed that has the potential to be used in surgical training and education. The results indicate that the simulator functions as intended but further advances in robustness are needed. In using multiple images for the various parts of the simulator, usability of the simulator was affected so further research into different interaction devices is needed to make improvements to this simulator. This device would need to allow the user to interact with the virtual objects while continuing to operate on the mobile platform. This will increase the cost of the simulator as users will need access to additional hardware; however, the improvements to usability should justify the increase in cost.

المنارة للاستشارات

www.manaraa.com

Chapter 3

3 Targeting Performance of Leap Motion In An Augmented Reality Environment

This chapter will assess the usability of the Leap Motion (LM) controller as a user input device on a mobile platform using an AR environment. This assessment comprised of participants using a pair of virtual hands to complete a series of tasks: the first being a set of pointing tasks, and the second a set of tracing tasks. For the first set of tasks, participants located virtual spheres and placed the index finger of one virtual hand in the center of each sphere. For the second set of tasks, participants traced the outside edge of various shapes. This interaction between the participant and the virtual objects was achieved using the LM. A total of seven participants completed the 15 sphere targeting tasks followed by 15 shape tracing tasks. The performance accuracy of each participant while completing these tasks was done using a Fitts' Law methodology and was used to assess the usability and robustness of the system.

3.1 Introduction

In the previous study, image tracking was used for both the simulator and the interactive tool. Some users had difficulty completing the targeting tasks, as the tool image would block the base image, and this would cause the image tracking to fail. When this happened the virtual objects disappeared, which required the participants to move the tool image so that tracking for both images could resume. Using the knowledge gained from the previous study, a different device was selected for interacting with the virtual objects. The LM controller was chosen for this study, as it did not cause image occlusion while still allowing for virtual interaction while running on the mobile platform (Fig. 10).

www.manaraa.com

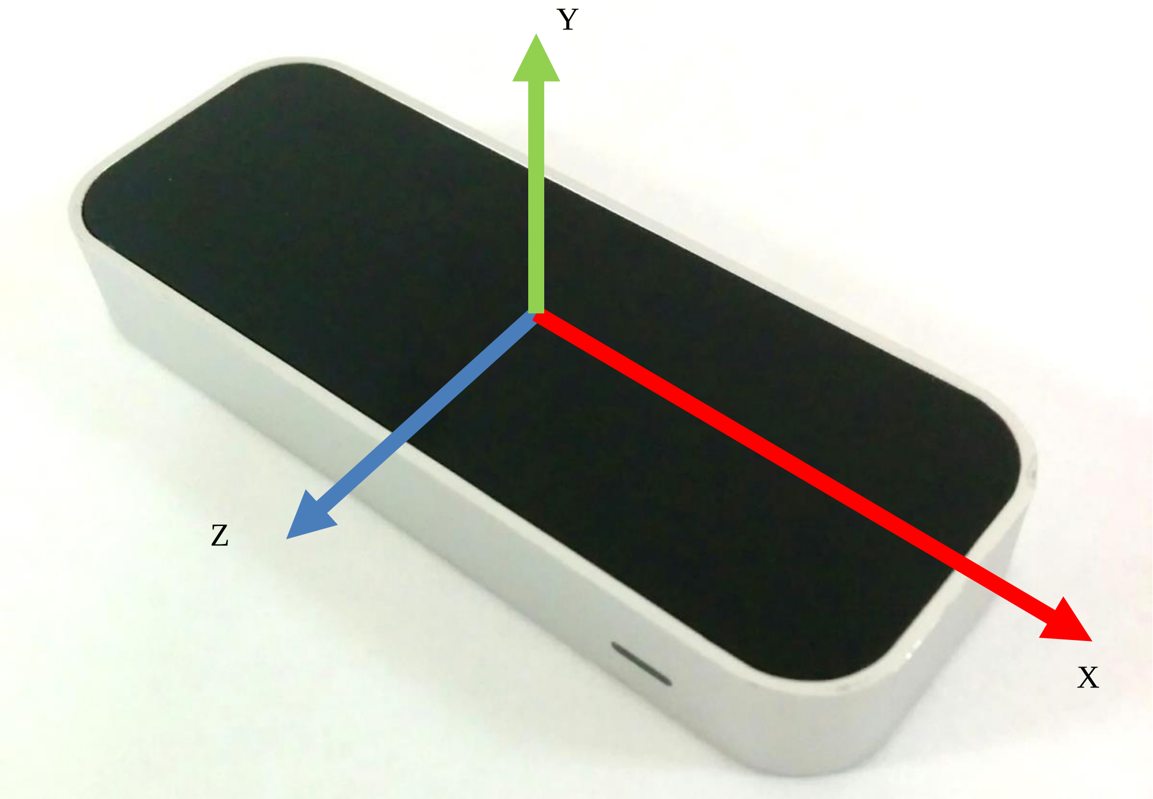

Figure 10: The LM controller with the 3D axis labeled.

The LM controller uses three infrared sensors and two infrared cameras to detect the position and orientation of the users hands when held over the controller [45][46][47]. It detects the individual finger positions and has a fingertip positional accuracy of 0.01 mm [48]. The operational field of view (FOV) for the controller is 25 mm to 600 mm above the controller with a range of 150° [45][46][47]. The LM controller may be connected to a computer or a mobile device using a USB cable. To run the controller using a smartphone, a special SDK package was installed onto the smartphone. This SDK package allows the LM to communicate with the AR application. The controller does not work on all smartphones available as it does require the smartphone to have enough power to run the application and the controller simultaneously. There is no other external power supply that can be used to run the controller and because of this, only smartphones that have an 800+ snapdragon processor will be able to successfully run the LM and all the associated applications. The LG Nexus 5 selected in the previous study has a snapdragon 800 processor, so it met the hardware requirements for the LM controller.

المنارة للاستشارات
www.manaraa.com

3.2 Methods

The AR environment for this study was developed using Unity3d (version 5.2.2). AR provides a more enhanced environment as the users have the ability to use the context of the real world when interacting with the virtual objects [22]. Image tracking for the virtual objects was done with Vuforia (version 5.06). This was utilized since the tracking on one image worked well from the previous study. All the spheres and shapes used in both parts of this study were loaded into the Unity3d program so that their locations and orientations were associated with the base image. The system was deployed on the LG Nexus 5 with the LM directly connected to the phone (Fig. 11).

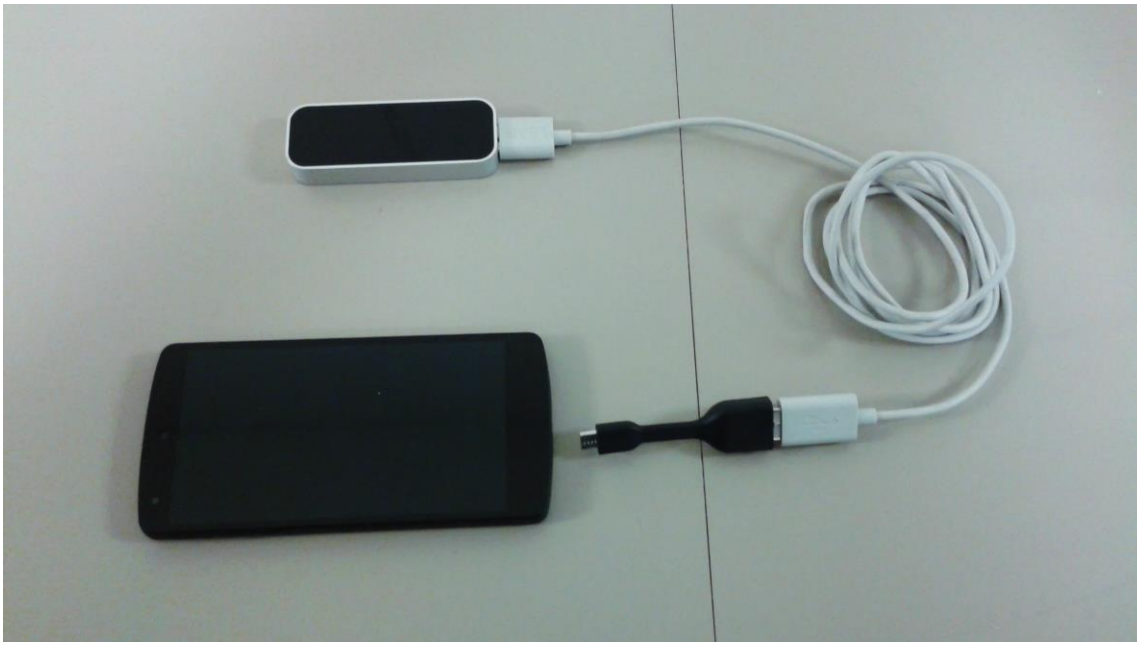

Figure 21: The setup of the smartphone with the LM controller. The LM uses a USB connector, so a USB to micro USB converter was needed to connect the LM directly to the Nexus 5.

This study consisted of two parts: the first part participants were instructed to place the tip of a virtual index finger within a sphere, and the second part participants were instructed to trace the outside edge of different shapes with the tip of the virtual index finger. All seven participants completed the study in the same order: first they completed the sphere pointing tasks, then completed the shape tracing tasks. The study was

المنارة للاستشارات
www.manaraa.com

conducted in this order so that all participants could learn how to use the system by completing relatively simple tasks, then move on to complete the more difficult tasks. The gender and handedness of the seven participants were recorded. Three participants were female and four were male, while two were left handed, one female and one male. The same spheres and shapes were used for all participants in the same order to ensure equality of task difficulty. The unit of measure that Unity3d uses for the virtual environment is a Unity unit (uu). For both parts of this study, 1 unity unit is equal to 216 mm.

3.2.1 Sphere Targeting Tasks

The first part of the study was used to determine how well participants could target simple spheres using the LM. A total of 15 sphere targeting tasks were designed with the spheres appearing in the same random locations for all participants (Fig. 12). The sphere size was the same for all tasks and only one sphere was visible to the participant for each task.

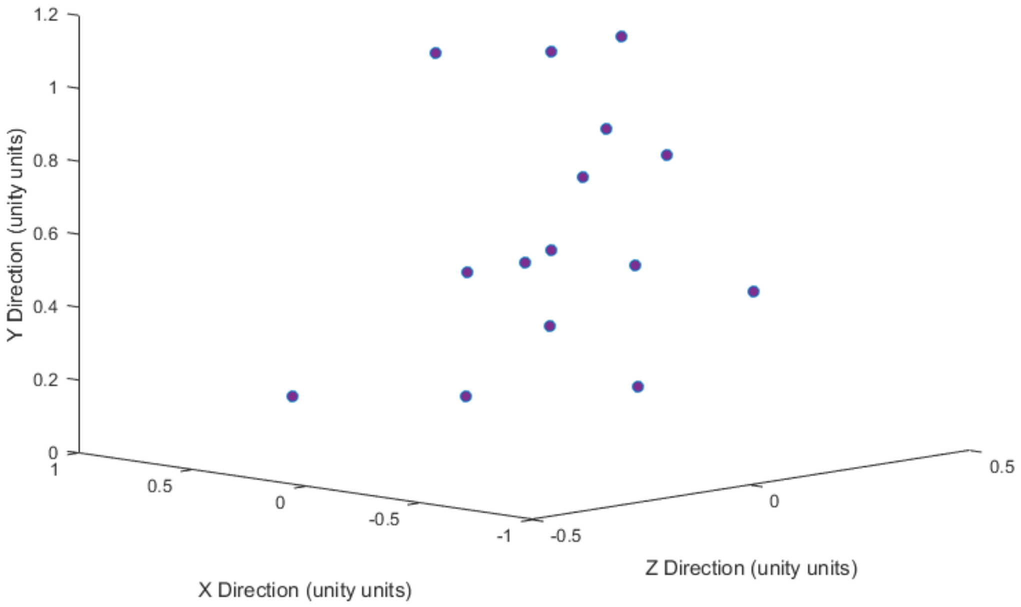

Figure 32: Location of all spheres within the AR environment.

المنارة للاستشارات

www.manaraa.com

The sphere positions were selected so that they would test the range of the LM. Figure 13 shows the base image that was selected, the virtual scene that was created in Unity3d with one of the spheres shown, as well as how that scene was presented to the participants when the application was running on the smartphone.

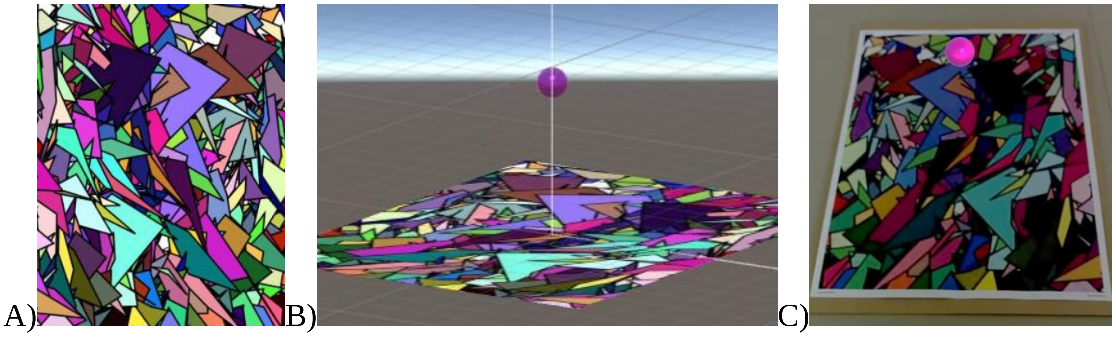

Figure 43: The base image for all spheres. A) The image that was selected. B) The image in a Unity scene with a sphere. C) The view of the same scene when run on the smartphone.

The participants interacted with the virtual objects by using virtual hands (Fig. 14). The application used the positional and rotational information from the LM to calculate where the virtual hands should be within the AR environment shown to the participants. These virtual hands therefore mimic the movements of the participant’s real hands.

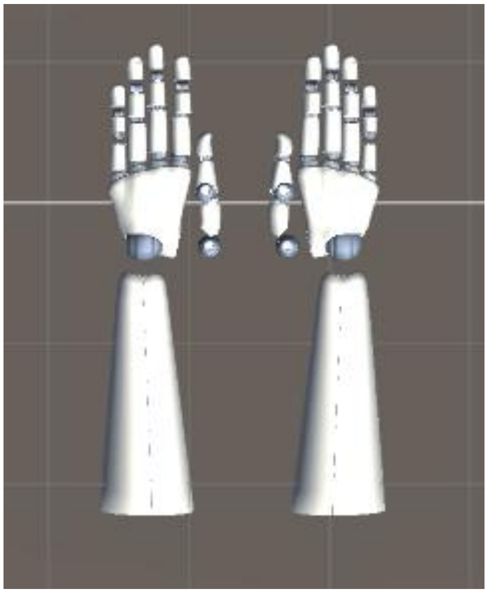

www.manaraa.com

Figure 54: The virtual robotic hands used in the application. The virtual hands mimic the movements of the users' hands when held above the LM.

The image tracking required the camera to have an unobstructed view of the image for continuous tracking. If the participants used their hands to interact with the virtual spheres, image occlusion is possible and therefore cause tracking loss, so the virtual hands provided the users with a means of interacting virtually, while always maintaining continuous image tracking. The base image was printed and placed on a flat surface. The participants were seated and could choose which hand they would use with the LM controller. All the participants chose to use their dominate hand, and the LM was placed such that the participant's hand could be easily held above the controller (Fig. 15).

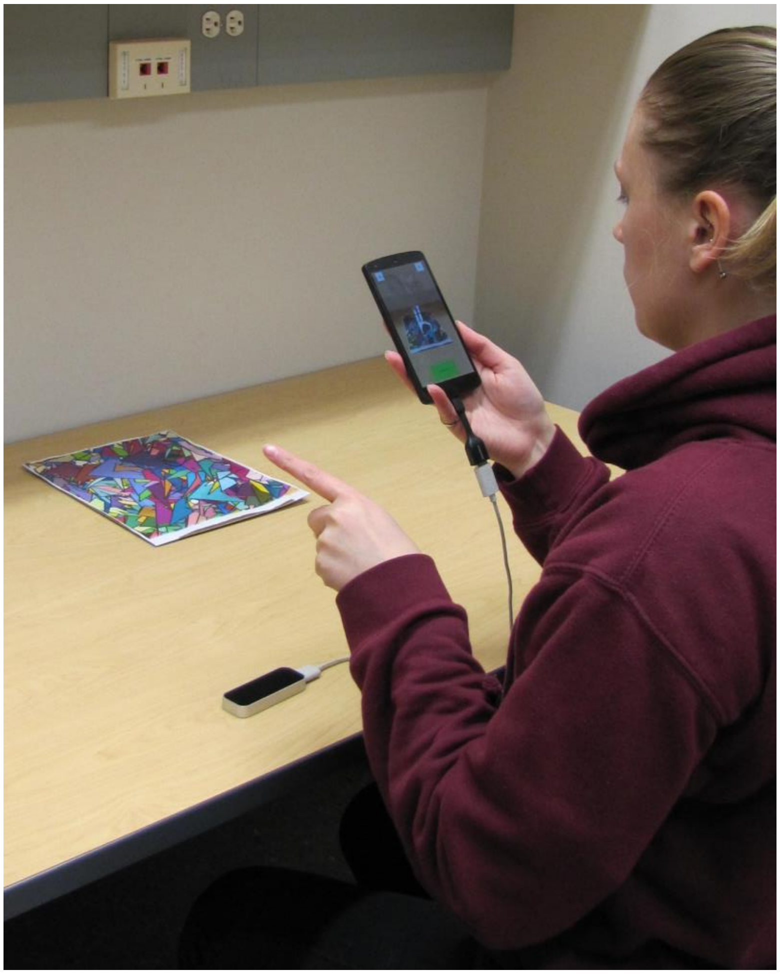

Figure 65: The setup for the sphere targeting tasks with a participant.

www.manaraa.com

The participants were instructed to move about the space to determine the exact location of the sphere, then to place the tip of the virtual index finger within the center of this sphere. They were informed that they were being timed but should complete the tasks as accurately as possible. When the participant felt they had placed the index finger correctly, they pressed the button at the bottom of the screen and then move onto the next task by pressing the button in the top right-hand corner of the screen (Fig. 16). The screen interface was designed so that the participants could easily interact with all of the buttons while holding the smartphone.

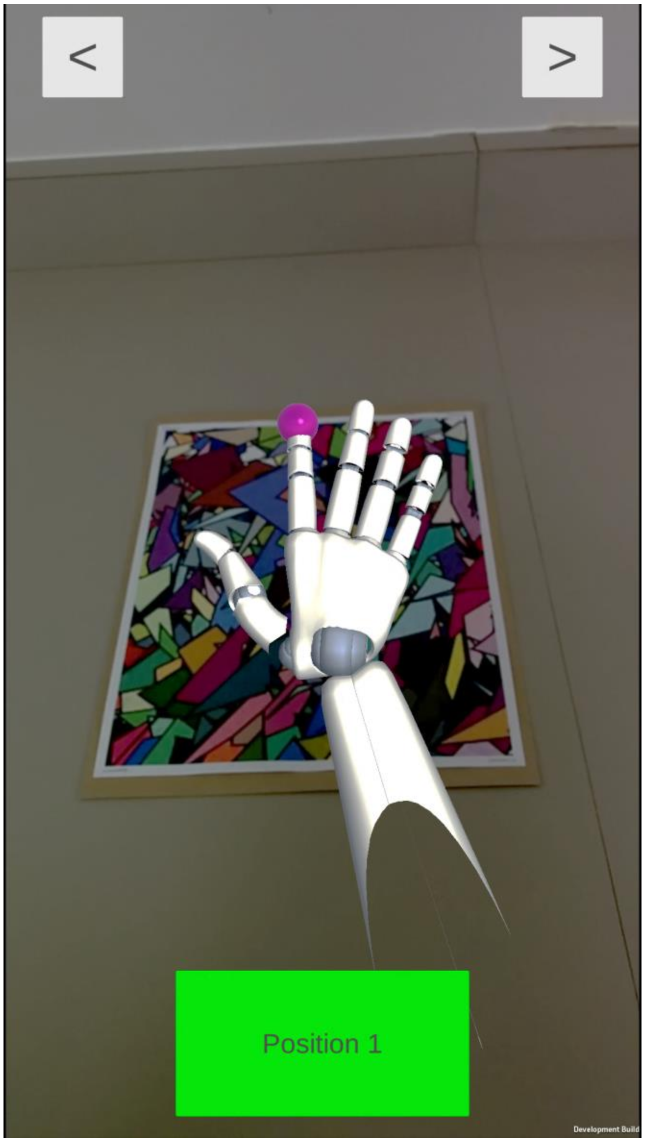

المنارة للاستشارات
www.manaraa.com

Figure 76: The screen view of the application as seen by the participants. The arrows at the top of the screen as for switching between spheres and the green button at the bottom of the screen records the position of the virtual index finger when pressed.

The application was designed so that it recorded the position of the tip of the virtual index finger for the duration of the task, and the time it took each participant to complete the task. The timer started when the new sphere became visible and finished when the user clicked the position button. The software to do this was written using C# and was directly integrated with Unity3d.

3.2.2 Shape Tracing Tasks

The second part of this study was used to determine how well participants could trace the outside edge of virtual shapes. To do this, three different shapes: squares, triangles and circles, were used. Each shape was employed in five tasks for a total of 15 tasks. During the first three tasks, the participants were shown each of the shapes in the center of the screen (Fig. 17).

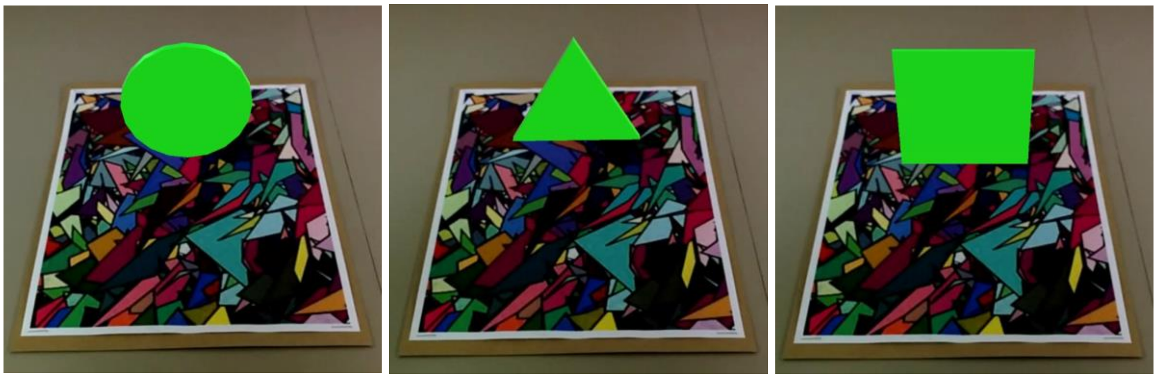

Figure 87: The first three shapes the participants were asked to trace.

For the remaining tasks, the order, size, position and orientation of the shapes were changed within the AR environment (Fig. 18). This was done to increase the difficulty from the initial three tasks.

المنارة للاستشارات

www.manaraa.com

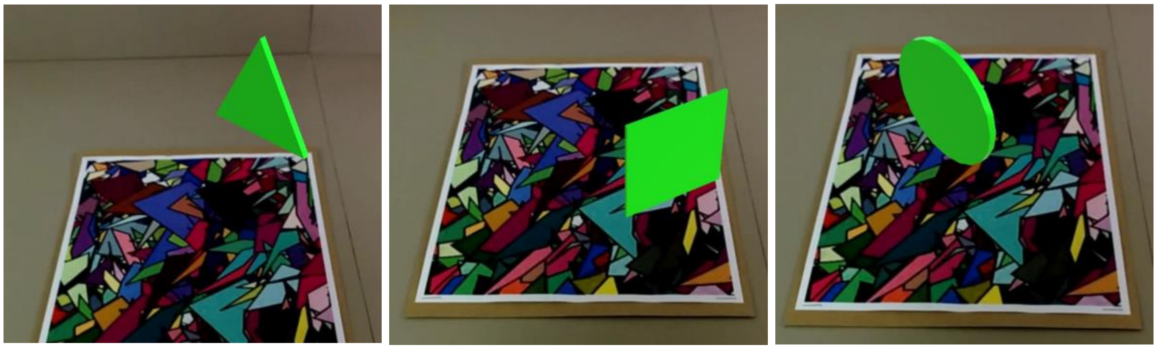

Figure 98: Examples of the change in orientation, position and size for the three different shapes that were presented to the participants.

The base image used for the sphere targeting tasks was used for these tasks. All the shapes were associated with the base image in Unity3d (Fig. 19).

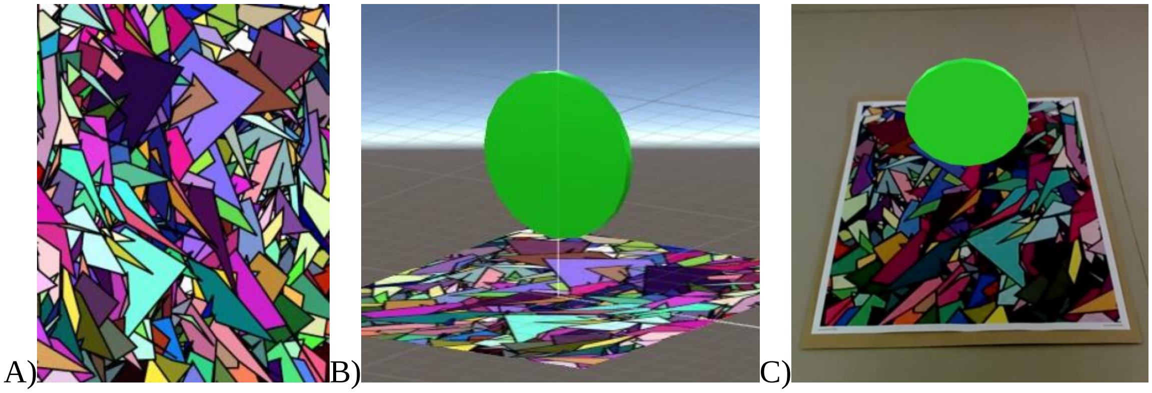

Figure 109: The base image for all shapes. A) The image selected. B) The image and a circle from a Unity scene. C) The same scene when run through the application on the smartphone.

The LM setup was arranged the same, with the participants using a virtual hand to interact with the virtual shapes. The same experimental design was used, with the base image being placed in front of the seated participants and the LM placed on the same side as the hand the participant selected. All of the participants again chose to use their dominate hand and were instructed to explore the AR environment. Participants were instructed to press the button at the bottom of the screen when they were ready to start tracing the shape (Fig. 20). The participants could begin tracing the shape from any point and were instructed to keep

المنارة للاستشارات
www.manaraa.com

the tip of the virtual hands as close to the outside edge of the shape as possible, while still touching the shape. Once they had completed tracing, the participant pressed the button at the bottom again before moving on to the next shape by pressing the buttons at the top of the screen. They were again informed that they were being timed while completing the tasks but they should complete the tasks as accurately as possible.

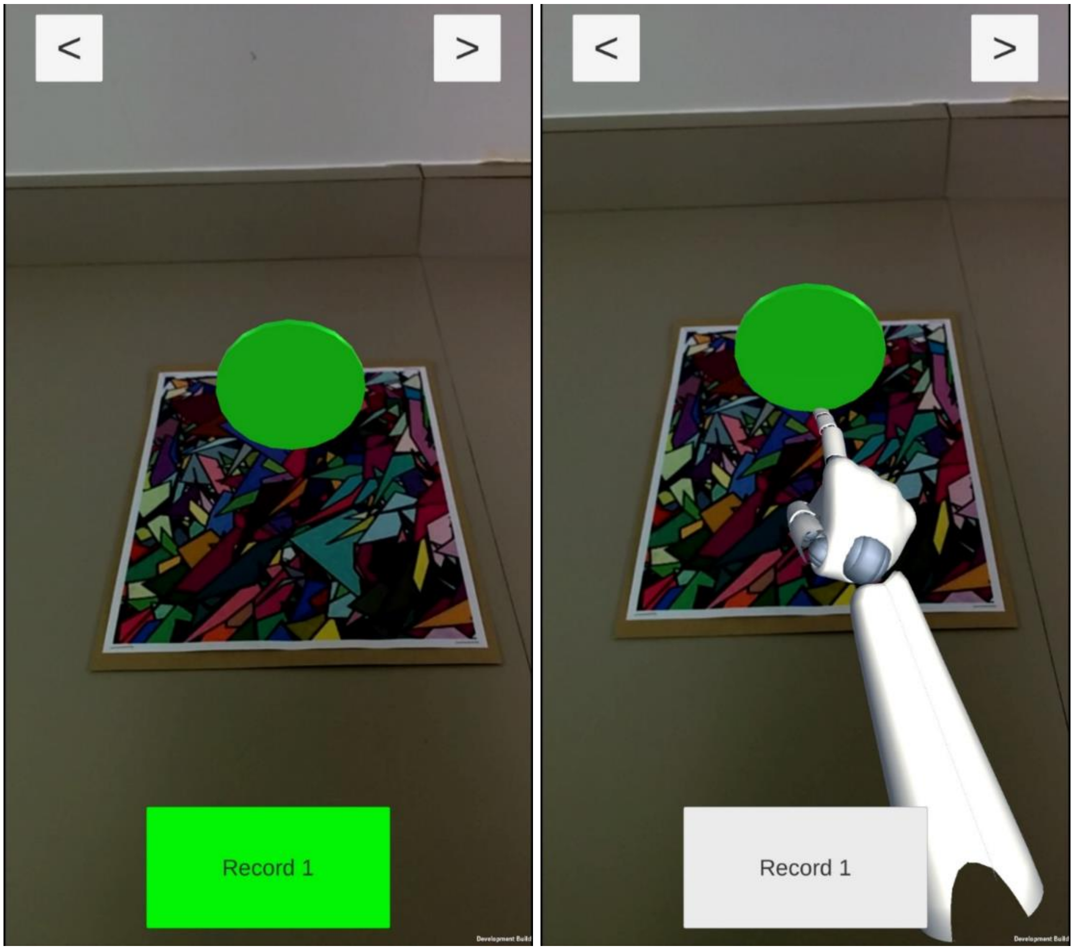

Figure 20: The view of the first tracing task to the user. When the participant was ready to start tracing, they pressed it and began tracing. The colour of the button changed to indicate the position information of the index finger was being recorded. The arrows at the top of the screen allowed the user to move between shapes.

The data for the position of the tip of the virtual index finger, the state of the record button and the time were recorded. The timer started when the shape became visible to the participant and stopped when the bottom button was pressed after the participant had

المنارة للاستشارات
www.manaraa.com

finished tracing. The fingertip position was recorded during the entire length of the task. The software to do this was written in C# and integrated with Unity3d.

3.3 Results

The results were analyzed from both parts separately using a Fitts' Law approach.

3.3.1 Sphere Targeting

The position of the index finger was recorded for the duration of the task, so that the exact approach the user took to place their fingertip could be observed (Fig. 21).

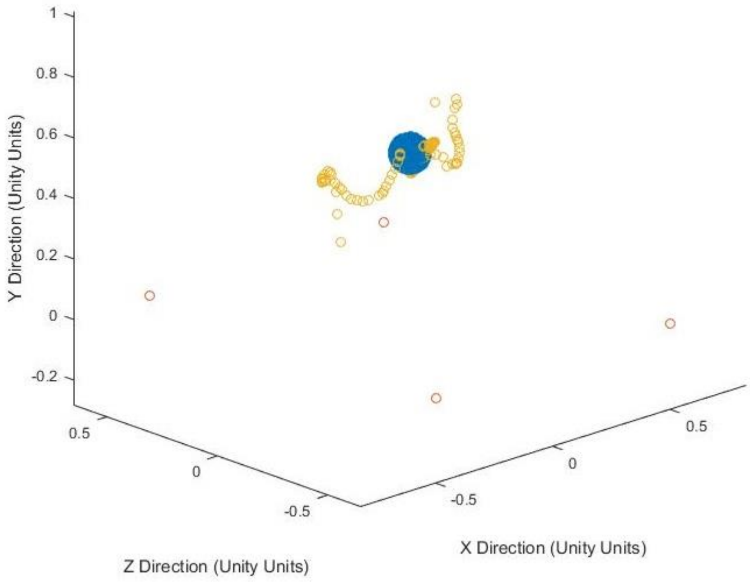

Figure 211: The information recorded from Unity. The path of the index finger is shown in yellow with the outside edge of the sphere shown in blue. The corners of the base image are shown in red.

The radius of each sphere was 0.0516 uu. The participant was considered to be accurate if they placed their fingertip inside the sphere. All distance calculations were performed using the center location of each sphere and the user selected position of the fingertip. This distance calculation is considered to be the participants' error in completing the tasks. The

المنارة للاستشارات
www.manaraa.com

error was first calculated in all three directions. The participants' accuracy was calculated using:

$$\text{Accuracy} = \log_2(1 + \frac{1}{error}) \tag{5}$$

The speed of each completed task was calculated using:

$$Speed = \frac{1}{time} \tag{6}$$

With time as the individual task completion time. The average task completion speed was 0.0647 Hz (SD 0.0493 Hz) and the average task accuracy was 4.0159 bits (SD 1.2860 bits) of all participants (Fig. 22).

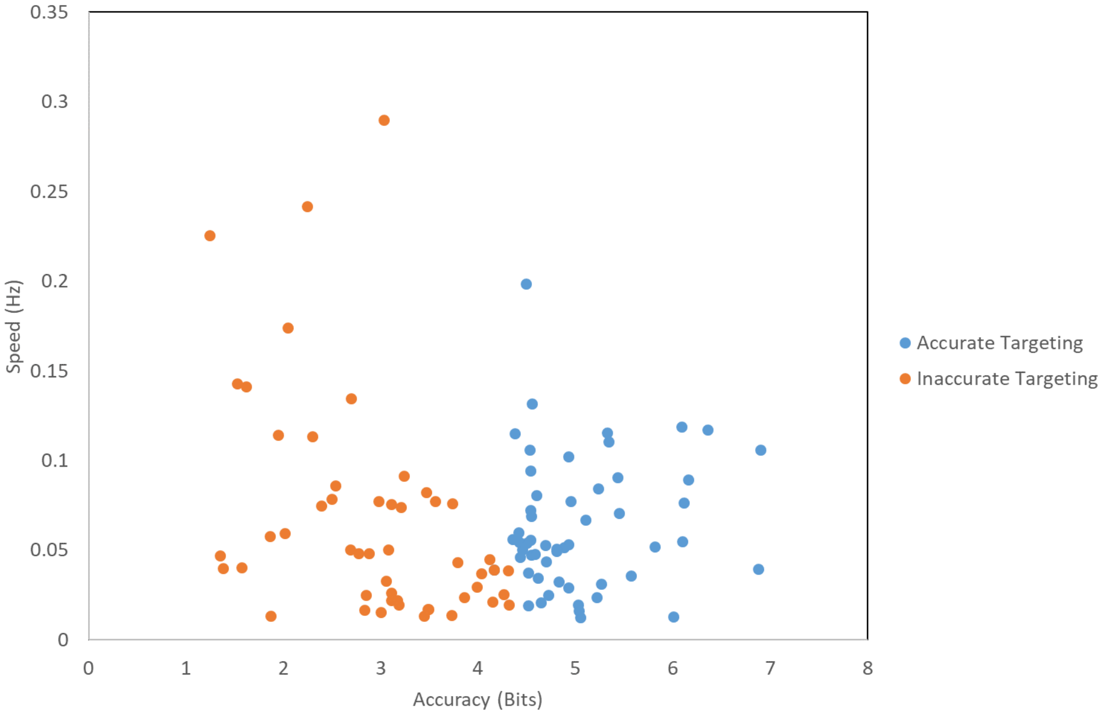

Figure 22: The speed and accuracy of sphere targeting for all participants. Correct fingertip positions are shown in blue.

For the 105 fingertip positions selected by the participants, only 54 were accurate. The average task completion time for all participants was 25.1831 s (SD 18.5018 s). The task completion times by user are shown in figure 23.

المنارة للاستشارات
www.manaraa.com

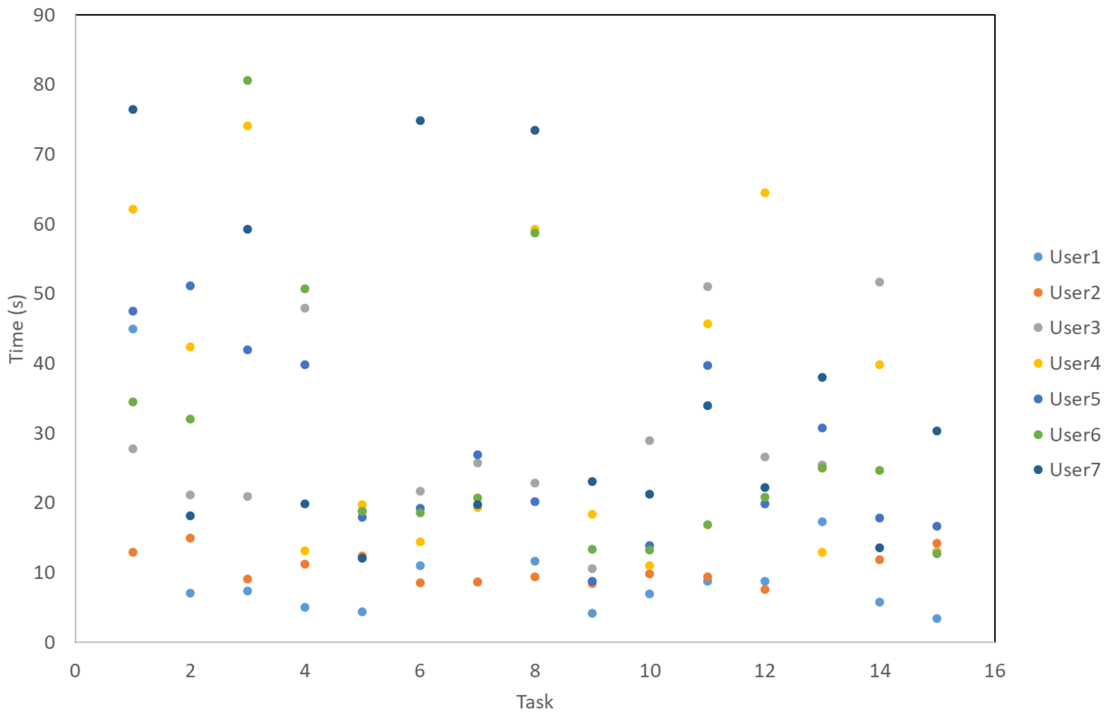

Figure 23: The task completion times by user.

As these targeting tasks require spatial reasoning, the error between the sphere center and the fingertip was calculated in each individual direction to determine if some sphere locations were more difficult for participants. Equation (5) and (6) were once again used to calculate the accuracy in each direction and the task completion speed. Of the three directions, the most accurate was the x direction, the width direction, with an average accuracy of 5.9122 bits (SD 1.6016 bits) (Fig. 24). The second most accurate was the y direction, the height direction, with an average accuracy of 5.8156 bits (SD 2.1596 bits) (Fig. 25). The z direction, the depth direction, was the least accurate with an average accuracy of 4.747 bits (SD 1.8004 bits) (Fig. 26).

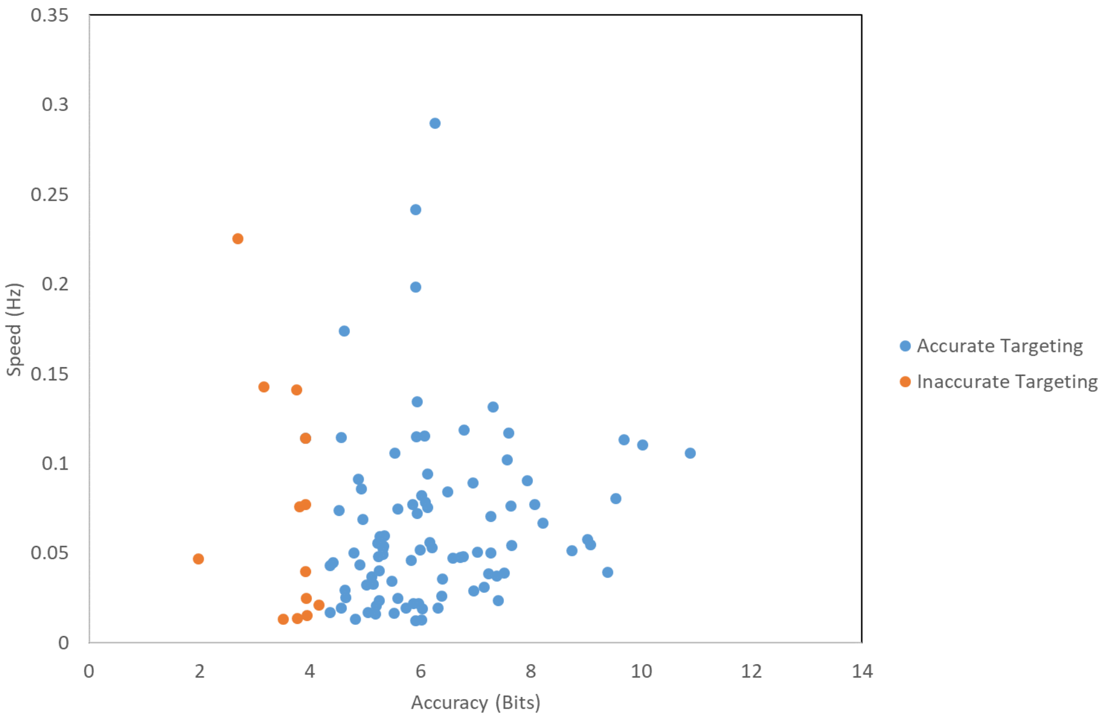

Figure 24: The speed and accuracy in the x direction (width direction) for all participants.

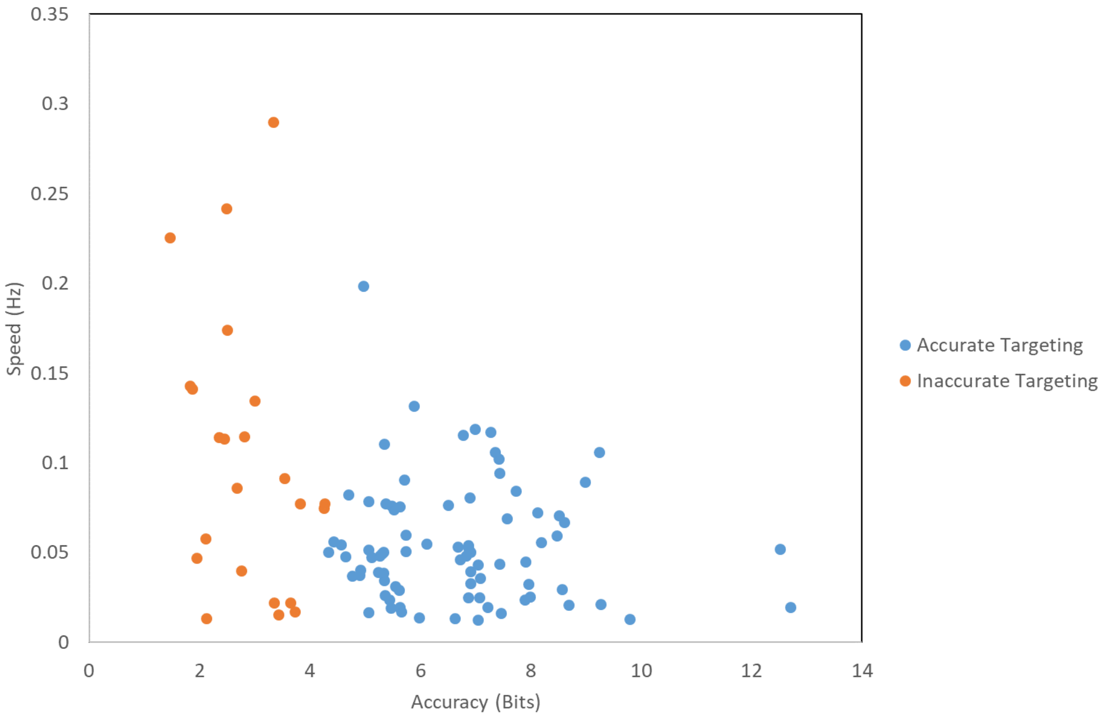

www.manaraa.com

Figure 25: The speed and accuracy in the y direction (height direction) for all participants.

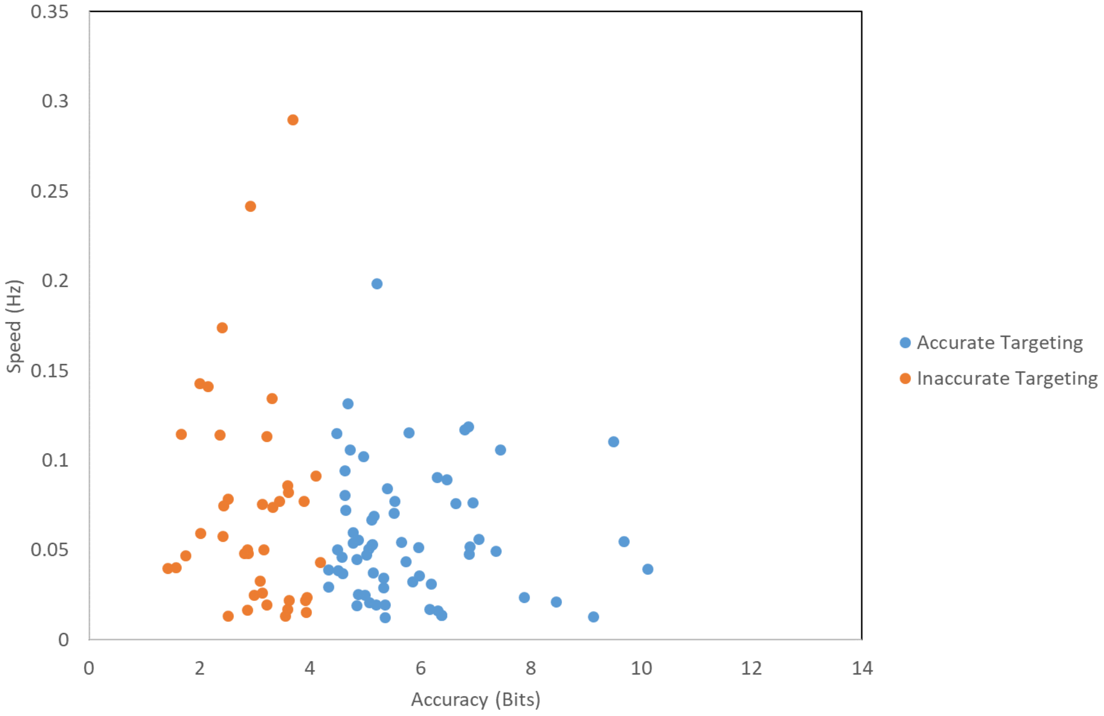

Figure 26: The speed and accuracy in the z direction (depth direction) for all participants.

Table 1 shows the average time, average distance error in three directions, and the average distance error in each of three directions for each user. The averages were computed using participant data from all 15 tasks.

Table 2: Average time, average combined distance and average distance in each direction for all users based on all target tasks.

User	Average Time (s)	Avg Distance (unity units)	Avg X Distance (unity units)	Avg Y Distance (unity units)	Avg Z Distance (unity units)
1	12.5905	0.280038	0.044904	0.215482	0.168116
2	12.95473	0.026035	0.006718	0.008905	0.020648

المنارة للاستشارات
www.manaraa.com

3	31.6582	0.041199	0.015622	0.017227	0.029653
4	40.06133	0.098245	0.038541	0.057432	0.056077
5	31.75773	0.077861	0.027337	0.024154	0.058247
6	31.45233	0.184395	0.021842	0.030927	0.177719
7	38.3646	0.135926	0.056961	0.040854	0.105796

3.3.2 Shape Tracing

The results from this study were analyzed by the task shape type. The fingertip path was separated into two components: the first was before the participant pressed the “Record Position” button, and the second was after the initial button press. This first section was recorded to observe what the participants did in preparation for tracing. Overall, this initial position data showed the users identifying the hand orientation needed to make tracing the shape easier and then moving their hand to the starting position. Figure 27 shows this separated fingertip positional data for the first three tasks for one participant with the outside edge of the shape.

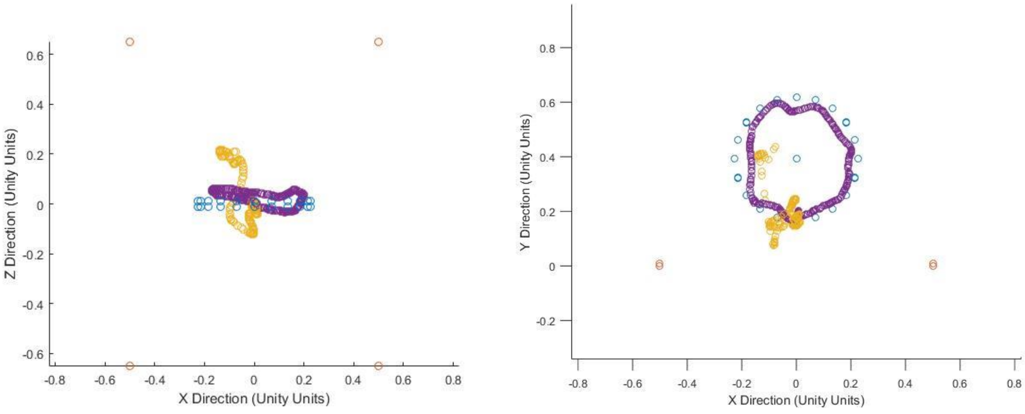

www.manaraa.com

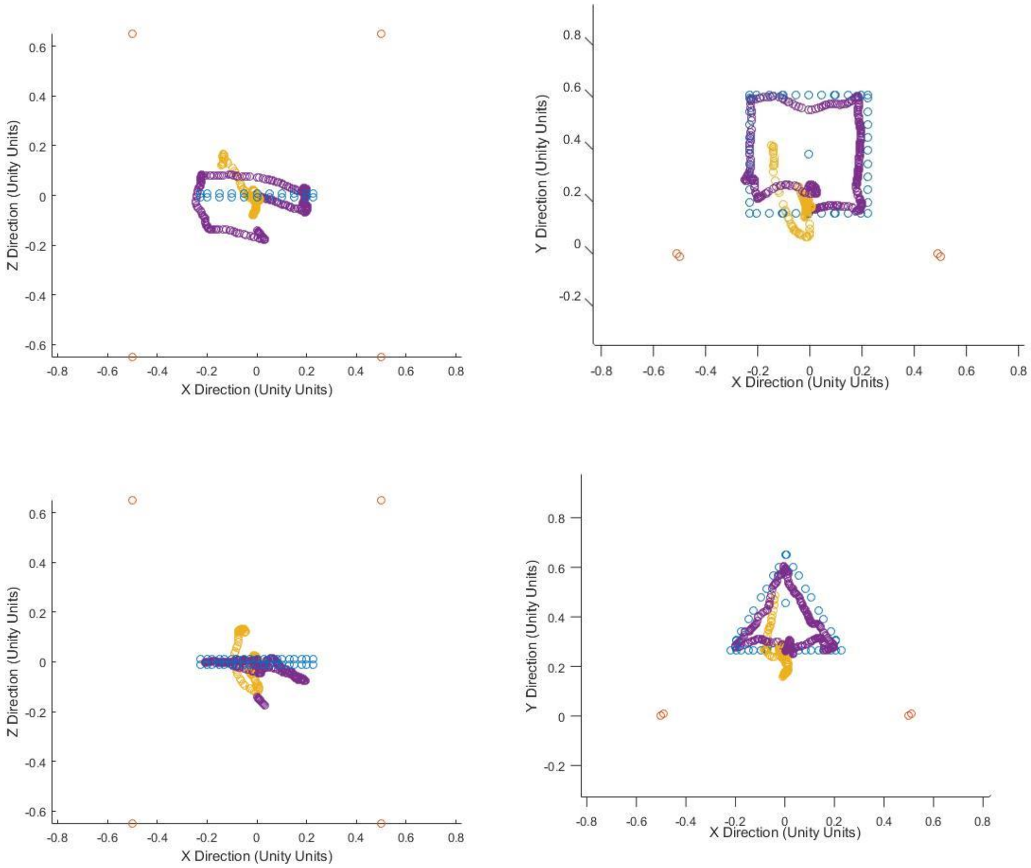

Figure 27: The fingertip path split into before the record button had been pressed, in yellow, and after the record button had been pressed, in purple. The outside edge of the shape was shown in blue with the corners of the base image shown in red.

3.3.2.1 Circle Tracing

The tracing of the circles was analyzed by calculating the distance from the center of the circle to the position of the index finger. Figure 28 shows the typical path of a user when tracing and this considered this a “good” trace.

www.manaraa.com

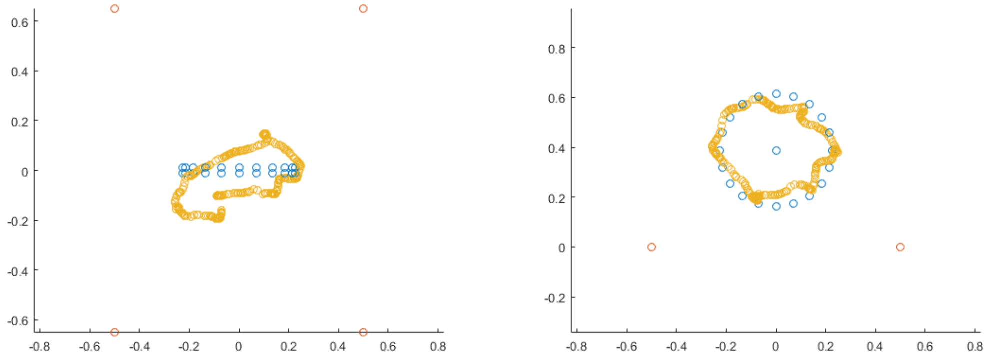

Figure 28: The fingertip path after the record button has been pressed for a "good" trace.

Not all users were successful in tracing the outside edge as seen in figure 29 which was considered a "poor" trace.

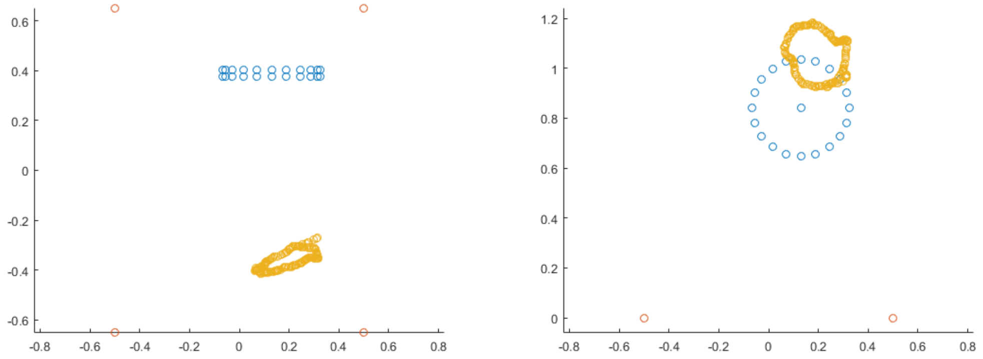

Figure 29: The fingertip path after the record button has been pressed for a "poor" trace.

The ideal path for the user to have traced would have been the outside edge of the circle. Figure 30 shows the distance from the center for both the "good" and "poor" trace with the outside edge distance shown.

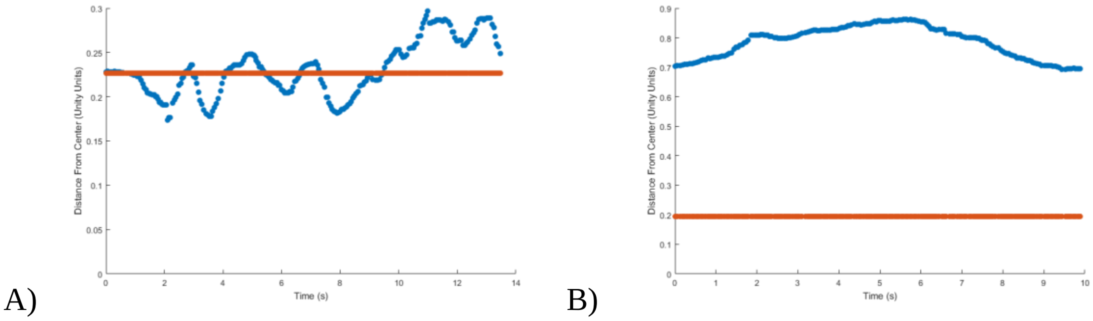

Figure 30: The distance from the center over time. A) The "good" trace in blue, the calculated edge of the circle in red. B) The "poor" trace in blue, the calculated edge of the circle in red.

A modified equation (3), which describes a user's path through a tunnel, was used to calculate each participant's performance for each circle. The Fitts' Law equation for a tunnel was used:

$$t = \frac{1}{IP} * \frac{A}{\sigma} \tag{7}$$

Where t is time, IP is the index of performance, A is the circumference of the task circle, and σ is the difference in the maximum distance and the minimum distance from the center of the circle. An example of σ for the "good" trace can be seen in Figure 31.

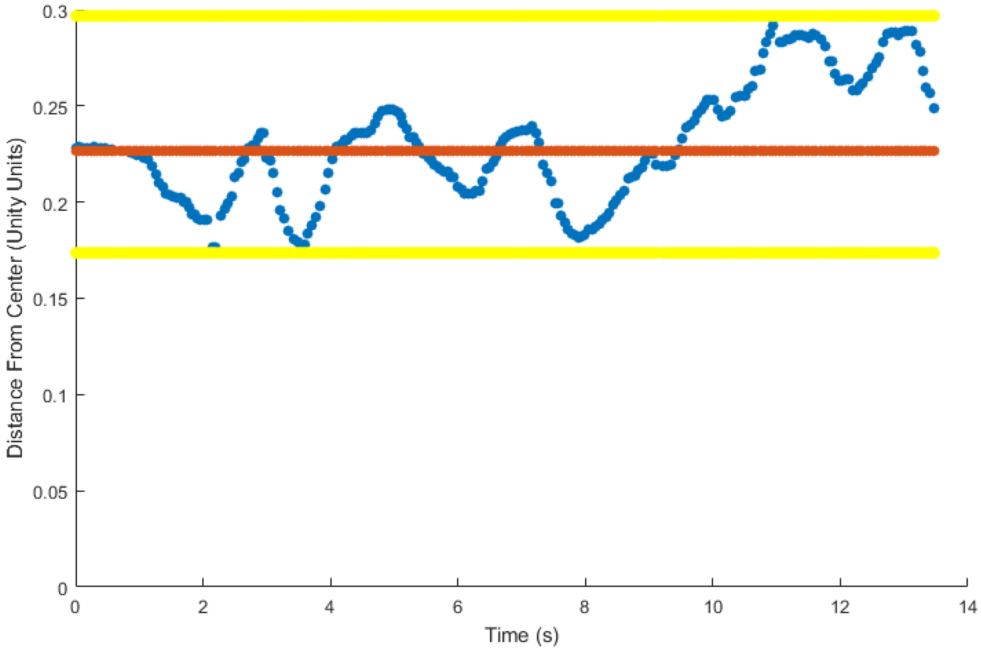

المنارة للاستشارات
www.manaraa.com

Figure 31: The maximum distance for this "good" trace was the top yellow line and the minimum distance was the bottom yellow line.

Some users showed a clear bias in their tracing of the circles. For these participants, the σ was calculated in the same manner, however the difference between the edge of the circle and the minimum value was used as the bias (Fig. 32).

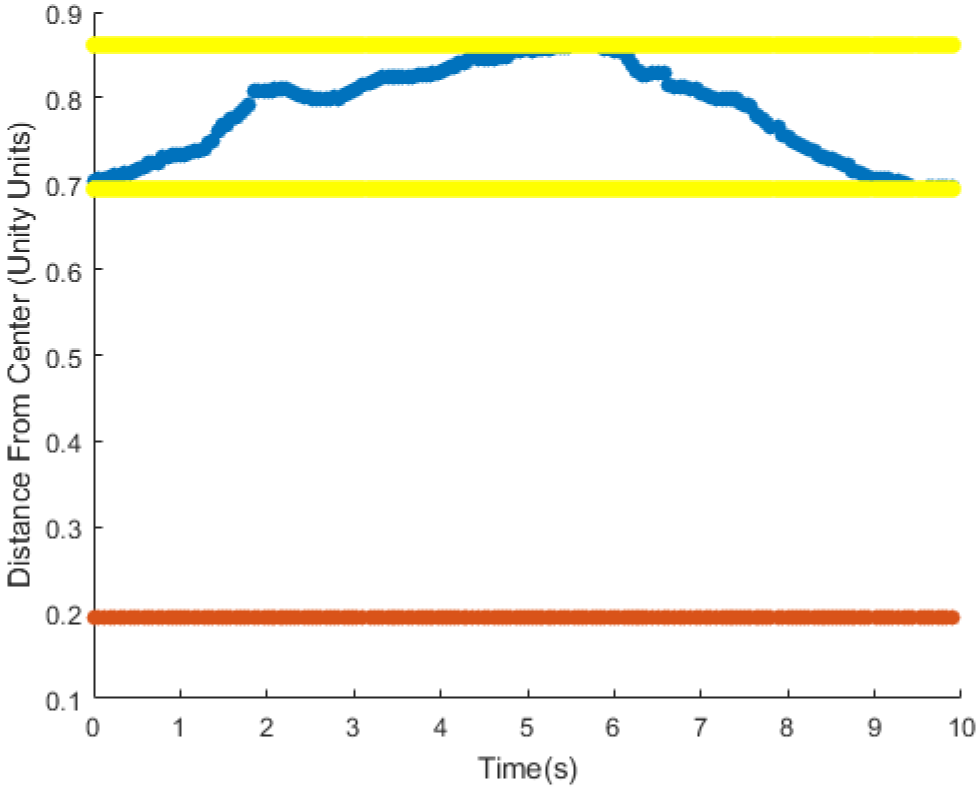

Figure 32: The maximum distance for this "poor" trace was the top yellow line and the minimum distance was the bottom yellow line. The bias was the difference between the minimum and the edge of the circle, as shown in red.

The error for all participants was calculated as:

$$error = \frac{A}{\sigma} + bias \tag{8}$$

If the participant did not show a bias, then the bias was equal to zero. The results for each participant can be seen in Table 2.

www.manaraa.com

Table 3: Average time, average combined distance and average distance in each direction for all users based on all target tasks.

User	Circle 1		Circle 2		Circle 3		Circle 4		Circle 5	
	σ	Bias	σ	Bias	σ	Bias	σ	Bias	σ	Bias
1	0.1176	0	0.2077	0	0.3244	0	0.1271	0.1737	0.1682	0.4995
2	0.0537	0	0.0593	0	0.1209	0	0.0377	0.0040 (<)	0.2450	0
3	0.1227	0	0.1316	0	0.0725	0	0.0837	0	0.0702	0
4	0.2074	0	0.0947	0	0.0794	0	0.0809	0	-	-
5	0.2013	0	0.3437	0.0991	0.4392	0	0.3194	0	0.2425	0
6	0.0892	0	0.1179	0	0.0618	0	0.1781	0.2491	0.5111	0.0659
7	0.2018	0	0.2634	0.1715	0.1164	0	0.0834	0.2591	0.0605	0

The accuracy for each task was calculated using equation (5) and the error calculated from equation (8). The speed was calculated using equation (6). The speed and accuracy results for all participants can be seen in Figure 33. The average speed was 0.1234 Hz (SD 0.0864 Hz) and the average accuracy was 0.1811 bits (SD 0.1141 bits).

المنارة للاستشارات

www.manaraa.com

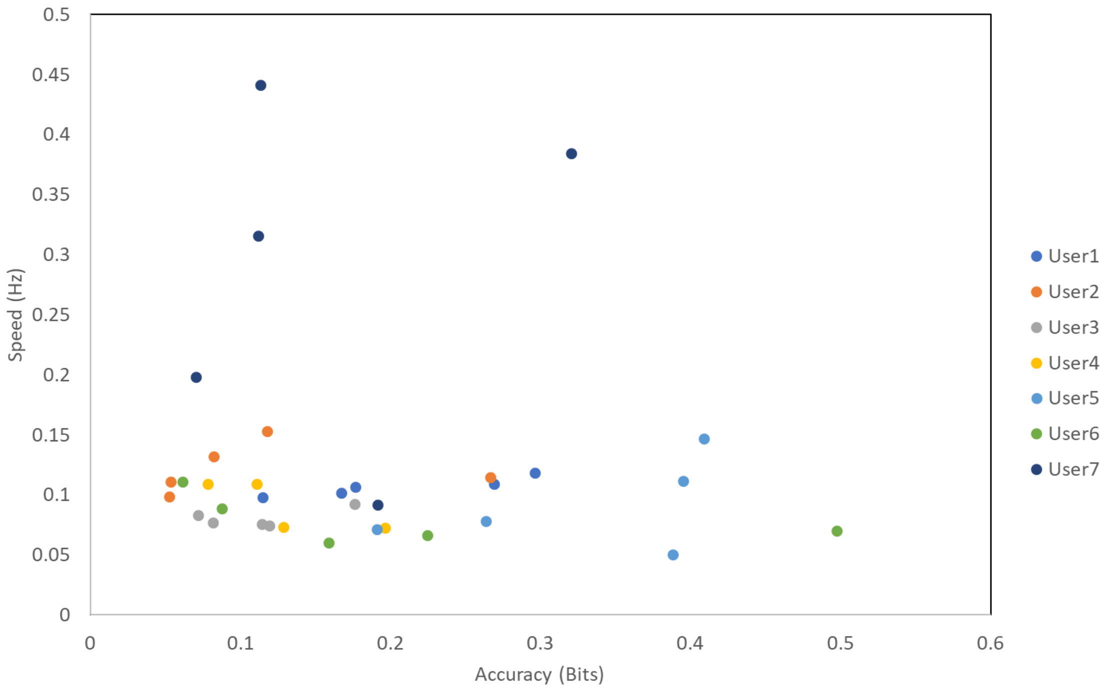

Figure 33: The speed and accuracy of circle tracing for all participants.

The average circle tracing time was 10.6751 s. The circle tracing times by participant can be seen in Figure 34.

المنارة للاستشارات

www.manaraa.com

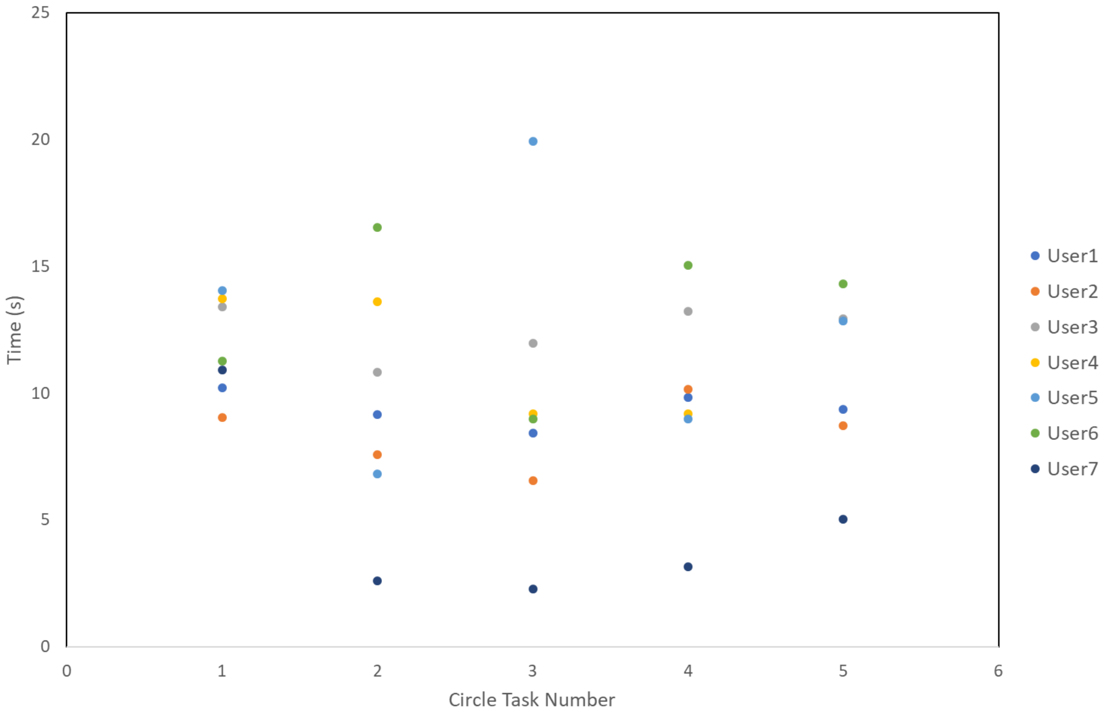

Figure 34: The circle tracing times for all participants.

3.3.2.2 Square Tracing

The tracing of the squares was analyzed by splitting the path into each individual side and calculating the distance between the fingertip position and the edge of the side. Figure 35 shows the path of a "good" trace.

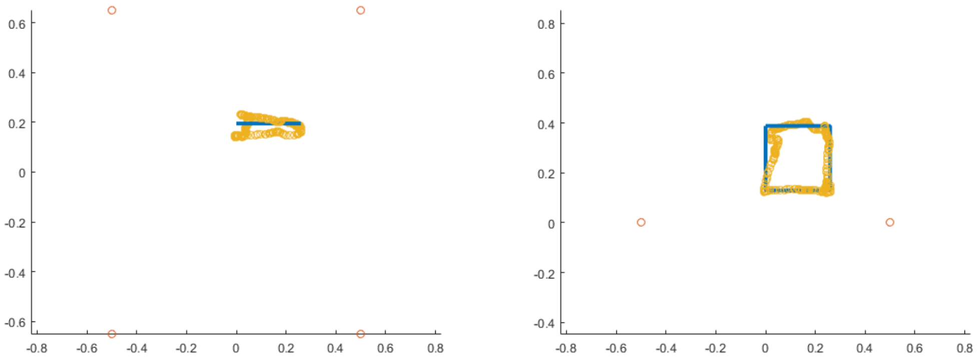

Figure 35: The fingertip path of a "good" trace after the record button has been pressed. The participant's path is shown in yellow, the outside edge of the square is shown in blue and the corners of the base image are shown in red.

المنارة للاستشارات

www.manaraa.com

The participants' path was split into the four sides of the square and the distance was calculated between the fingertip position and that side edge of the square. Figures 36 shows this distance for each side of the square for the "good" trace.

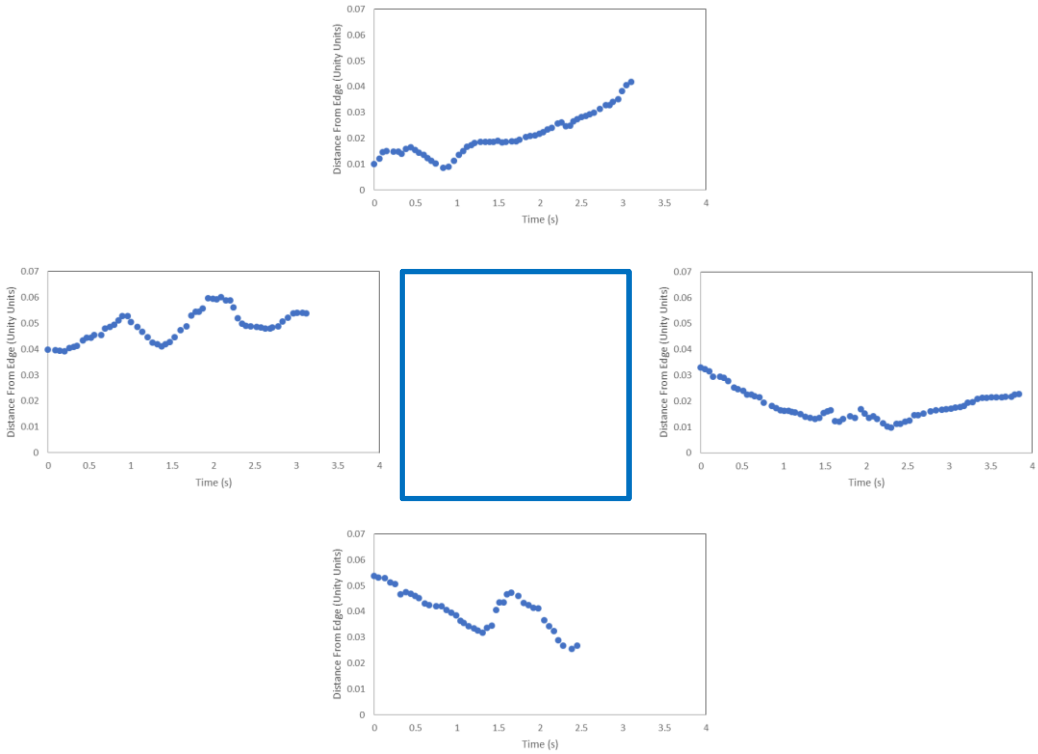

Figure 36: The distances between the fingertip and the outside edge of the square for the "good" trace.

Figure 37 shows the typical path of a "poor" trace.

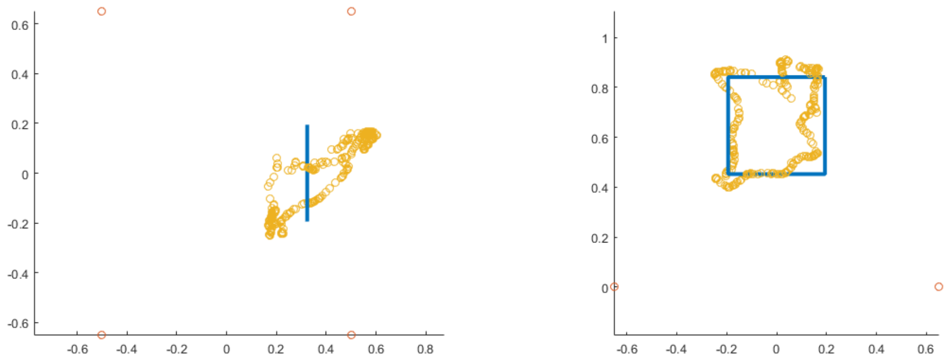

www.manaraa.com

Figure 37: The fingertip path of a "poor" trace after the record button had been pressed. The participant's path is shown in yellow, the outside edge of the square is shown in blue and the corners of the base image are shown in red.

Figures 38 shows the distances between the fingertip position and outside edge of the shape by side for the "poor" trace.

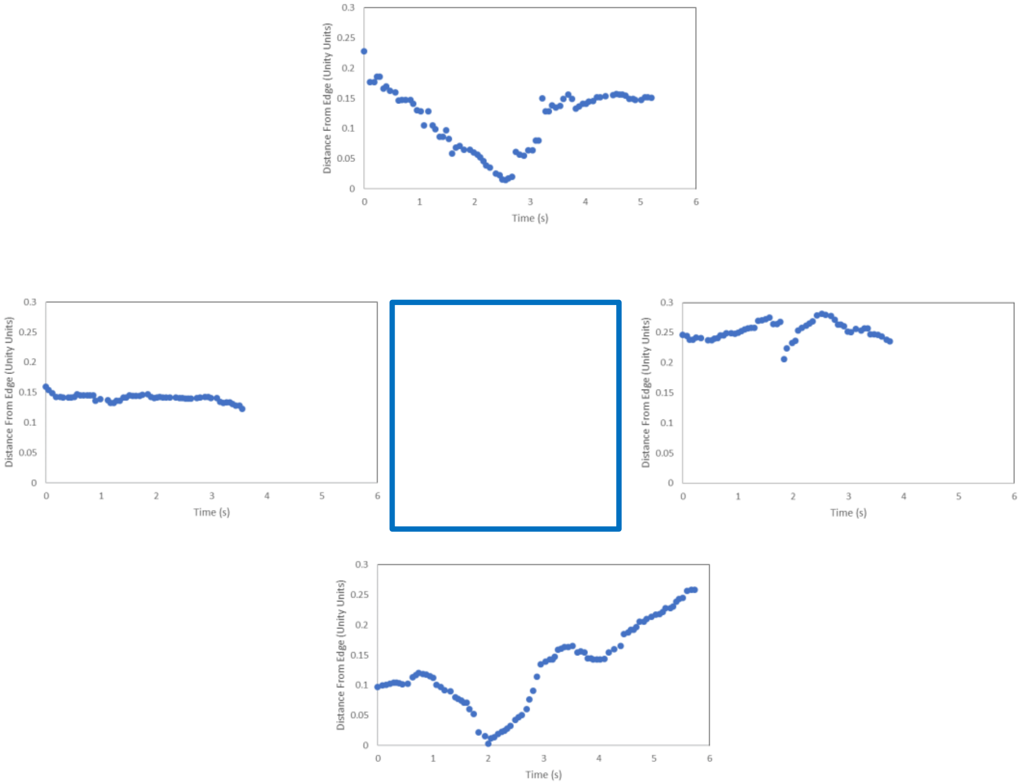

Figure 38: The distances between the fingertip and the outside edge for the square for the "poor" trace.

A modified Fitts' Law equation was used for this analysis. Each point error was calculated as the distance away from the closest point on that side of the square. The average of these distance errors was calculated and was considered the error for that side of the square. Equation (5) was used to calculate the accuracy with the average error used as the error and equation (6) was used to calculate the speed of tracing for that side. The speed and accuracy for all participants can be seen in Figure 39. The average speed was 0.4324 Hz (SD 0.3536 Hz) and the average accuracy was 3.8202 bits (SD 0.9160 bits).

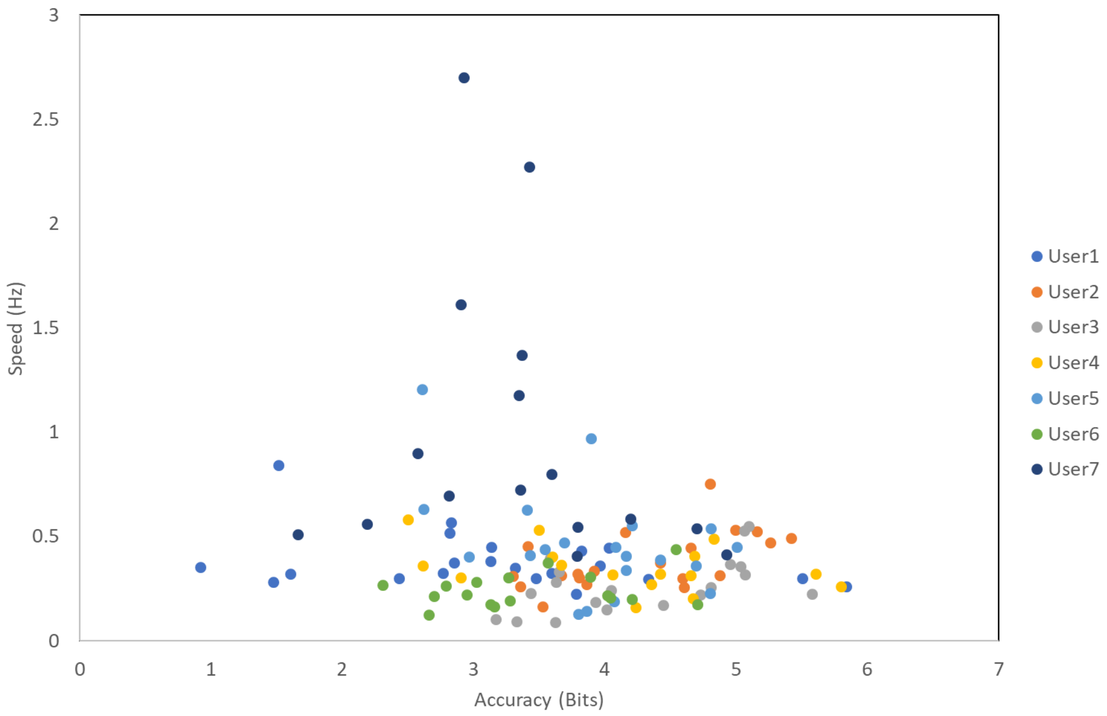

Figure 39: The speed and accuracy of each square traced by side for all participants.

The average time per side was 3.2336 s. The square tracing times by participant can be seen in figure 40.

www.manaraa.com

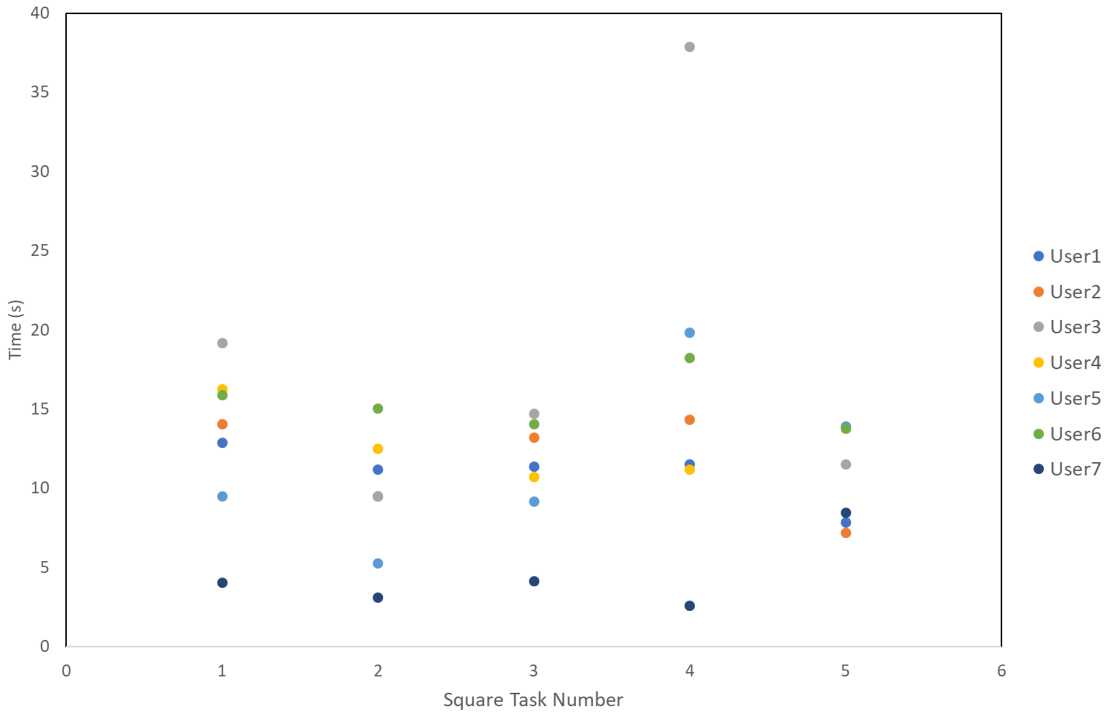

Figure 40: The square tracing times for all participants.

3.3.2.3 Triangle Tracing Results

Similar analysis was completed for the triangle shape tracing. The fingertip path was split into each side of the triangle and the distance was calculated between the fingertip position and the outside edge of the side. Figure 41 shows a typical "good" triangle trace.

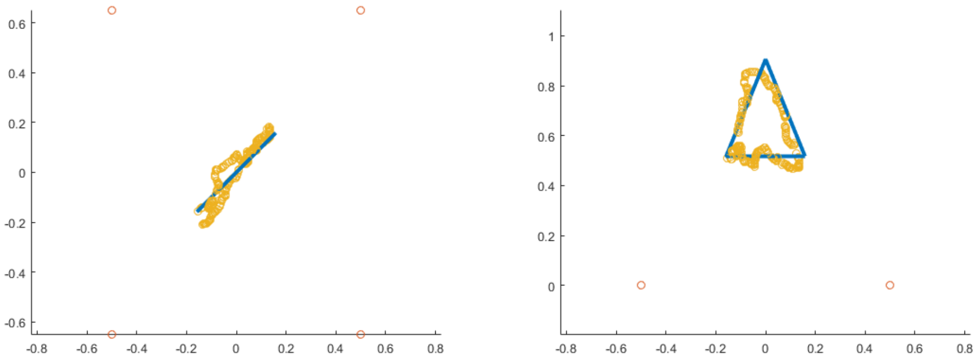

Figure 412: The fingertip path after the record button had been pressed for a "good" trace. The fingertip path is shown in yellow, the outside edge of the triangle is shown in blue and the corners of the base image are shown in red.

www.manaraa.com

Figures 42 shows the distances calculated for each side of the triangle for the “good” trace.

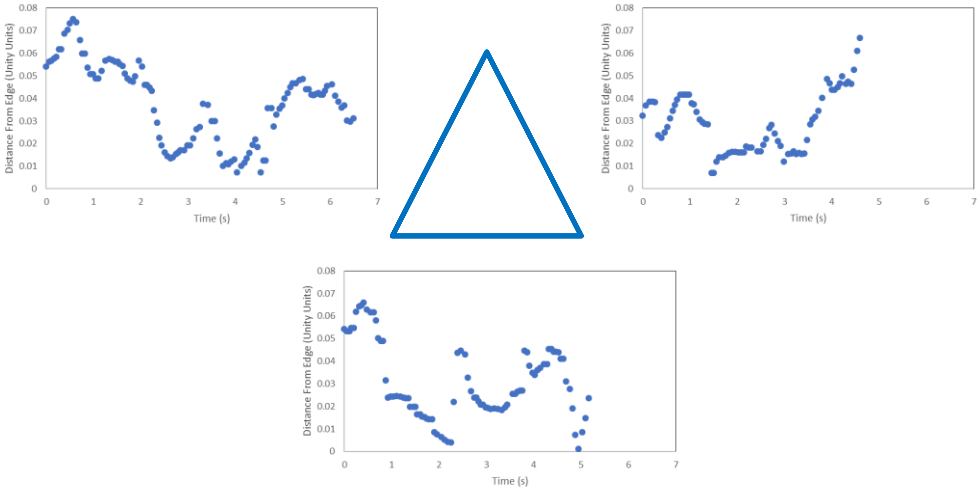

Figure 42: The distance between the fingertip position and the outside edge of side one of the triangle for the “good” trace.

A typical fingertip path for a “poor” triangle trace can be seen in figure 43.

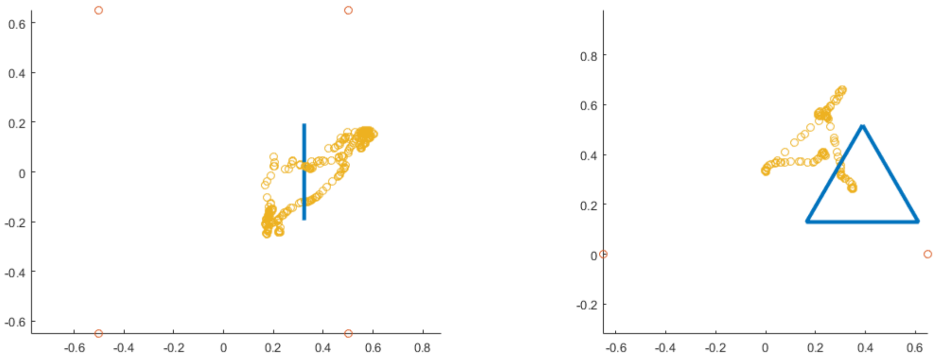

Figure 43: The fingertip path after the record button has been pressed for a “poor” trace. The fingertip path can be seen in yellow, the outside edge of the triangle can be seen in blue and the corners of the base image can be seen in red.

Figures 44 shows the distances calculated between the fingertip path and each side of the triangle for the “poor” trace.

المنارة للاستشارات

www.manaraa.com

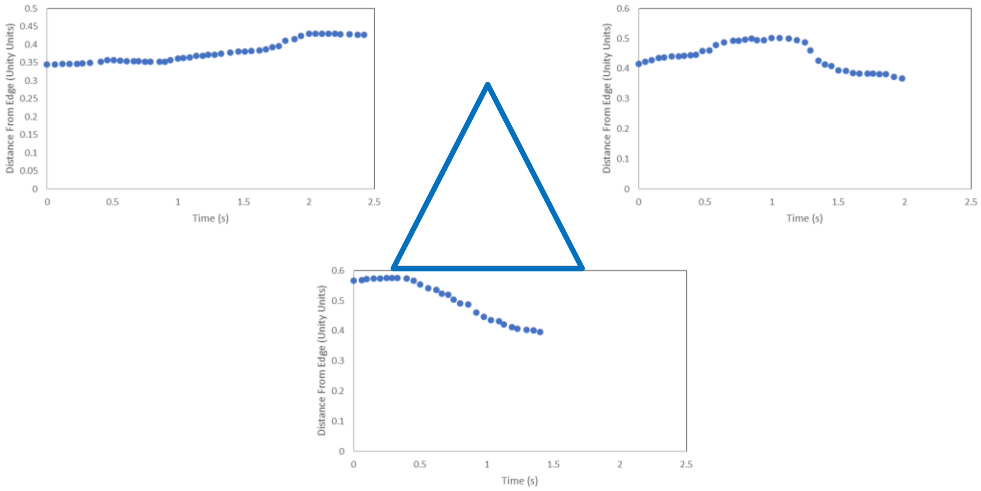

Figure 44: The distances between the fingertip position and the outside edge of the triangle for the “poor” trace.

The distance errors were calculated similarly to that of the square with the average distance error per side calculated. Equation (5) was again used to calculate the accuracy of each side of the triangle with the speed calculated using equation (6) and the tracing time for each side. The speed and accuracy for all participants can be seen in Figure 45. The average speed was 0.3183 Hz (SD 0.1599 Hz) and the average accuracy was 3.5962 bits (SD 1.0067).

www.manaraa.com

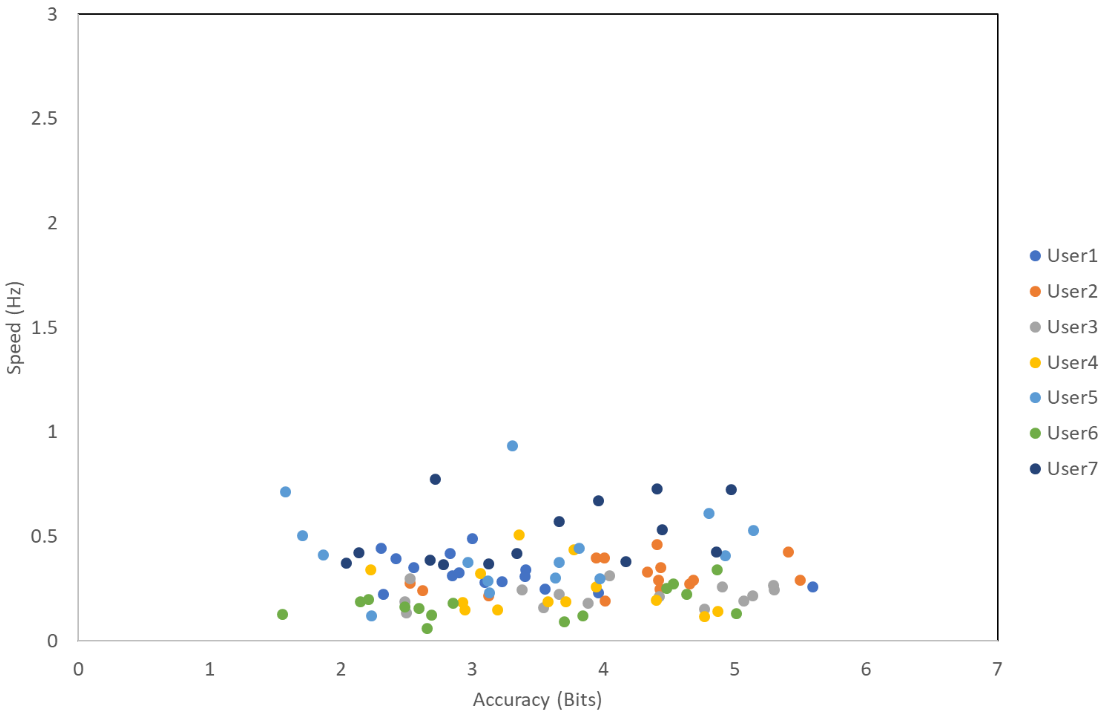

Figure 45: The speed and accuracy for the triangle traced by side for all participants.

The average time per side was 4.0196 s. The triangle tracing times by participant can be seen in Figure 46.

المنارة للاستشارات
www.manaraa.com

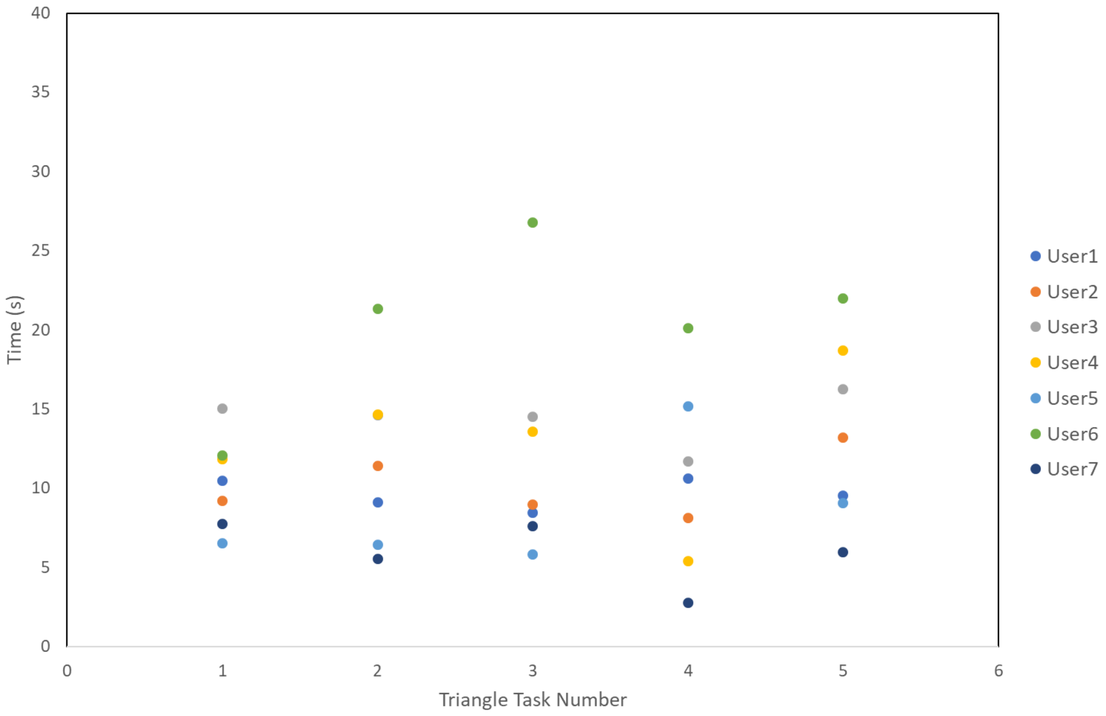

Figure 46: The triangle tracing times for all participants.

3.4 Discussion

3.4.1 Sphere Targeting Tasks

These results show that participants were less accurate if they completed the tasks quickly. It was observed that four of the participants' task completion times deceased as they completed more tasks, however this was not observed for the remaining participants. Five of the participants experienced some tracking issues with the system. These tracking issues were both with the base image and with the LM. This lead to longer completion times, as the participants would either have to move the smartphone in towards the image to pick up the image tracking or place their hand directly over top of the controller and hold it there until the hand tracking resumed. Once the tracking resumed, the participants could then complete the task. This effect was observed in Figure 14. Participants 4 and 7 both experienced tracking loss on several tasks. The image tracking loss occurred due to participant movement to a position located too far away from the image, whereas the LM tracking loss may have been attributed to the lighting conditions or the location of

www.manaraa.com

participants’ jewelry. This could have interfered with the infrared cameras identifying the participants’ fingers. These errors were often solved by changing the lighting so it was less direct or by having the participant remove their jewelry; however, it was found that this did not solve all of the tracking problems. Participants were more accurate in the x direction, the width direction, and the y direction, the height direction, than they were in the z direction, the depth direction. This is similar to findings in other studies focusing on 3D pointing tasks [22][49][50]. Depth perception is difficult in VR as the user does not have the same visual clues as they do in reality to determine how far away an object is from them [51][52]. AR does not have that difficultly to the same extent as VR because the user can use the surrounding environment to try to determine how far away from the virtual objects they are; however, many people still experience difficultly in estimating depth [22][52]. These findings explain why the participants were worse in the depth direction. The angle at which the participants held the smartphone may also account for differences calculated in accuracy in the x and y directions. The participants angled the phone to view the spheres located on the outer edge of the field of view instead of moving to view the spheres from a better position.

3.4.2 Shape Tracing Tasks

Once again, it was observed that as participants completed the tracing tasks quickly, they were more inaccurate. On average, participants were quicker at tracing the circles than they were at tracing the squares or the triangles. Between the squares and the triangles, the squares had a higher accuracy (0. 4324 and 03183 bits). The triangles were the slowest traced shapes. This could be because the squares require the participant to move their hand in either a horizontal or vertical direction; however, the triangle has only one side where they can move in the horizontal direction. The other two sides require a combination of movement in both horizontal and vertical directions which is a more difficult spatial reasoning task. There were also some tracking issues with the tracing that were not solved. An example of this was observed for user 6 in figure 37, as this participant had a much longer tracing time for square 3 then for any of the other squares. When there were tracking issues, the user would have to stop tracing and sometimes move their hand away from the shape to have the hand tracking resume. This would

المنارة للاستشارات

www.manaraa.com

affect the distance calculations and lead to a higher error on that side of the shape. The decrease in task time trend previously seen in the early part of this study was not observed for the subsequent shape tracing tasks. This could be due to the fact the shapes further on in the study were more difficult to trace then the initial three shapes, as the later shapes were not always orientated to face the participants. A larger circle on an angle would take more time to trace than first circle as it was facing the participants and was located in the middle of the base image. Overall, participants reported that the system design was very easy to learn and very intuitive.

3.5 Conclusion

The purpose of this study was to evaluate the performance and usability of the LM controller on our AR mobile environment. This would determine if the LM could be used for a mobile base medical training simulator. Overall, the system functioned as intended, and participants found the system very easy to learn and use. Participants did have difficulty in estimating the depth of the virtual objects, even when they could use the surroundings as a guide. The LM did work well on the mobile platform and made it very easy for participants to interact with the virtual environment. Further work is needed to improve the tracking robustness and perception of depth within the AR platform.

المنارة للاستشارات
www.manaraa.com

Chapter 4

4 Leap Motion Simulator Design and Evaluation

The purpose of this study is to design a medical training simulator and test is against the NeuroTouch training simulator, which is a commercially available medical procedure training simulator. An augmented reality (AR) interface had been designed that can be used with both simulators using the Google cardboard 3D glasses. The AR simulator has been integrated with the Leap Motion (LM) as the interactive device. The simulator was tested with 16 novice users and two expert neurosurgeons. They were asked to complete 40 targeting tasks that comprised of four practice ellipsoid targeting tasks and 36 ventricle targeting tasks. The simulator has been evaluated by comparing the user performance between the two systems.

4.1 Introduction

This final study has been designed to develop and test a medical simulator, based on the LM, against a training simulator. For this, the NeuroTouch has been selected. This simulator is able to simulate various types of procedures and uses high resolution graphics and a mechanical arm to do so [17]. There are many training modules that can be used to train different skill sets and knowledge [17]. To compare the designed simulator against the NeuroTouch, it must have similar functionality. To ensure the performance between the two simulators can be compared, it was decided that the same display should be used and participants should complete the same tasks. For this, an AR display for the virtual objects was selected, as it can be overlaid onto the physical components of the NeuroTouch. The display should be viewed stereoscopically to improve the depth perception that was an issue with the previous study. Using the results from the first study, the Google cardboard 3D glasses were selected for this. The display will not affect the functions of the NeuroTouch as the users will be viewing virtual objects. The AR simulator is being used to simulate ETV procedures, so the NeuroTouch "Burr Hole Selection" module was loaded. This limits the amount of information that can be recorded from the NeuroTouch. Similar information will need to be recorded from the LM simulator so that the two can be compared. The virtual interaction by the participant

المنارة للاستشارات

www.manaraa.com

with the LM should the similar to how the participant will complete the tasks with the mechanical arm of the NeuroTouch. These criteria were used in the development of the LM simulator and the AR display.

4.2 Methods

The simulator was designed using an AR environment. This was done because the participants would be using the environment for both the NeuroTouch and LM simulator. The virtual objects could be overlaid onto the real-world components of the NeuroTouch and would not interfere with the movement of the mechanical arm [53]. The AR environment was designed using Unity (version 5.2.2f). It was decided that image tracking would again be used to overlay the virtual objects onto the physical simulator. Vuforia (version 6.2.10) was used and integrated with Unity. A multi-image cube was used instead of a flat 2-dimensional image (Fig. 47). This would give the users more freedom to move around in the environment without causing the image tracking to be lost [54].

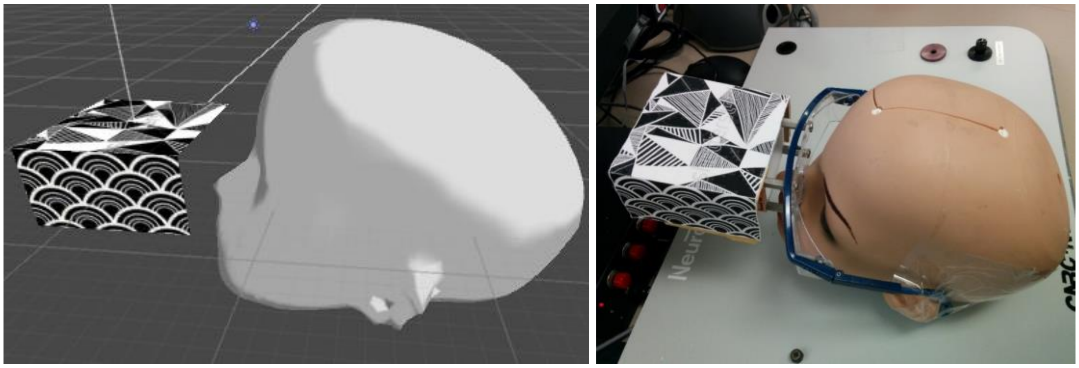

Figure 47: The multi-image cube for overlaying the virtual objects on to the physical simulator.

The multi-image cube was secured to a pair of glasses that were then attached to the physical head [55]. This was done so that the cube did not interfere with the range of motion of the mechanical arm [55]. The virtual mannequin head was then given a transparent colouring so that the physical head could be seen through the virtual head (Fig. 48).

www.manaraa.com

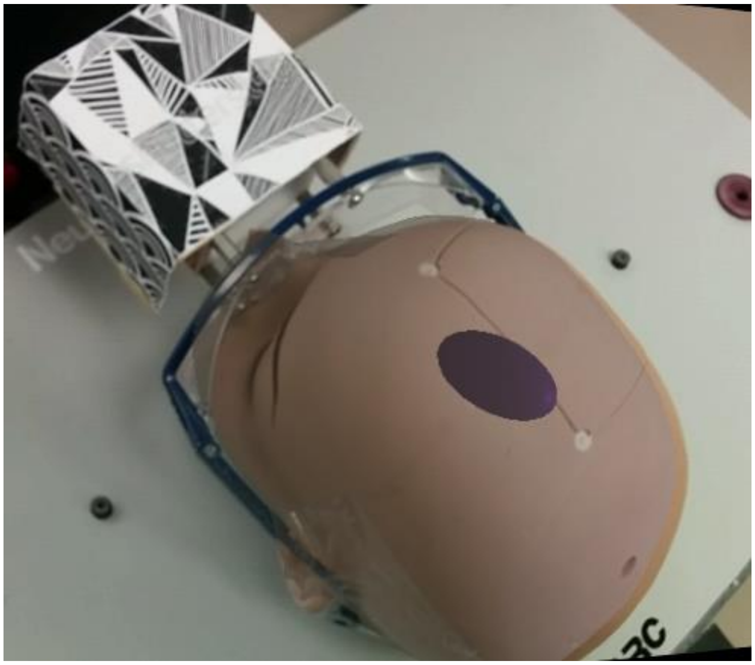

Figure 48: The transparent virtual head overlaid with the physical head.

The google cardboard 3D glasses environment set up was done with Unity. This allowed the virtual objects to be presented in a stereoscopic view (Fig. 49). The previous study found that participants had difficulty with depth perception so the glasses were used to help provide the participants with the missing distance cues that are present in the real world.

www.manaraa.com

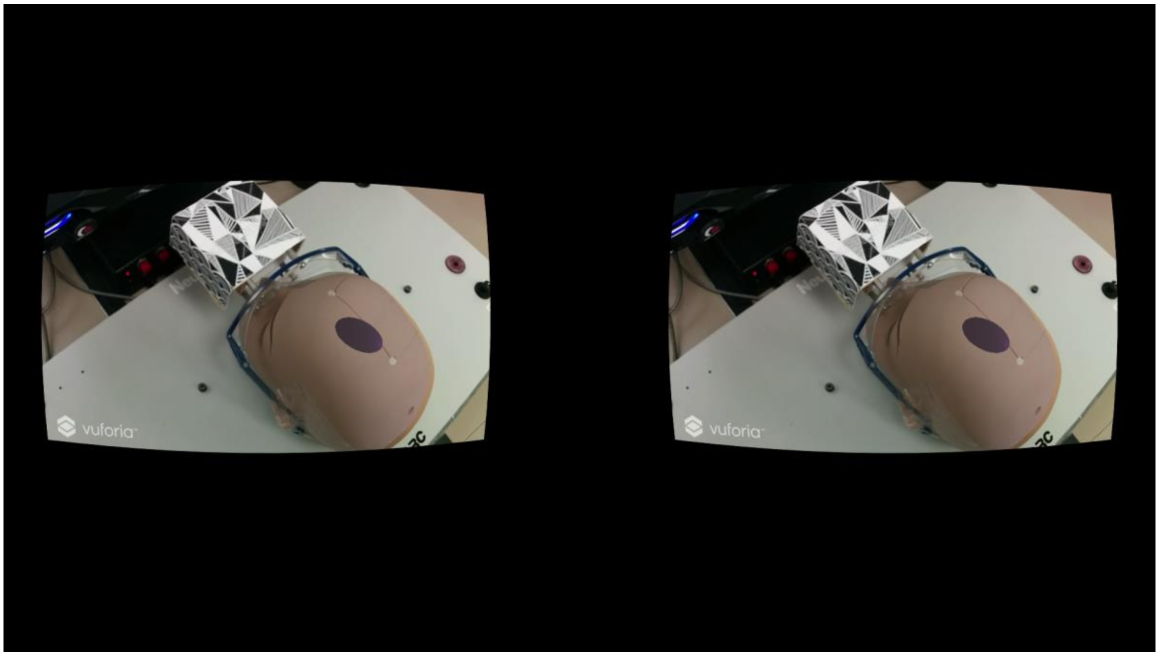

Figure 49: The stereoscopic view of the simulator through the Google Cardboard glasses.

The NeuroTouch has several different modules that can be run. For this study, the “Burr Hole Selection” module was loaded. This module records the final location and orientation of the end of the tool. The LM simulator was designed so that is was similar to the NeuroTouch. The robotic hands were once again used so that the participants’ actual hands did not cause tracking loss with the image cube (Fig. 50). The index finger of the participants’ hands would act as the virtual tool and the fingertip location and orientation were tracked for the duration of the tasks.

المنارة للاستشارات

www.manaraa.com

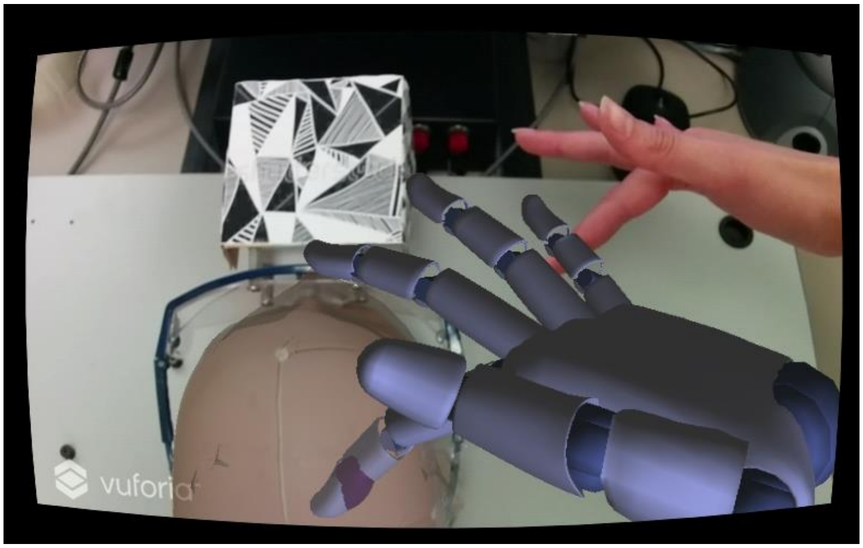

Figure 50: The LM robotic hand index finger was used as the tool for this simulator.

The study was designed with 40 targeting tasks. The first four tasks were training tasks and used ellipsoids in various shapes and sizes. These tasks were similar to those used in the first study. For the NeuroTouch, the participants were instructed to place the tool tip on the skull and orientate it so the trajectory would pass through the longest axis of the ellipsoid (Fig. 51). Once the user felt the tooltip was in the correct location and orientation, they would press the right foot pedal and that would record the task completion time, position and angle of the tooltip. For the LM, the participants were instructed to place the virtual index finger through the longest axis of the ellipsoid (Fig. 52). The virtual index fingers could pass through the virtual mannequin head so the participants could explore the environment within the head. As the index finger was the tool, participants were instructed to keep their index finger straight to mimic the NeuroTouch tool. When the user felt the finger was in the correct location, they would press the action button on the glasses. This would end the recording of the virtual index finger's location and orientation and record the task completion time.

المنارة للاستشارات

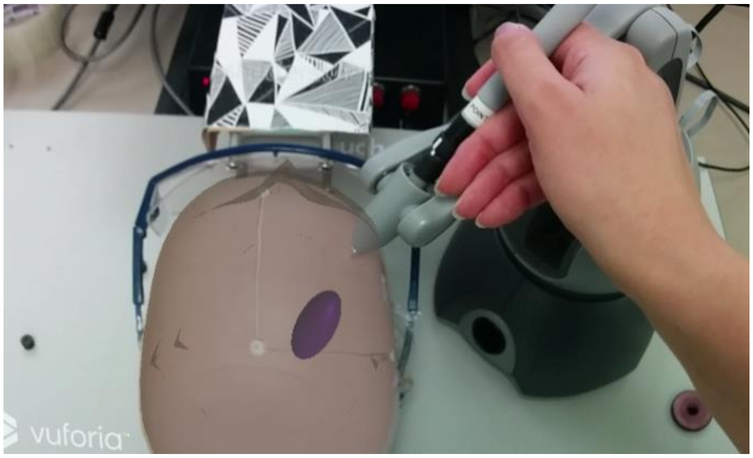

Figure 513: The NeuroTouch tool had to be placed on the physical skull and orientation so that the trajectory from the end of the tool would pass through the longest axis of the visible ellipsoid.

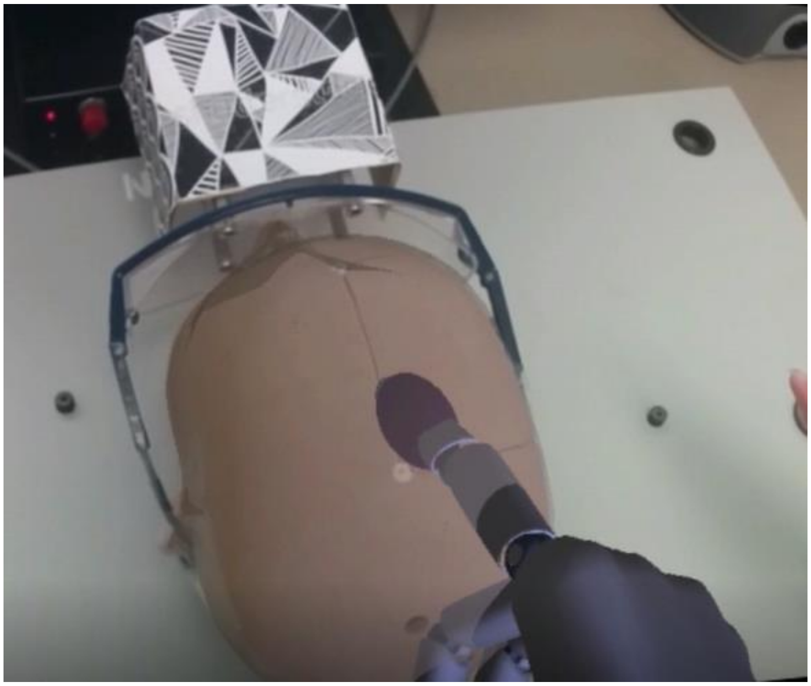

Figure 52: The LM virtual hands could pass through the virtual head so the index finger could be placed through the ellipsoid.

The NeuroTouch “Burr Hole Selection” program only records one set of data. A separate program was developed with Unity that would record the time, position and orientation for each task when the button was pressed (Fig. 53).

www.manaraa.com

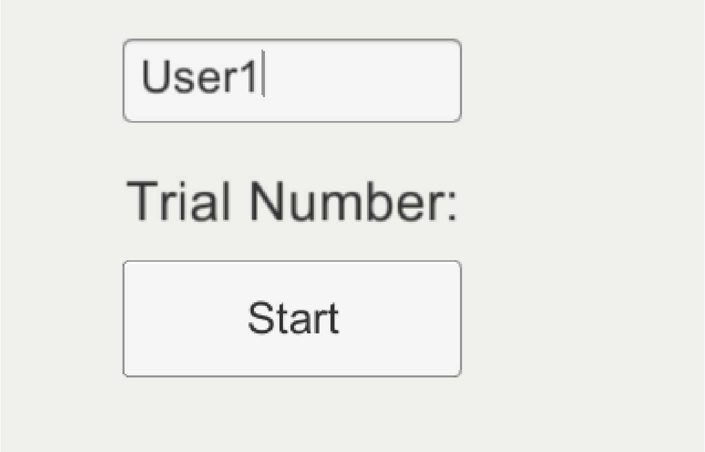

User1

Figure 53: The interface of the program used to copy the position and location of the NeuroTouch tooltip and the task completion time.

The remaining 36 targeting tasks used ventricles. The ventricles were segmented from 9 t1 MRI scans. The segmentation was done using Blender and the meshes were imported into Unity. The NeuroTouch can only target the right side of the mannequin head so the ventricles were mirrored as the left side of the ventricles could then be targeted. These extra targets brought the total number of ventricles to 18 and they were duplicated in the same order for a total of 36 tasks. The right anterior horn of each ventricle was highlighted in red (Fig. 54). Most participants did not have a background in anatomy. This was done so that anatomical knowledge was not required to complete the tasks.

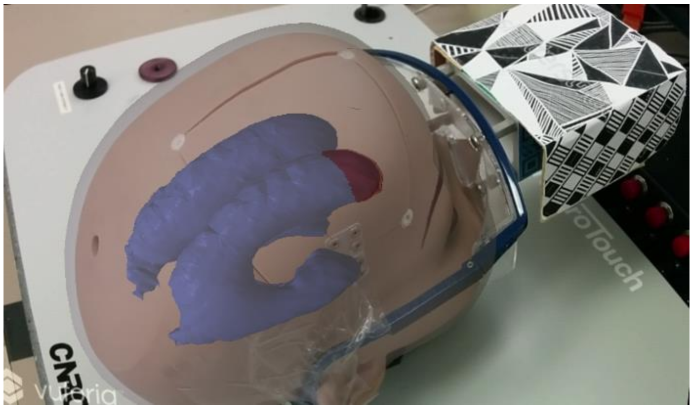

Figure 54: An example of one of the ventricles with the right anterior horn highlighted in red.

المنارة للاستشارات
www.manaraa.com

For these tasks, the participants were asked to place the NeuroTouch tooltip so that its trajectory would pass through the highlighted region without passing through any other visible structures (Fig. 55). There were also instructed to avoid areas such as the mannequin face as these are not areas where surgeons would place the tooltip. Once again, when they were confident in their selection, they would press the foot pedal and the same data would be recorded.

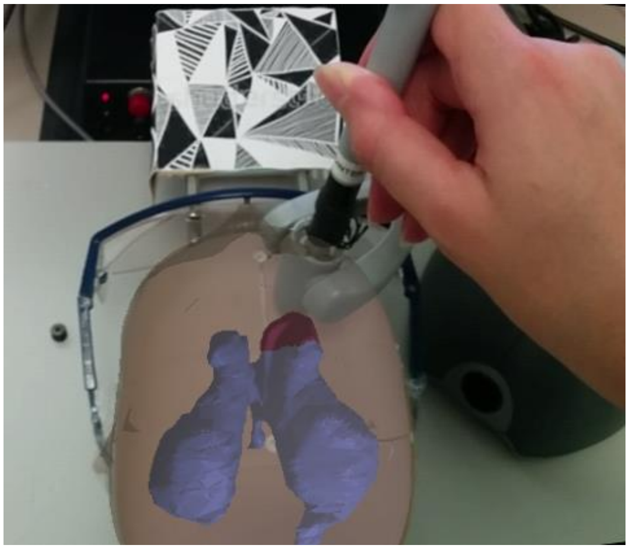

Figure 55: An example of how a user would place the NeuroTouch tool so that the trajectory from the tooltip would pass through the highlighted region of the ventricle.

When using the LM, the participants were instructed to place the index finger through the highlighted region of the ventricle so that the index finger did not touch any of the other structures (Fig. 56). They were also instructed to orientate the index finger so that the trajectory did not pass through areas such as the mannequin face. Once they were confident in the placements of the index finger, they would press the action button and the same data would be recorded. The participants were informed that they were being timed for each of the 40 tasks but they should complete the tasks as accurately as possible.

www.manaraa.com

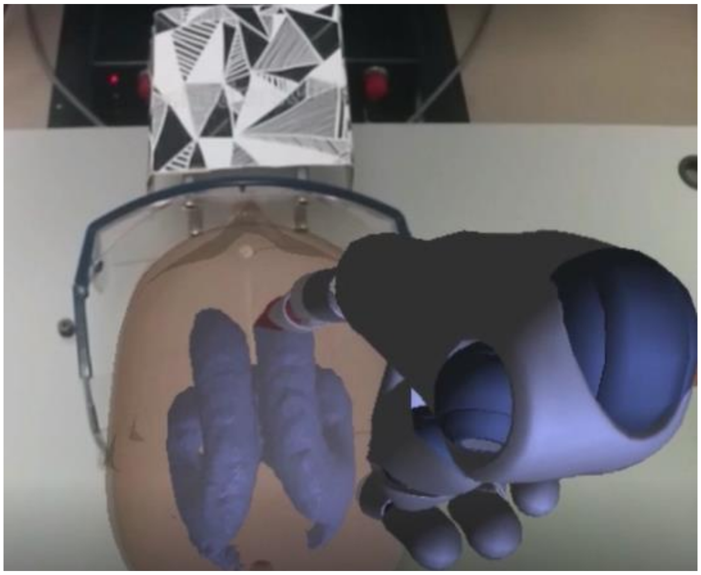

Figure 56: An example of how a user would place the LM index finger so that it passes through the highlighted region of the ventricle.

The NeuroTouch and LM simulators had a similar setup. The NeuroTouch mechanical arm was located on the right side of the mannequin head with the right foot pedal placed near the participants' foot (Fig. 57). The LM was placed in the same position as the NeuroTouch. Participants could move the LM controller to more comfortable position (Fig. 58).

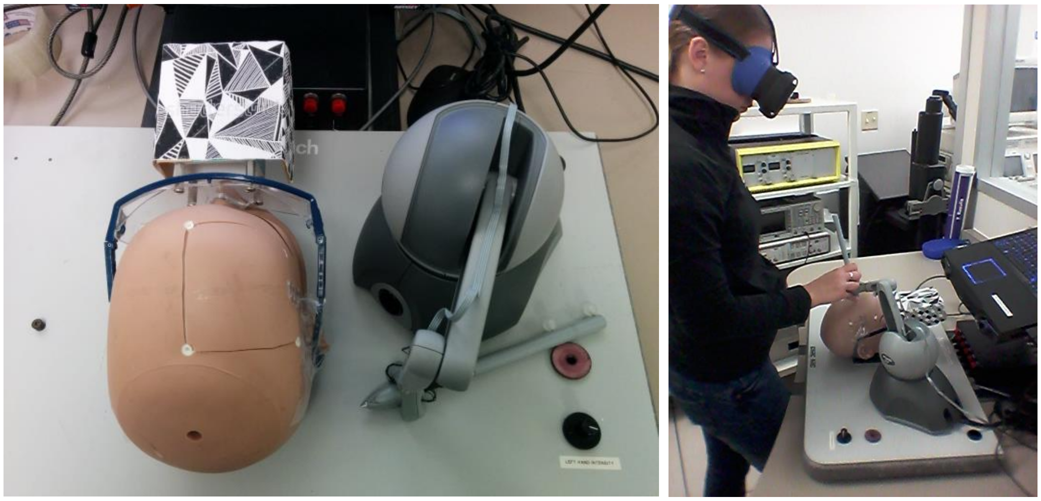

Figure 57: The setup of the NeuroTouch.

www.manaraa.com

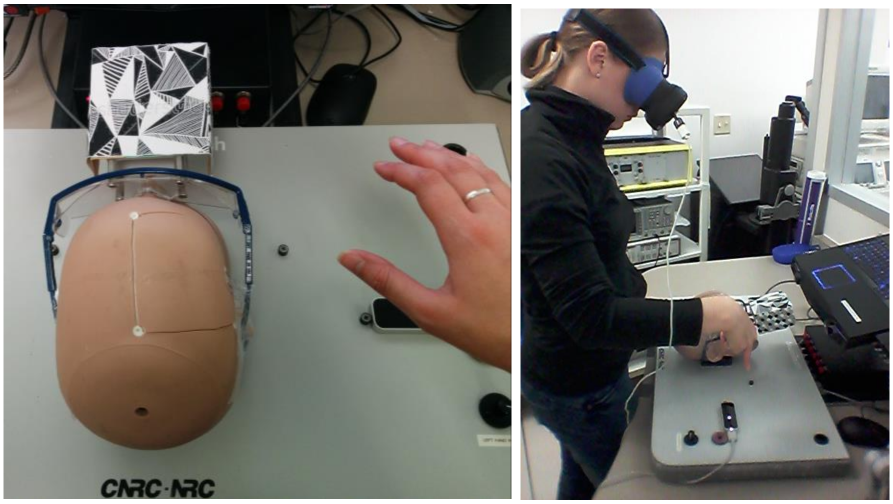

Figure 58: The setup of the LM.

In total, 18 participants were recruited for this study with 16 participants being novices and two being expert surgeons. The 18 participants were split into two groups. One group started the study with the NeuroTouch simulator, and the second started with the LM simulator. Both groups contained one of the experts. Of the 18 participants, 17 chose to use their right hand and one chose their left.

4.3 Results

For each of the ventricles used, one of the expert surgeons drew the correct targeting trajectory through it (Fig. 59). These will be used to compare the participants' trajectories.

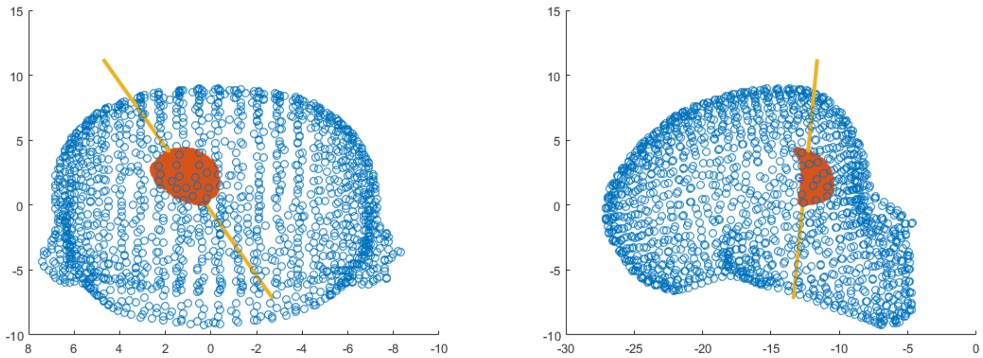

Figure 59: An example of a "correct" trajectory through the right anterior horn.

www.manaraa.com

The data collected from both simulators was processed the same way. The participants' trajectories were calculated from the collected data and compared against the "correct" trajectory. The "correct" trajectories were also given a center value (Fig. 60). The center is the midpoint in the line that passes through the ventricle.

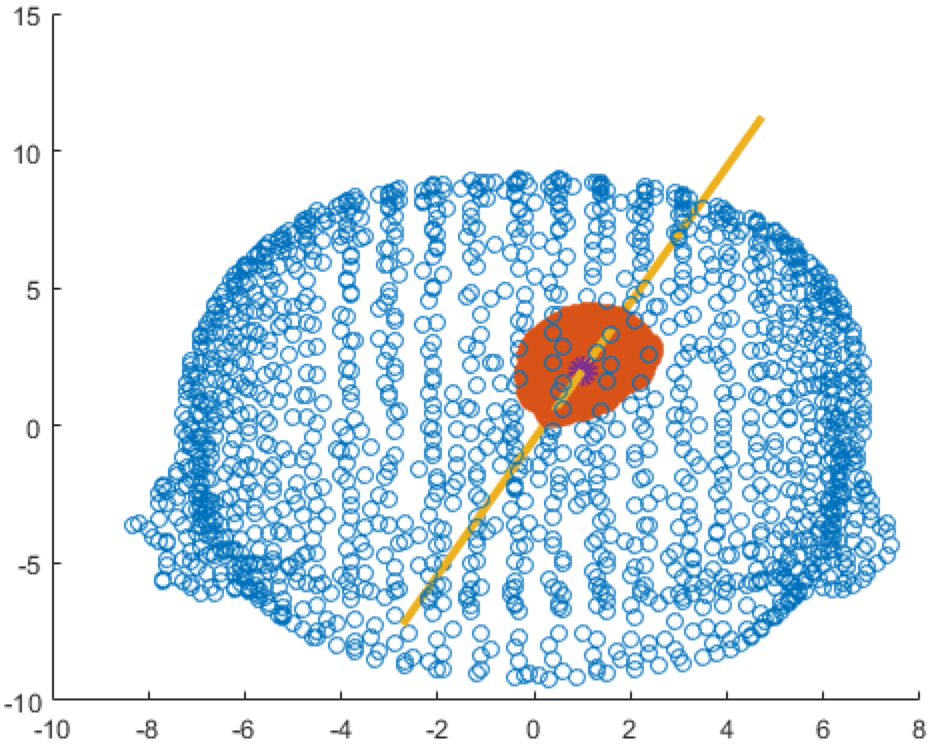

Figure 60: An example of a "correct" trajectory and its center through the right anterior horn.

The performance of the participants was measured by calculating the difference in the angle between their trajectory and the "correct" trajectory, and the distance between the center of the "correct" trajectory and the closest point on the participants' trajectory. The NeuroTouch data comprised of a point and a set of angles. From this each participant's trajectories could be calculated. An example of a "good" participant trajectory can be seen in figure 61 and an example of a "poor" participant trajectory can be seen in figure 62.

المنارة للاستشارات

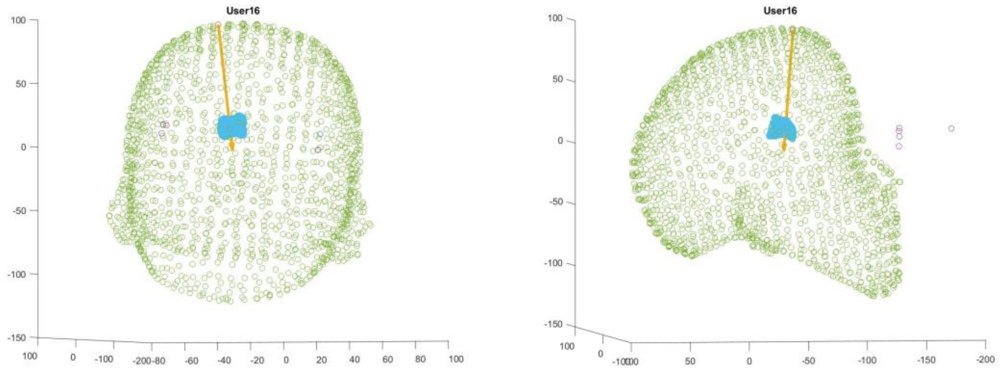

Figure 614: An example of a “good” participant trajectory through the right anterior horn using the NeuroTouch.

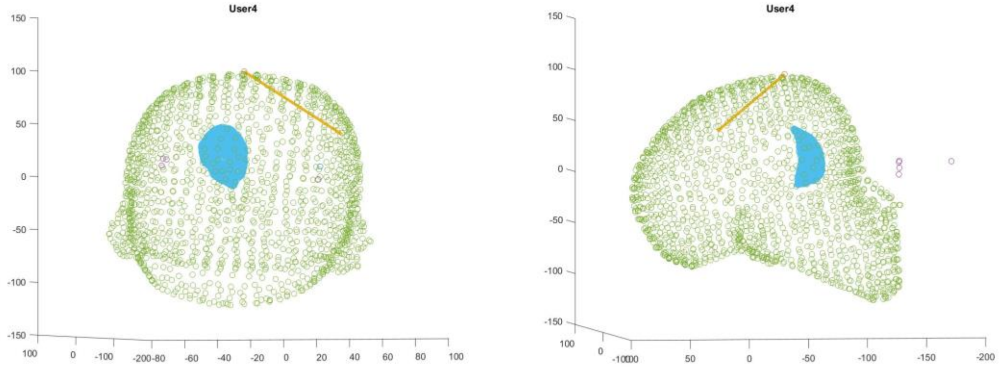

Figure 62: An example of a “poor” participant trajectory through the right anterior horn using the NeuroTouch.

These trajectories were then compare with the “correct” trajectories. Figure 63 and figure 64 show the “good” and “poor” trajectories with the “correct” trajectories.

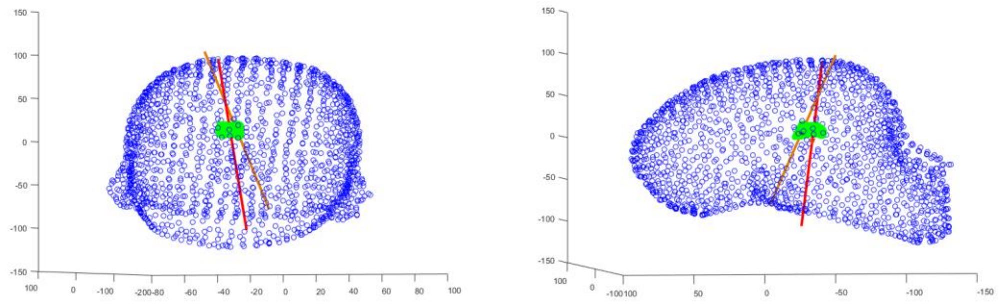

Figure 63: An example of a "good" participant NeuroTouch trajectory in red with the "correct" trajectory in gold.

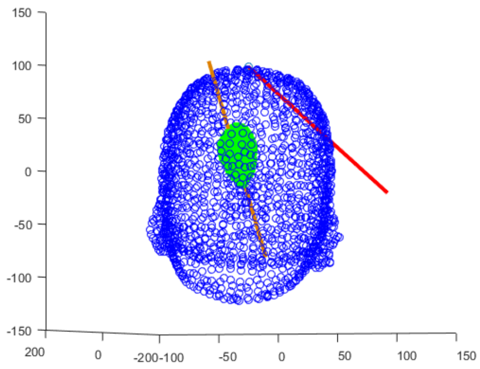

Figure 64: An example of a "poor" participant NeuroTouch trajectory in red with the "correct" trajectory in gold.

The angle between these two trajectories was calculated along with the closest distance from the center point to the trajectory. The data collected from the LM provided more information than the NeuroTouch. The entire path the participant took before selecting the final trajectory was recorded (Fig. 65).

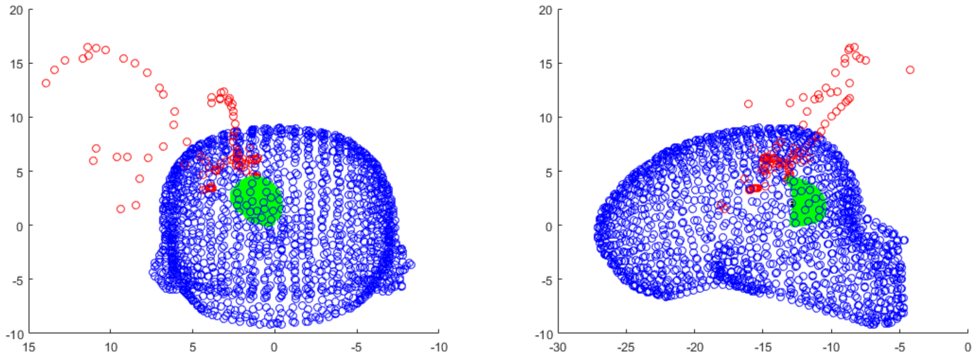

Figure 65: The entire path a participant moved their index finger, in red, before selecting the final trajectory.

An example of a "good" participant trajectory can be seen in figure 66 and a "poor" participant trajectory can be seen figure 67.

المنارة للاستشارات

www.manaraa.com

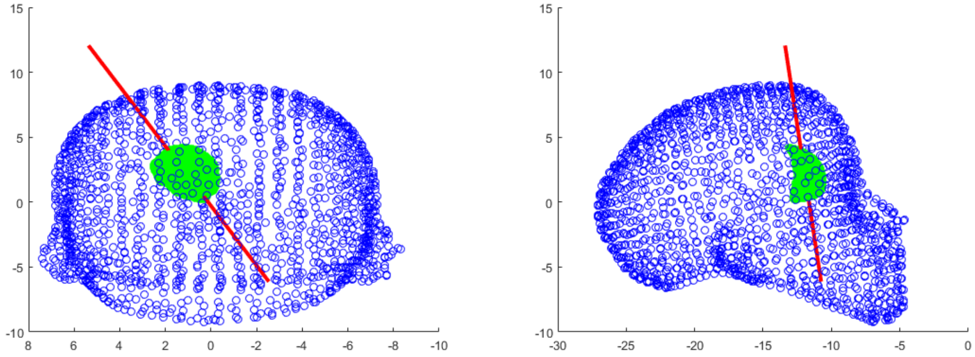

Figure 66: An example of a "good" participant trajectory through the right anterior horn using the LM.

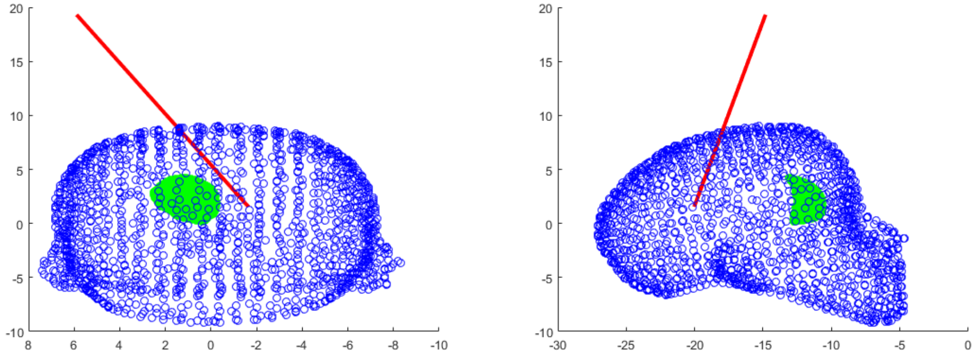

Figure 67: An example of a "poor" participant trajectory through the right anterior horn using the LM.

These trajectories were compared against the "correct" trajectory in the same manner as the trajectories from the NeuroTouch as seen in figure 68 and figure 69.

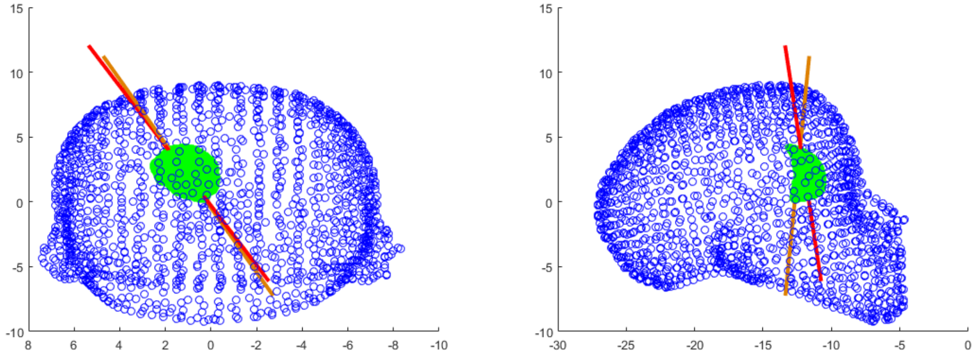

www.manaraa.com

Figure 68: An example of a "good" participant LM trajectory in red with the "correct" trajectory in gold.

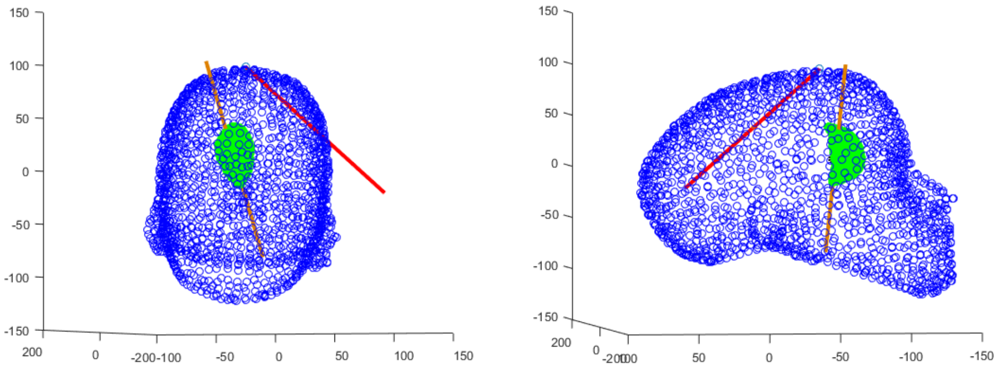

Figure 69: An example of a "poor" participant LM trajectory in red with the "correct" trajectory in gold.

The angle between the participant and "correct" trajectory was calculated and the closest distance from the center to the trajectory was calculated.

Overall, the novices and experts did not perform well with the NeuroTouch. The distance performance has been calculated by using a modified Fitts' Law equation. Participant performance uses speed and the index of performance, or accuracy. Speed has been calculated using equation (5). Accuracy has been calculated using equation (6). Error is the closest distance between the center of the right anterior horn mesh and the participant selected trajectory. The novice NeuroTouch performance can be seen in figure 70 and the expert performance in figure 71. The mean novice speed was 0.2545 Hz (SD 0.2738 Hz) and the mean expert speed was 0.5145 Hz (SD 0.3477 Hz). The mean novice distance accuracy was 0.2717 bits (SD 0.3899 bits) and the mean expert distance accuracy was 0.0925 (SD 0.1210 bits).

www.manaraa.com

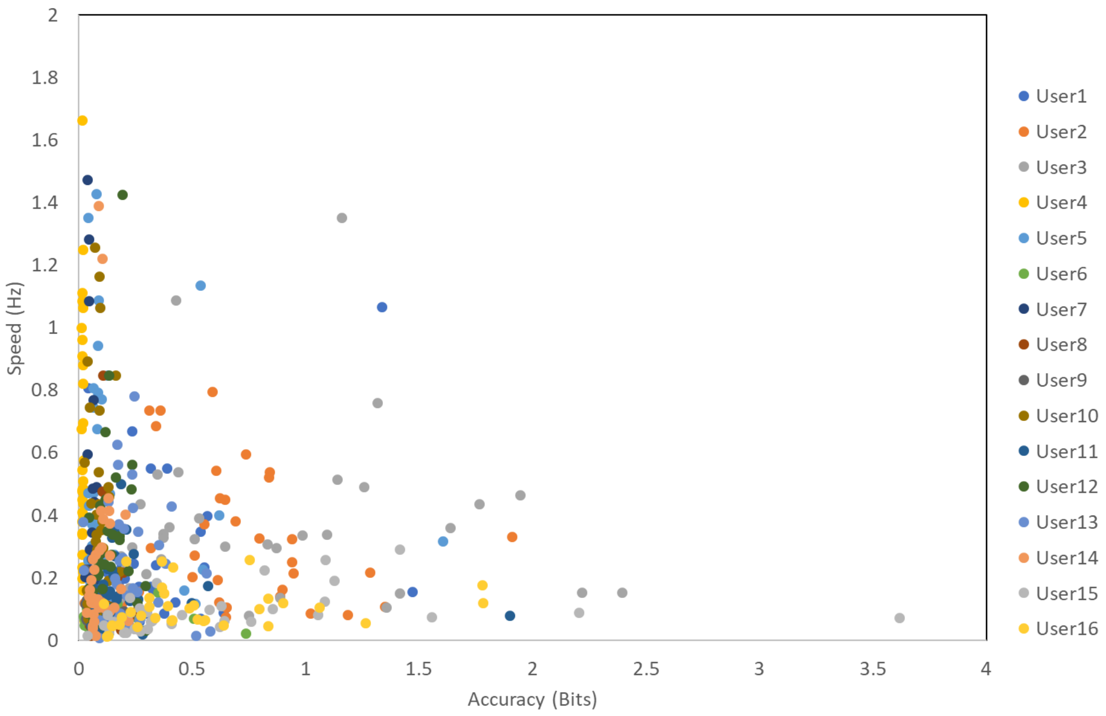

Figure 70: Novice distance performance for the NeuroTouch.

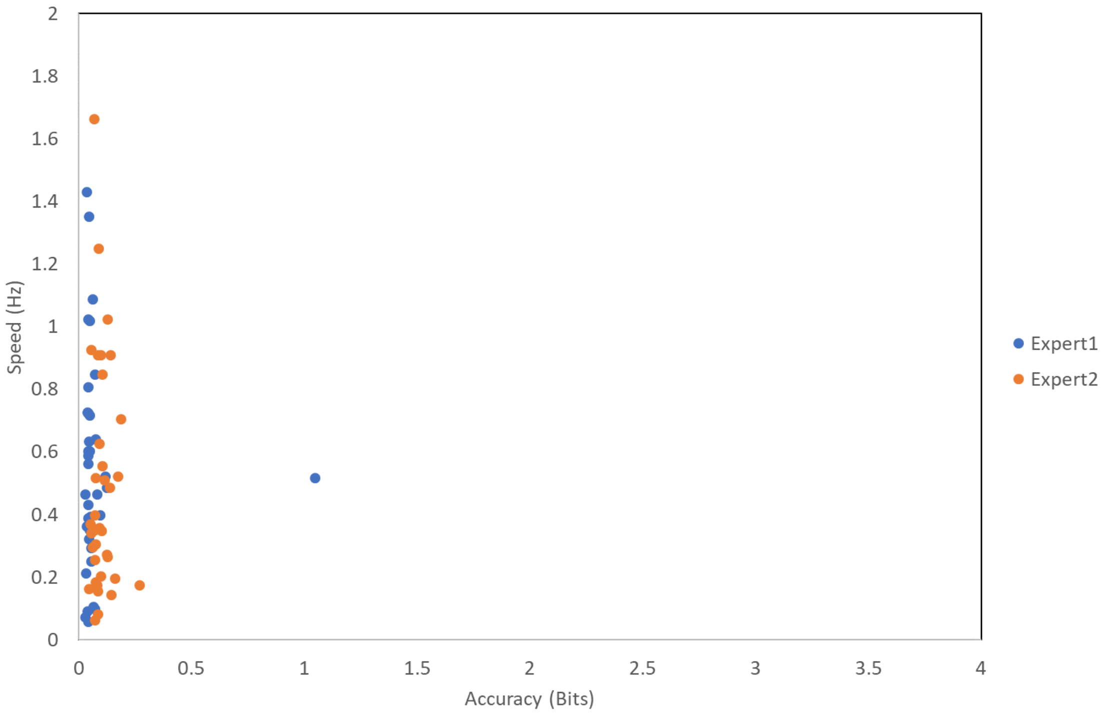

Figure 715: Expert distance performance for the NeuroTouch.

المنارة للاستشارات

www.manaraa.com

The participant angle performance has been determined using speed and angle accuracy. Speed for the angle performance is the same at equation (7). Accuracy has been calculated using:

$$\text{Accuracy} = \log_2\left(1 + \frac{1}{error}\right) \tag{9}$$

Error is the difference between the expert trajectory and the participant selected trajectory. The novice NeuroTouch angle performance can be seen in figure 72 and the expert angle performance in figure 73. The mean novice angle accuracy was 0.1171 bits (SD 0.08960 bits) and the mean expert angle accuracy was 0.1022 bits (SD 0.0701 bits).

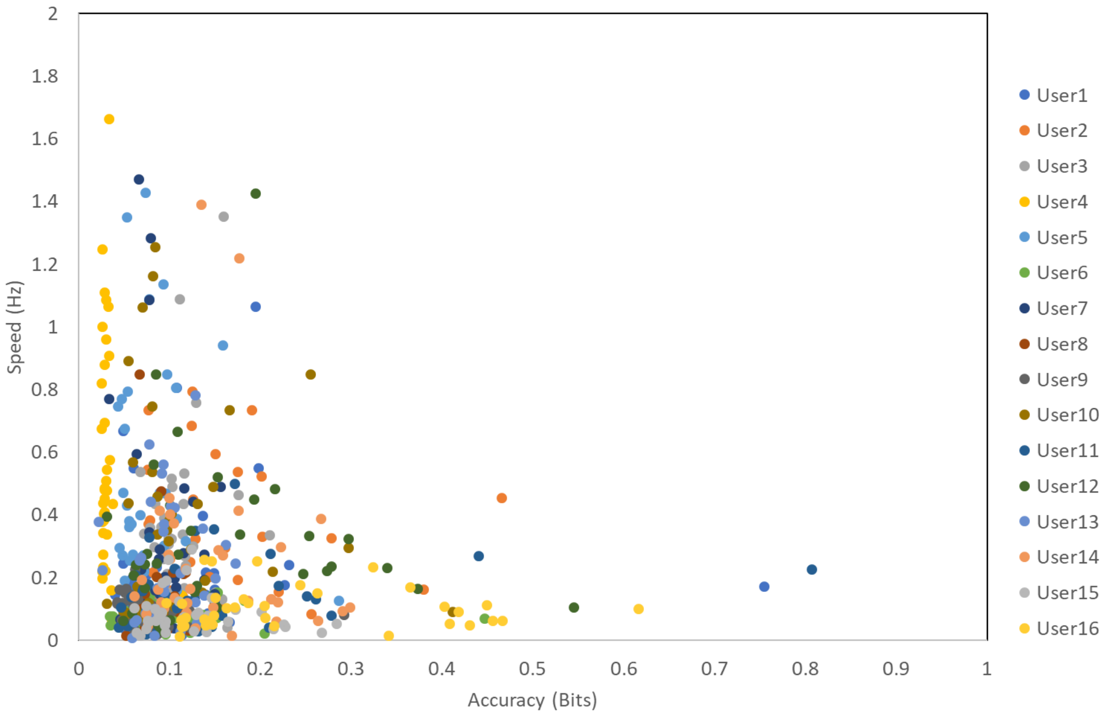

Figure 72: Novice angle performance for the NeuroTouch.

www.manaraa.com

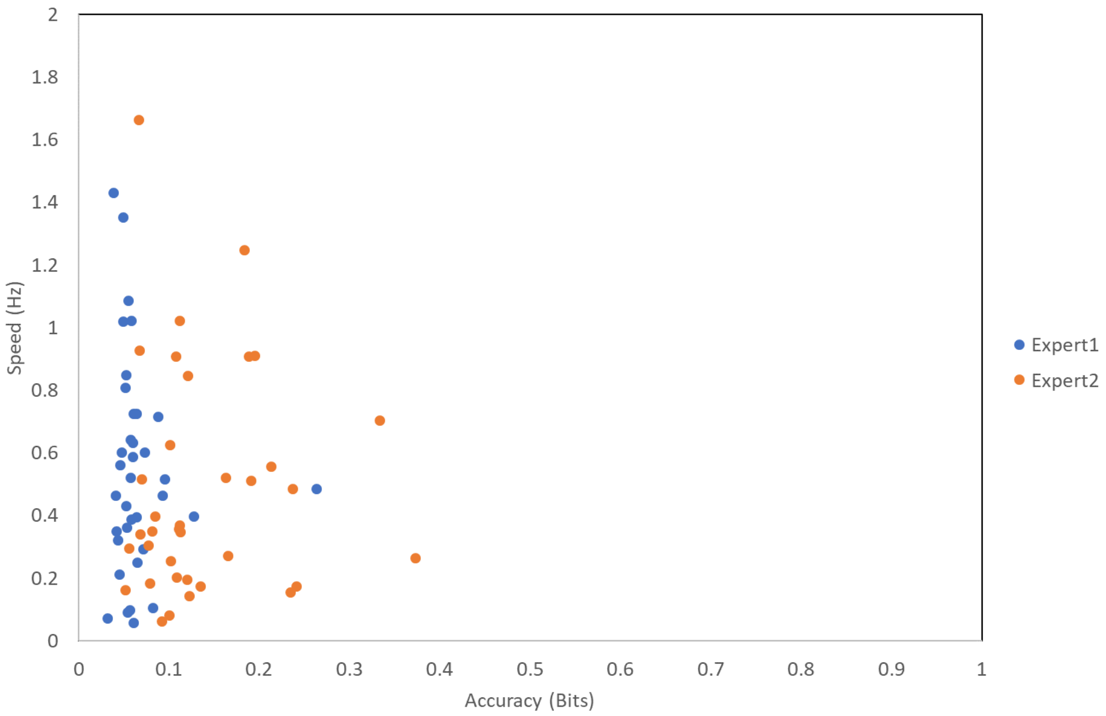

Figure 73: Expert angle performance for the NeuroTouch.

Both groups had improved performance using the LM simulator. The novice LM distance performance can be seen in figure 74 and the expert distance performance in figure 75. The distance performance with the LM has been calculated the same as distance performance with the NeuroTouch. The mean novice speed was 0.1927 Hz (SD 0.1769 Hz) and the mean expert speed was 0.1938 Hz (SD 0.1308 Hz). The mean novice distance accuracy was 0.3585 bits (SD 0.4474 bits) and the mean expert distance accuracy was 0.4581 bits (SD 0.3501 bits).

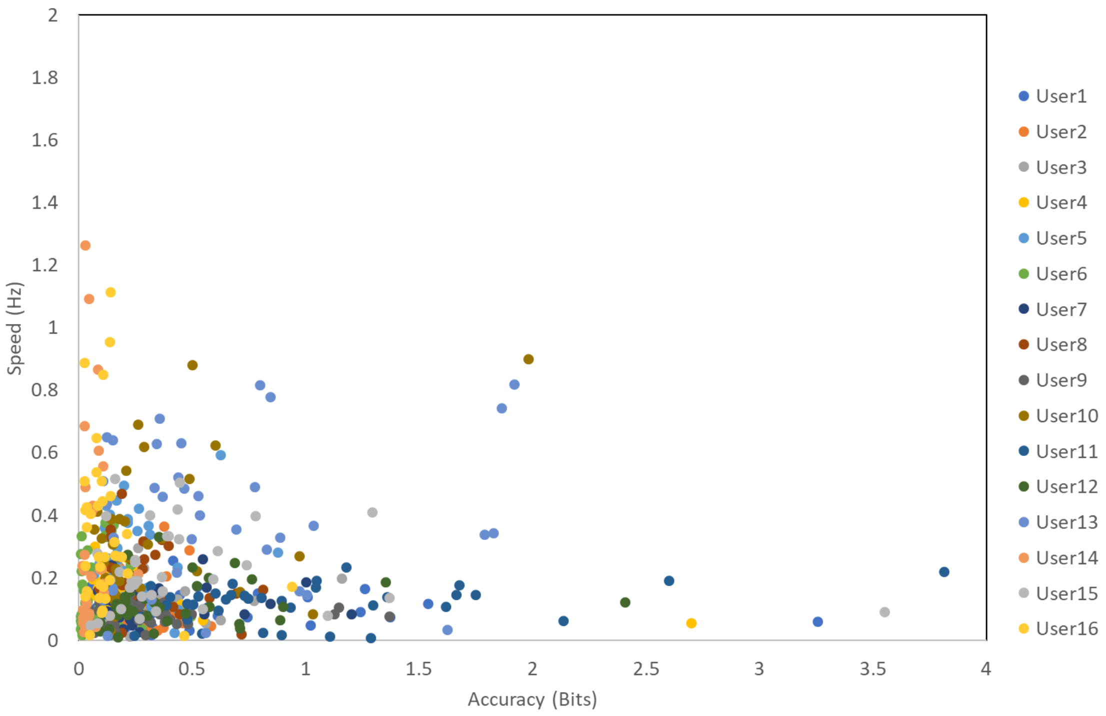

Figure 74: Novice distance performance for the LM.

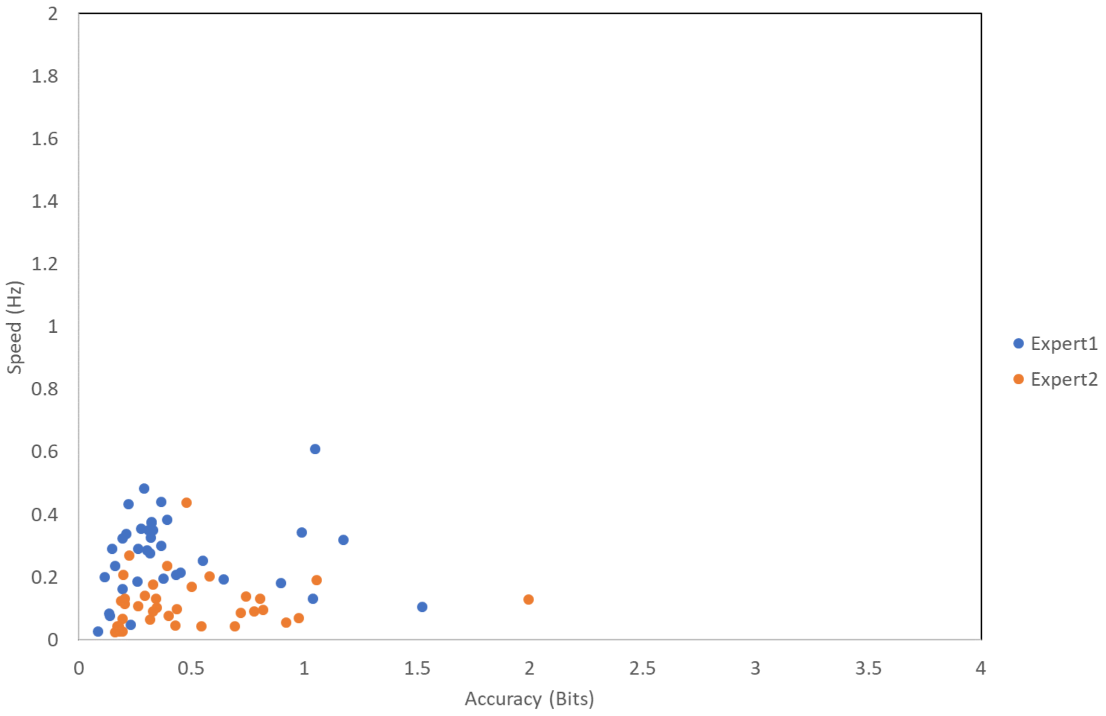

Figure 75: Expert distance performance for the LM.

www.manaraa.com

The novice LM angle performance can be seen in figure 76 and the expert angle performance in figure 77. The LM angle performance has been calculated the same as the NeuroTouch angle performance. The mean novice angle accuracy was 0.0540 bits (SD 0.0663 bits) and the mean expert angle accuracy was 0.0397 bits (SD 0.0095 bits).

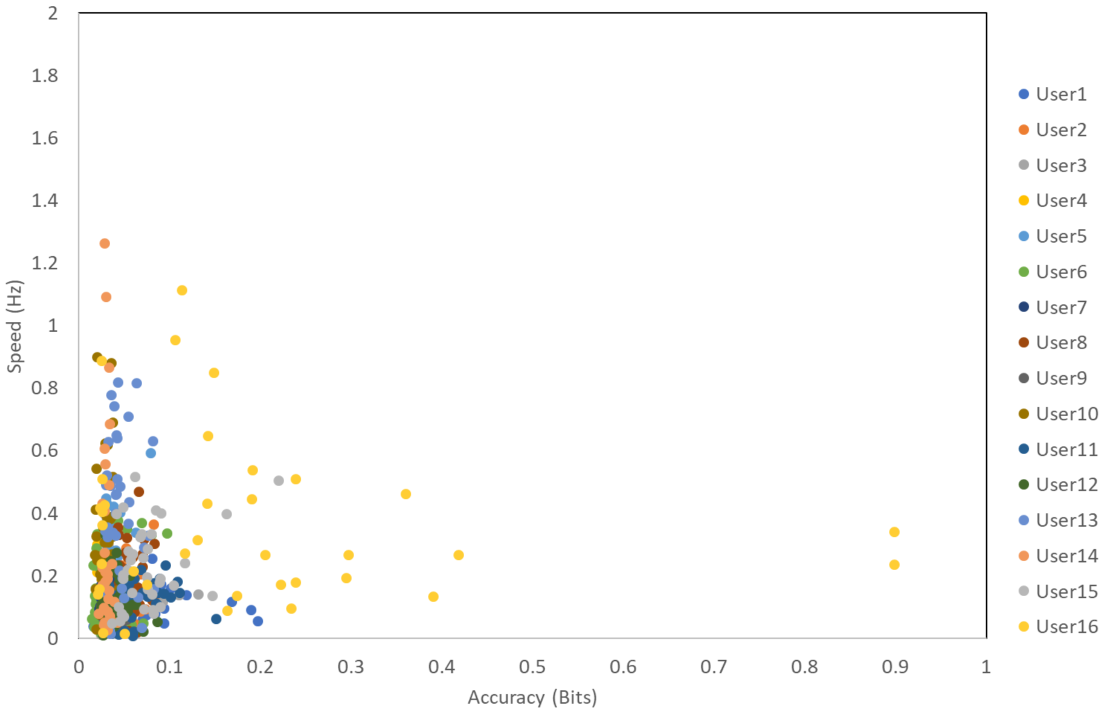

Figure 76: Novice angle performance for the LM.

www.manaraa.com

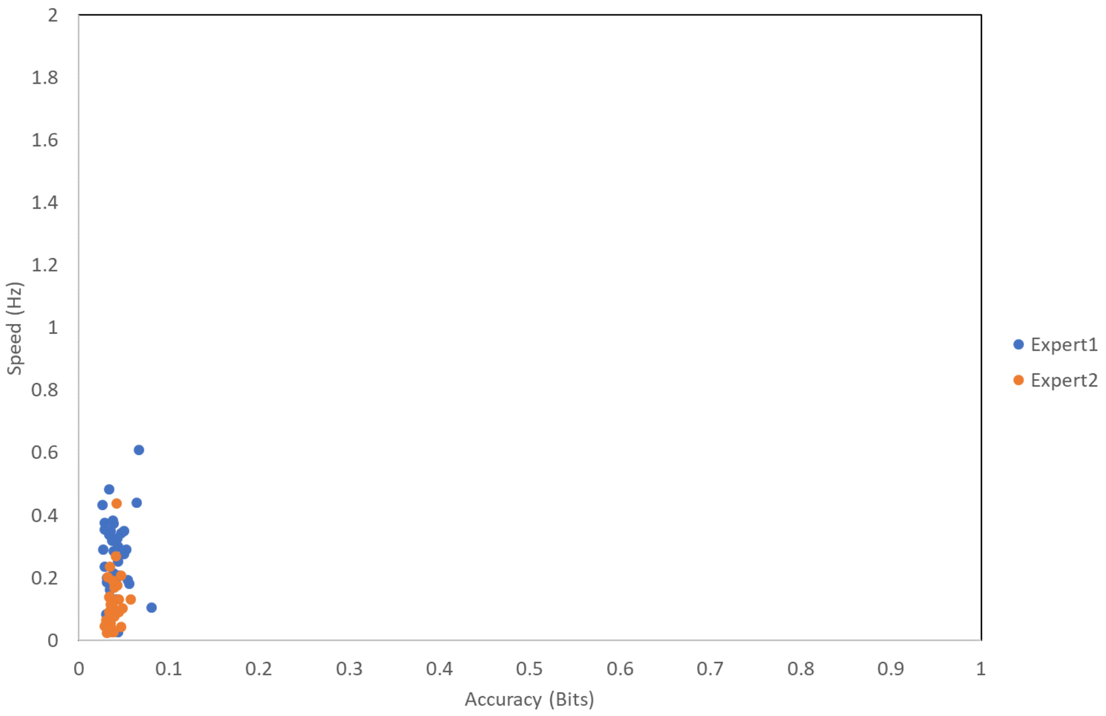

Figure 77: Expert angle performance for the LM.

The overall task completion times did decrease as the participants completed more tasks. The average novice task completion times for the NeuroTouch and the LM can be seen in figure 78 and the average expert task completion times for the NeuroTouch and the LM can be seen in figure 79.

www.manaraa.com

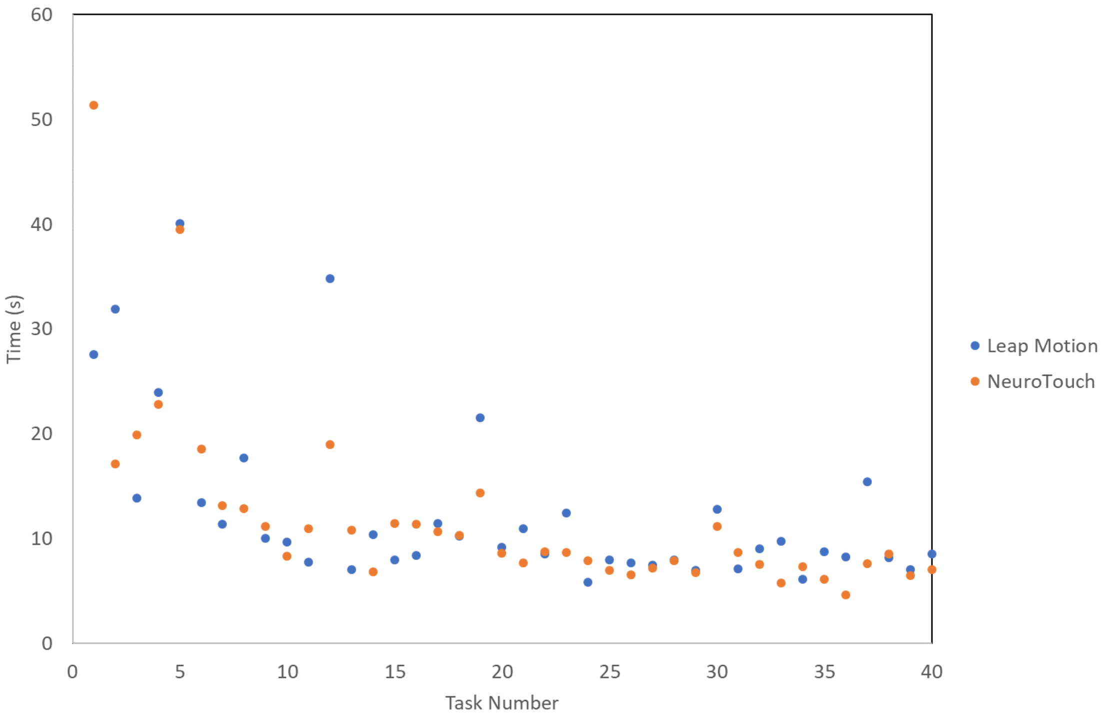

Figure 78: The average novice task completion times for both NeuroTouch and LM.

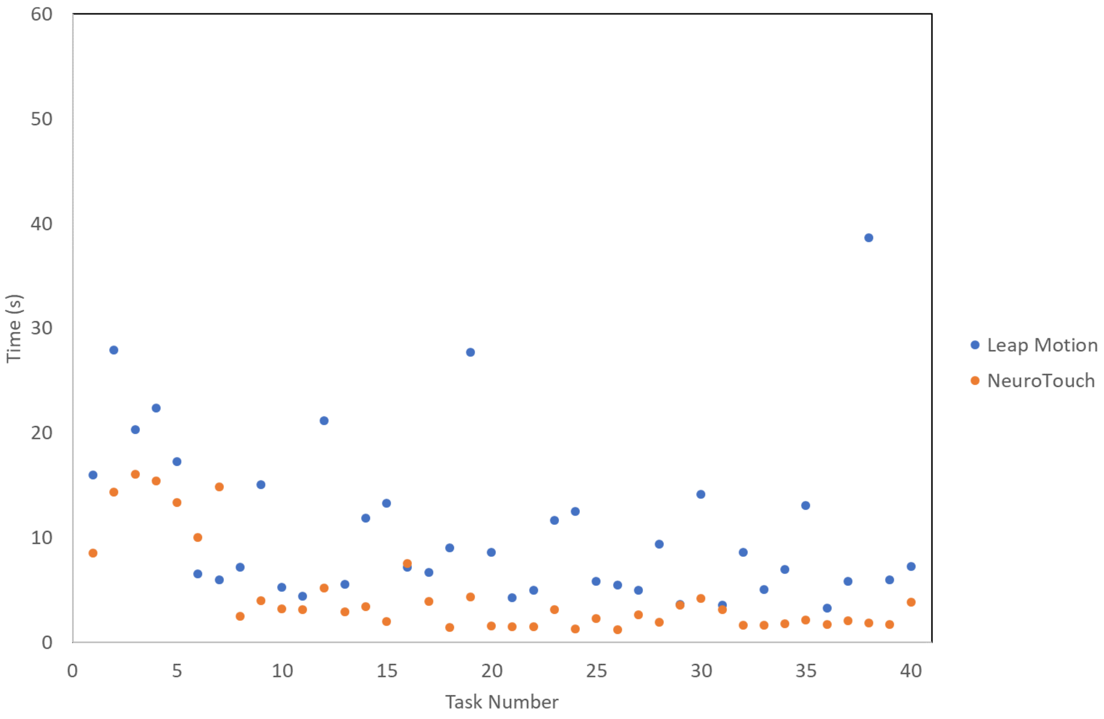

Figure 79: The average expert task completion times for both NeuroTouch and LM.

www.manaraa.com

4.4 Discussion

The ventricles were placed within the mannequin in positions that were not anatomically correct. This meant the experts could not rely on their knowledge of anatomical structures when selecting their trajectories. This explains why there was little difference in the expert and novice performance using the NeuroTouch. The experts had better performance when using the LM then the NeuroTouch; however, they slightly poorer angle performance when using the LM. Although, the anatomical context had been removed from the tasks, the experts would still perform the tasks on the NeuroTouch as though they were performing an ETV procedure. They would have a general idea of what the "correct" angle of trajectory would be. When using the LM, all the participants would have been affected by the lack of depth perception because of the AR. Participants may have over compensated for this causing the angle differences to be higher with the LM. Some of the participants did not follow all of the instructions when selecting their trajectories and selected ones that passed through regions they were instructed to avoid, such as the face. This would have caused them to have worse angle performance. The LM allowed the participants to explore the virtual environment within the head; therefore, the experts were able to target more accurately without the use of their anatomical knowledge. The experts were more consistent with their targeting error on both devices than the novices. The experts and novices completed in the NeuroTouch tasks with similar times. The experts did complete the LM tasks slower than they completed the NeuroTouch tasks and this helps explains their improved performance when using the LM. If participants completed the task quickly, they were more inaccurate then when they performed the tasks slowly. This can be seen across the study and is an overall trend in the data. This is not observed as strongly in the angles of the LM data which suggests that users may have been biased in their selection of a trajectory due to the nature of the virtual environment. All the participants reported that the LM system was very intuitive and easy the use. Most enjoyed the ability to explore the virtual environment. Some of the users reported that the AR system was more difficult to use with the NeuroTouch as the objects appeared to be floating above the mannequin head instead of appearing to be within it. This is a known difficultly with AR [56]. Because the virtual objects are being overlaid onto the stream from the camera, it is very difficult to

www.manaraa.com

have them appear under real life objects, such as the NeuroTouch tool. Edge detection is one method that can be used for this; however, there is limited processing resources available on the smartphone, a majority of which is used for the display. There were some image tracking problems when participants used the NeuroTouch. Although a multi-image cube was used, the tool arm sometimes would block enough of the top image that the application would lose tracking. There were some hand tracking problems reported with the LM. These issues were not as common as in the previous study. Both of these problems would have increased the task completion times and are a source of noise within the data. The LM system was intriguing to the participants and most preferred it to the NeuroTouch.

4.5 Conclusion

The purpose of this study was to create a medical simulator from commercially available and inexpensive technology and test is against a medical simulator. Overall, the designed simulator functioned as intended with good reported usability from the participants. There were some robustness problems due to image cube occlusion that caused some problems with the virtual objects and there were some LM hand tracking problems. Participants found the LM simulator more intuitive to use than the NeuroTouch and were more accurate in their performance.

www.manaraa.com

Chapter 5

5 Conclusion

The purpose in conducting this research was to design and test a medical simulator then perform a comparison test with a commercially available medical simulator. The NeuroTouch simulator was selected as the testing simulator for this study. The design criteria specified that the simulator had to be easily accessible, inexpensive, robust, and have similar functionality as the NeuroTouch. This novel Leap Motion (LM) simulator does not rely on technology that is difficult for most students to obtain and, assuming the user already has a smartphone with enough processing power to run the LM, the cost of the simulator is around $100. This can be broken down into two separate components; the cost of the LM, which is available online or at most electronic stores, and the 3D glasses. There are many variations of 3D glasses that will work with the simulator so the user can select a pair that best suits their needs. This is significantly less expensive than the training simulators utilized by educational institutions. The other part of the LM simulator that the user would require is the image markers used, which are easily accessible and may be printed at home. The LM simulator did have some robustness issues. Each stage in the testing of the LM simulator successfully achieved improvements upon the issues identified from the previous stage; however, there are still some tracking problems. Qualitative feedback about the simulator was positive, as all of the participants that tested the LM simulator found it very easy to learn how to use and enjoyed the AR environment. The simulator was designed so that it included more functionality then the NeuroTouch. The movement of the head mounted display (HMD), as this tracked the users' movement, and the position and orientation of the virtual hands were recorded for the duration of the full study. This is more information about the users' movements than what is provided by the NeuroTouch which could assist in improving their metacognitive awareness, performance and procedural knowledge for the skills involved in the training.

المنارة للاستشارات

www.manaraa.com

5.1 Simulator design

5.1.1 HMD

The smartphone functioned well as the display for the simulator, as there were no participant reports of any issues with the smaller field of view (FOV), or weight when wearing the smartphone in the 3D glasses. The 3D glasses selected were only able to interact with the display through the action button pressed by the user, which did limit the functionality that could be included in each application. The smartphone had enough processing power to handle the rendering demand from the application and power the LM. The application did put a strain on the battery of the smartphone, as the display takes a lot of power to run, so it was found that only a set number of people could test in one day as the phone needed time to recharge in between users. The battery would be depleted after two users had run through the simulator. This would not be an issue if the simulator is run on a user’s personal phone as they will be using it for their own use.

5.1.2 Image Tracking

Image tracking was one of the two robustness issues that was consistently observed with the simulator. Although the image tracking worked really well in testing, it did not require a significant disturbance for a user to lose tracking. To address this issue, the images were changed several times to make them more intricate. Vuforia uses distinct points on the image as markers, so the more distinct points are in the image, the better the tracking. The high level of intricacy allowed the algorithm to compensate if more of the image was blocked, as long as enough of these distinct points could still be identified. There is a trade off with this highly complex image as the smartphone camera has a set resolution, and most do not have high resolution. If an image has too many small points, then the algorithm will not be able to detect the points unless the camera is positioned close to the image. This is unrealistic for the purposes of the simulator, thus images were selected so there were enough distinct points that if part of the image was occluded, the tracking would not be lost. The images utilized were also formatted to be large enough that the user could sit at a reasonable distance from the image and have the enough points

المنارة للاستشارات

detected by the algorithm to start tracking. Using one image instead of two greatly improved the tracking performance of the simulator.

5.1.3 Leap Motion

The LM was a very intuitive device and made interacting with the virtual environment more interesting and compelling for the users. Integrating the device with the virtual environment was very straight forward and the device did perform as intended. The LM was the second source of the robustness problems with the simulator, as it only works on smartphones with the minimum snapdragon processor; however, the alpha release of the LM software development kit (SDK) is not overly efficient. It was found that if any other applications were running on the smartphone at the same time as the simulator application then the application's run speed decreased significantly. This is something that LM says will be improved in the beta release. The LM also had some other tracking issues where it would mirror which hand was seen by the user. This did not affect the tracking of the system as it was set to record which ever hand was present in the scene, but it was a bit of a distraction to the users. The connection between the LM and smartphone worked well for the purposes of the simulator.

5.1.4 VR and AR Environment

Using the virtual environments was found to be the most difficult for users. The virtual simulator only contained a virtual head and the objects targeted during the pointing tasks completed by the users. This was done to minimize the number of objects that the application had to render and track. This meant that users did not have other structures that could be used to generate a sense of depth, which may have impacted their performance. The simulator was then changed to use augmented reality (AR), as it was thought that this might help the users with depth perception issues, but it was found that while it did help improve performance, depth was still difficult for users to estimate. Even when the AR was paired with the 3D glasses, this depth perception was still an issue. This is something that will need to be addressed in future work. The AR environment was very compelling for the users as they found it very interesting to see virtual objects overlain on reality. This did lead to some interesting feedback, as users felt

المنارة للاستشارات
www.manaraa.com

that the objects were floating nearer to them or on top of real life objects. This is unfortunately something that cannot be change. The applications render the virtual objects over top of the stream from the camera. The objects size and orientation can be adjusted, but the rendering is still done as an overlay, which is a factor that affects the depth perception. It is difficult for the user to estimate depth using the real world if the virtual objects appear in front. This is another area that could be addressed in future work; however, there is limited processing power available on a smartphone, with much of it claimed by the application, display and the powering of the LM.

5.2 Future Directions

There are several areas that could be further investigated with future work. First would be to improve the visual aspects so that the virtual objects look like they are behind real-life objects. This could be done by creating an edge detection algorithm that would find the edge of a user’s hands or the edge of a tool. Another algorithm would also need to be created for the purpose of splitting objects, so that the section that passed through the area were edges have been detected would not be rendered. Unity uses several meshes for objects with its environment. These meshes would need to be split and the section removed for every frame. This is take a lot of processing resources, which may not be available on the current generation of smartphones. Further development with the LM could be made with respect to these features once the beta android version has been released, although there is not a release date currently set for this version.

An additional study that could be conducted would be to investigate the effect of different contrast on user performance. This study would ask participants to complete pointing task but the contrast of the objects would vary for each task. The contrast could be varied in several ways including changing the transparency of the shader attached the objects or by adjusting the sharpness of the object edges. This would cause the object to become more blurred. The impact of this change would be measured in the change of the user performance. The user would perform the same pointing tasks with the objects that had high contrast (opaque shader and sharp edges) and then vary either the transparency or the sharpness.

www.manaraa.com

References

[1] K. E. Roberts, R. L. Bell, and A. J. Duffy. “Evolution of Surgical Skills Training.” World Journal of Gastroenterology. 2006, 12, (20), pp. 3219–3224.

[2] G. Ahlberg, T. Heikkinen, L. Iselius, C-E. Leijonmarck, J. Rutqvist, and D. Arvidsson. "Does training in a virtual reality simulator improve surgical performance?." Surgical endoscopy. 2002, 16, (1), pp. 126-129.

[3] A. Hamed, G. Alzhrani, A. Winkler-Schwartz, F. Alotaibi, N. Gelinas-Phaneuf, V. Pazos, N. Choudhury, J. Fares, R. DiRaddo, and R. F. Del Maestro. "Neurosurgical virtual reality simulation metrics to assess psychomotor skills during brain tumor resection." International journal of computer assisted radiology and surgery. 2015, 10, (5), pp. 603-618.

[4] A. G. Gallagher, and C. U. Cates. "Virtual reality training for the operating room and cardiac catheterisation laboratory." The Lancet. 2004, 364, (9444), pp. 1538-1540.

[5] M. Oishi, M. Fukuda, G. Ishida, A. Saito, T. Hiraishi, and Y. Fujii. “Presurgical simulation with advanced 3-dimensional multifusion volumetric imaging in patients with skull base tumors.” Neurosurgery. 2011, 68, pp. 188.

[6] S. C. Shamsunder, and M. Manivannan. "Haptic guided laparoscopy simulation improves learning curve." Studies in health technology and informatics. 2008, 132, pp. 454.

[7] J. Kim, B. Ahn, S. De, and M. A. Srinivasan. “An efficient soft tissue characterization algorithm from in vivo indentation experiments for medical simulation.” The international journal of medical robotics and computer assisted surgery. 2008, 4, (3), pp. 277–285.

[8] L. Soler and J. Marescaux. “Patient-specific surgical simulation.” World journal of surgery. 2008, 32, (2), pp. 208–212.

[9] W. J. Ang, M. E. Hopkins, R. Partridge, I. Hennessey, P.M. Brennan, I. Fouyas, M. A. Hughes. “Validating the use of smartphone-based accelerometers for performance assessment in a simulated neurosurgical task.” Neurosurgery. 2014;10, pp. 57-65

[10] S. Chan, F. Conti, K. Salisbury, and N. H. Blevins. “Virtual reality simulation in neurosurgery: technologies and evolution.” Neurosurgery. 2013, 72, (1)., pp. A154–A164.

[11] D. Waller and J. Miller. “A desktop virtual environment trainer provides superior retention of a spatial assembly skill.” Conference Summary on Human Factors in Computing Systems. 1998, pp. 339–340.

المنارة للاستشارات

www.manaraa.com

[12] B. Dunkin, G. Adrales, K. Apelgren, and J. Mellinger. “Surgical simulation: a current review.” Surgical endoscopy. 2007, 21, (3), pp. 357–366.

[18] K. Abhari, J. S. Baxter, E. S. Chen, A. R. Khan, C. Wedlake, T. M. Peters, S. de Ribaupierre, and R. Eagleson. “Use of a Mixed-Reality System to Improve the Planning of Brain Tumour Resections: Preliminary Results.” Augmented Environments for Computer-Assisted Interventions, 2013, pp. 55–66.

[13] R. A. Kockro and P. Y. Hwang. “Virtual temporal bone: an interactive 3-dimensional learning aid for cranial base surgery.” Neurosurgery. 2009, 64, (5), pp. 216–230.

[14] P. P. Banerjee, C. J. Luciano, G. M. Lemole Jr, F. T. Charbel, M. Y. Oh. “Accuracy of ventriculostomy catheter placement using a head-and hand-tracked high-resolution virtual reality simulator with haptic feedback.” Journal of Neurosurgery. 2007, 107, pp. 515-521.

[15] G. M. Lemole Jr, P. P. Banerjee, C. Luciano, S. Neckrysh, F. T. Charbel. “Virtual Reality in Neurosurgical Education: Part-Task Ventriculostomy Simulation With Dynamic Visual and Haptic Feedback.” Neurosurgery. 2007; 61, (1), pp.142-149.

[16] R. Armstrong, R. Eagleson, S.D. Ribeaupierre. “Patient-Specific Pipeline to Create Virtual Endoscopic Third Ventriculostomy Scenarios.” Medicine Meets Virtual Reality 21: NextMed/MMVR21. 2014 ;196, pp. 14.

[17] S. Delorme, D. Laroche, R. DiRaddo, R. F. Del Maestro. “NeuroTouch: a physics-based virtual simulator for cranial microneurosurgery training.” Neurosurgery. 2012;71, pp. 32-42.

[18] W. J. Ang, M. E. Hopkins, R. Partridge, I. Hennessey, P. M. Brennan, I. Fouyas, M. A. Hughes. “Validating the use of smartphone-based accelerometers for performance assessment in a simulated neurosurgical task.” Neurosurgery. 2014, 10, pp. 57-65

[19] Pagano, Koreen, Angela Haddad, and Tai Crosby. “Virtual Reality-Making Good On the Promise of Immersive Learning: The effectiveness of in-person training, with the logistical and cost-effective benefits of computer-based systems.” IEEE Consumer Electronics Magazine. 2017, 6, (1), pp. 45-47.

[20] Amer, Ahmed, and Phillip Peralez. “Affordable altered perspectives: Making augmented and virtual reality technology accessible.” Global Humanitarian Technology Conference, 2014, 201, pp. 603-608.

[21] Azuma, Ronald T. “A survey of augmented reality.” Presence: Teleoperators and virtual environments. 1997, 6, (4), pp. 355-385.

www.manaraa.com

[22] Kim, Sung Lae, Hae Jung Suk, Jeong Hwa Kang, Jun Mo Jung, Teemu H. Laine, and Joonas Westlin. “Using Unity 3D to facilitate mobile augmented reality game development.” IEEE Internet of Things. 2014, pp. 21-26.

[23] Lindeman, Robert W. “A low-cost, low-latency approach to dynamic immersion in occlusive head-mounted displays.” IEEE Virtual Reality. 2016, pp. 221-222.

[24] Jie, Jiang, Kuang Yang, and Shen Haihui. “Research on the 3D game scene optimization of mobile phone based on the Unity 3D engine.” IEEE Computational and Information Sciences. 2011, pp. 875-877.

[25] Wang, Sa, Zhengli Mao, Changhai Zeng, Huili Gong, Shanshan Li, and Beibei Chen. “A new method of virtual reality based on Unity3D.” IEEE International Conference on Geoinformatics. 2010, pp. 1-5.

[26] Anglin, J. M., T. Sugiyama, and S-L. Liew. “Visuomotor adaptation in head-mounted virtual reality versus conventional training.” Scientific Reports. 2017, 7.

[27] Egger, Jan, Markus Gall, Jürgen Wallner, Pedro Boechat, Alexander Hann, Xing Li, Xiaojun Chen, and Dieter Schmalstieg. “HTC Vive MeVisLab integration via OpenVR for medical applications.” PloS one. 2017, 12, (3).

[28] Rakkolainen, I., M. Turk, and T. Höllerer. “A Superwide-FOV Optical Design for Head-Mounted Displays.” 2016.

[29] Niehorster, Diederick C., Li Li, and Markus Lappe. “The Accuracy and Precision of Position and Orientation Tracking in the HTC Vive Virtual Reality System for Scientific Research.” i-Perception. 2017, 8, (3).

[30] K. Abhari, J. S. Baxter, E. S. Chen, A. R. Khan, C. Wedlake, T. M. Peters, S. de Ribaupierre, and R. Eagleson, “Use of a Mixed-Reality System to Improve the Planning of Brain Tumour Resections: Preliminary Results,” Augmented Environments for Computer-Assisted Interventions. 2013, pp. 55–66.

[31] Kress, Bernard C., and William J. Cummings. “11-1: Invited Paper: Towards the Ultimate Mixed Reality Experience: HoloLens Display Architecture Choices.” SID Symposium Digest of Technical Papers. 2017, 48, (1), pp. 127-131.

[32] Kovács, Péter Tamás, Niall Murray, Gregor Rozinaj, Yevgeniya Sulema, and Renata Rybárová. “Application of immersive technologies for education: State of the art.” IEEE Interactive Mobile Communication Technologies and Learning. 2015, pp. 283-288.

[33] Höllerer, Tobias, and Steve Feiner. “Mobile augmented reality.” Telegeoinformatics: Location-Based Computing and Services. Taylor and Francis Books Ltd., London, UK 21 (2004).

www.manaraa.com

[34] Olson, J. Logan, David M. Krum, Evan A. Suma, and Mark Bolas. “A design for a smartphone-based head mounted display.” IEEE Virtual Reality Conference. 2011, pp. 233-234.

[35] Rosedale, Philip. “Virtual Reality: The Next Disruptor: A new kind of worldwide communication.” IEEE Consumer Electronics Magazine. 2017, 6, (1), pp. 48-50.

[36] Guna, Jože, Grega Jakus, Matevž Pogačnik, Sašo Tomažič, and Jaka Sodnik. “An analysis of the precision and reliability of the leap motion sensor and its suitability for static and dynamic tracking.” Sensors. 2017, 14, (2), pp. 3702-3720.

[37] M. Kramers, R. Armstrong, S. M. Bakhshmand, A. Fenster, S. de Ribaupierre, and R. Eagleson, “A Mobile Augmented Reality Application for Image Guidance of Neurosurgical Interventions.” American Journal of Biomedical Engineering. 2013, 3, (6), pp. 169–174, 2013.

[38] R. Armstrong, S. de Ribaupierre, and R. Eagleson, “A Software System for Evaluation and Training of Spatial Reasoning and Neuroanatomical Knowledge in a Virtual Environment.” Computer Methods and Programs in Biomedicine. 2014.

[39] Grossman, Tovi, and Ravin Balakrishnan. “Pointing at trivariate targets in 3D environments.” Proceedings of the SIGCHI conference on Human factors in computing systems. 2004, pp. 447-454.

[40] Accot, Johnny, and Shumin Zhai. “Beyond Fitts' law: models for trajectory-based HCI tasks.” Proceedings of the ACM SIGCHI Conference on Human factors in computing systems. 1997, pp. 295-302.

[41] Zhai, Shumin, Jing Kong, and Xiangshi Ren. “Speed–accuracy tradeoff in Fitts’ law tasks—on the equivalency of actual and nominal pointing precision.” International journal of human-computer studies. 2004, 61, (6), pp. 823-856.

[42] Zhai, Shumin, William Buxton, and Paul Milgram. “The “Silk Cursor”: investigating transparency for 3D target acquisition.” Proceedings of the SIGCHI Conference on Human Factors in Computing Systems. 1994, pp. 459-464.

[43] Kabbash, Paul, and William AS Buxton. “The “prince” technique: Fitts' law and selection using area cursors.” Proceedings of the SIGCHI conference on Human factors in computing systems. 1995, pp. 273-279.

[44] Al Delail, Buti, Luis Weruaga, and M. Jamal Zemerly. “CAViAR: Context aware visual indoor augmented reality for a university campus.” Web Intelligence and Intelligent Agent Technology. 2012, 3, pp. 286-290.

[45] Han, Jihyun, and N. E. Gold. “Lessons Learned in Exploring the Leap Motion™ Sensor for Gesture-based Instrument Design.” Goldsmiths University of London. 2014.

المنارة للاستشارات

www.manaraa.com

[46] Krastev, Georgi, and Magdalena Andreeva. “A software tool for experimental study leap motion.” International Journal of Computer Science & Information Technology. 7, (6), pp. 145-53.

[47] Coelho, Joanna C., and Fons J. Verbeek. “Pointing task evaluation of leap motion controller in 3D virtual environment.” Creating the Difference. 2014, 78.

[48] Weichert F, Bachmann D, Rudak B, Fisseler D. “Analysis of the Accuracy and Robustness of the Leap Motion Controller.” Sensors (Basel, Switzerland). 2013, 13, (5), pp. 6380-6393.

[49] DW Cool, MJ Connolly, S Sherebrin, R Eagleson, JI Izawa, J Amann, A Fenster “Repeat Prostate Biopsy Accuracy: Simulator-based Comparison of Two- and Three-dimensional Transrectal US Modalities.” Radiology. 2010, 254, (2), pp. 587-594.

[50] Abhari, K, de Ribaupierre, S, Baxter, J, Peters, T, and Eagleson, R “The Role of Augmented Reality in Training the Planning of Brain Tumor Resection.” Augmented Reality Environments for Medical Imaging and Computer-Assisted Interventions, LNCS AE-CAI. 2013, 8090, pp.241-248.

[51] M Kramers, R Armstrong, SM Bakhshmand, A Fenster, S de Ribaupierre, R Eagleson “A Mobile Augmented Reality Application for Image Guidance of Neurosurgical Interventions.” American Journal of Biomedical Engineering. 2013, 3, (6), pp. 169-174.

[52] Drascic, D., and Milgram, P. “Perceptual issues in augmented reality.” Proceedings-Spie The International Society For Optical Engineering. 1996, pp. 123-134.

[53] Azuma RT. “A survey of augmented reality.” Presence: Teleoperators and virtual environments. 1997; 6, (4), pp. 355-385

[54] Amin, D. and Govilkar, S. “Comparative study of augmented reality SDK’s.” International Journal on Computational Science & Applications. 2015, 5, (1), pp.11-26.

[55] Armstrong R, Wright T, de Ribaupierre S, Eagleson R. “Augmented Reality for Neurosurgical Guidance: An Objective Comparison of Planning Interface Modalities.” International Conference on Medical Imaging and Virtual Reality. 2016, pp. 233-243

[56] Diaz, C., Walker, M., Szafir, D.A., Szafir, D. “Designing for Depth Perceptions in Augmented Reality.”. IEEE International Symposium on Mixed and Augmented Reality Conference Proceedings. 2017.

المنارة للاستشارات

www.manaraa.com

Curriculum Vitae

Name:	Trinette Wright	
Post-secondary Education and Degrees:	McMaster University Hamilton, Ontario, Canada 2009-2013 B.Eng.	
Related Work Experience	Teaching Assistant The University of Western Ontario 2015-2017 *Teaching Assistantships*	
	Programming Fundamentals for Engineers	(2015-2016)
	Hardware, Software Co Design	(2017)

Publications:

Wright, T., de Ribaupierre, S., & Eagleson, R. Leap Motion Targeting Performance in an Augmented Reality Workspace. IEEE Consumer Electronics Magazine. (2017)

Wright, T., de Ribaupierre, S., & Eagleson, R. Design and Evaluation of an Augmented Reality Simulator using Leap Motion. Healthcare Technology Letters. (2017).

Armstrong, R., Wright, T., de Ribaupierre, S., & Eagleson, R. Augmented Reality for Neurosurgical Guidance: An Objective Comparison of Planning Interface Modalities. In International Conference on Medical Imaging and Virtual Reality. (2014). pp. 233-243.

Conferences:

R. Armstrong, T. Wright, R. Eagleson, S. de Ribaupierre, A VR system for medical simulation using Google Cardboard and Vuforia, CARS, Heidelberg, Germany, 2016.

Professional Affiliations:

2013 – 2017	**Professional Engineers of Ontario** Engineer In Training

www.manaraa.com